CLIMATOLOGY OF AIR MASS TRANSPORT TO CAPE POINT

by

CHELEDI EVANS TSHEHLA

Submitted in fulfillment of the academic requirements for the degree of

MASTER OF SCIENCE

In the School of Environmental Sciences, University of KwaZulu-Natal, Durban

December 2008

ABSTRACT

Air transport climatology to Cape Point (South Africa; 34.21°S, 18.29°E) was examined by analyzing 5-day kinematic back trajectories at both 300 and 5000 m above ground level for the period 2001-2003. Trajectories were computed using the Hybrid Single-Particle Lagrangian Integrated Trajectory model version 4 (HYSPLIT-4). A multivariate statistical procedure, known as cluster analysis was performed separately for the whole data set, and for yearly and seasonal trajectories, in this way trajectories were classified into distinct transport pathways showing interannual and seasonal variations.

The influence of weather systems such as semi-permanent subtropical continental anticyclones, transient ridging anticyclones originating in the midlatitude westerlies, and baroclinic disturbances in the westerlies on major transport patterns were also discussed.

Cluster analysis results identified seven transport flow patterns to Cape Point (northerly, north-easterly, south-easterly, southerly, south-westerly, westerly and north-westerly). Similar year to year gross features of atmospheric transport patterns were observed at the 5000 m level, however, variability in transport patterns was observed at the 300 m level. Both spring and summer mean clusters exhibit a south-easterly transport associated with trade winds, while autumn and winter show recirculation associated with anticyclones dominating over the interior of South Africa during this period. The influence of the 2002/2003 ENSO (El Ninõ-Southern Oscillation) proved to be insignificant on flow characteristics of Cape Point. Other features such as recirculation of air across southern Africa were also observed. The flow height characteristics of the 5-day cluster means to Cape Point affirmed that South Africa lies in the descending component of the Hadley cell circulation. The autumn and winter cluster means show greater wind shear between the 300 and 5000 m levels.

PREFACE

The research described in this thesis for Master of Science was carried out in the School of Environmental Sciences, University of KwaZulu-Natal, Durban, from January 2006 to December 20008.

These studies represent original work by the author and have not otherwise been submitted in any form for any degree or diploma to any tertiary institution. Where use has been made of others it is duly acknowledged in the text.

DECLARATION

I, **Cheledi Evans Tshehla** declare that

1. The research reported in this thesis, except where otherwise indicated, is my original research.
2. This thesis has not been submitted for any degree or examination at any other university.
3. This thesis does not contain other persons' data, pictures, graphs or other information, unless specifically acknowledged as being sourced from other persons.
4. This thesis does not contain other persons' writing, unless specifically acknowledged as being sourced from other researchers. Where other written sources have been quoted, then:
   a. Their words have been re-written but the general information attributed to them has been referenced.
   b. Where their exact words have been used, then their writing has been placed in italics and inside quotation marks, and the source being detailed in the thesis and in the Reference section.
5. This thesis does not contain text, graphics or tables copied and pasted from the Internet, unless specifically acknowledged, and the source being detailed in the thesis and in the Reference section.

Signed…….

University of KwaZulu-Natal, Durban, December 2008

ACKNOWLEDGEMENT

I would like to express my sincere gratitude and deepest appreciation to:

- Prof. R Diab, my supervisor, for her guidance, vision, critical comments, encouragement and for editing the manuscript.
- The librarians of the South African Weather Service, Karin and Anastasia, for helping with the quest to find articles.
- The staff at National Oceanic and Atmospheric Administration, Barbara Stunder and Roland Draxler for their assistance in running the windows-based HYSPLIT model to cluster trajectories.
- Prof. W.A Landman for his assistance in proof reading chapter 2.
- The South African Weather Service for funding my studies.
- My late parents, Mamohlomi and Petros Tshehla who were always there for me to offer their support and assistance.

TABLE OF CONTENTS

LIST OF SYMBOLS

$x(t)$	three dimensional position at t
$V(t)$	parcel velocity vector
T	interpolated temperature
P	parcel start pressure
σ	internal trajectory model terrain-following coordinates
Z_{top}	top of the trajectory model coordinate system
Z_{msl}	height of model at mean sea level
Z_{gl}	height of model at ground level
z	model's internal height
k	model's internal index
T_0	surface temperature
θ	potential temperature at pressure P

LIST OF FIGURES

LIST OF PLATES

LIST OF TABLES

LIST OF ABBREVIATIONS

agl	above ground level
amsl	above mean sea level
ARL	Air Resources Laboratory
ATG	Auto Trajectory Generator
BL	Boundary Layer
CFC	Chlorofluorocarbon
CH_4	Methane
CO	Carbon monoxide
CO_2	Carbon dioxide
COAMPS	Coupled Ocean Atmosphere Mesoscale Prediction System
DJF	December-January-February
DRC	Democratic Republic of Congo
ECMWF	European Center for Medium Range Weather Forecasting
ENSO	El Ninõ-Southern Oscillation
GAW	Global Atmospheric Watch
gpm	Geopotential meter
hPa	Hectopascal
HYSPLIT	HYbrid Single-Particle Lagrangian Integrated Trajectory
IMK-IFU	Institut für Meteorologie und Klimaforschung, Atmosphäriche Umweltforschung
ITCZ	Intertropical Convergence Zone
JJA	June-July-August
MAM	March-April-May
MM5	Fifth-Generation Mesoscale Model
N	Northerly
NCAR	National Center for Atmospheric Research
NCEP	National Center for Environmental Prediction
NE	North-easterly
NW	North-westerly
NOAA	National Oceanic and Atmospheric Administration
N_2O	Nitrous oxide
O_3	Ozone
RAMS	Radiation Measurement System
SAFARI	Southern Africa Fire-Atmosphere Research Initiative
SAST	South African Standard Time
SAWS	South African Weather Service
S	Southerly
SE	South-easterly
SW	South-westerly
SO_2	Sulphur dioxide
SON	September-October-November

SST	Sea Surface Temperature
TSV	Total Spatial Variance
TRACM	Trace gas Research and Atmosphere Change Monitoring
UTC	Coordinated Universal Time
W	Westerly
WMO	World Meteorological Organization

CHAPTER 1

INTRODUCTION

1.1 Background

Among the various consequences of increasing population and economic growth in many areas of the world are serious pollution problems. These problems can result from both local emissions and from the long-range transport of pollutants from outside the local area. As a result, understanding the atmospheric transport climatology at a particular location is crucial to determining the relationship between measured trace gases and aerosols and their regions of origin. This is particularly important in the case of a measuring station that is established in order to provide measurements of background concentrations of pollutants, such as the Global Atmospheric Watch (GAW) baseline monitoring stations of the World Meteorological Organization (WMO).

The Cape Point station is one such station in the GAW network (Fig. 1.1). It is rated among the best WMO baseline atmospheric monitoring stations because of its long record of operation (>30 years). The first trace gas measurements, *viz.* carbon monoxide (CO) and chlorofluorocarbons (CFC-11) started at Cape Point in 1977, when the station was managed by the Council for Scientific and Industrial Research (CSIR) of South Africa in collaboration with the Max-Planck Institute for Chemistry, Germany. Subsequently, in 1986, collaboration with the Fraunhofer Institute (IFU), which is now IMK-IFU of the Research Center Karlsruhe, was initiated, and in 1995, the station was officially incorporated into the WMO-GAW network. Two years later, the Trace gas Research and Atmosphere Change Monitoring (TRACM) division of the South African Weather Service (SAWS) took over the management of the station from CSIR.

The Cape Point monitoring programme has expanded over the years, and now includes monitoring greenhouse gases such as carbon dioxide (CO_2), methane (CH_4), nitrous oxide (N_2O) and surface ozone (O_3), as well as halocarbons, CO, radon, sulphur dioxide (SO_2) and aerosols.

The mission of the Cape Point monitoring station is to make reliable, comprehensive observations of the chemical composition and selected physical characteristics of the atmosphere on a regional scale and to provide the scientific community with the means to predict future atmospheric states. A detailed description of the sampling line and trace gas measuring methods together with quality control and assurance procedures are given in WMO [2002].

Measurements of the chemical composition of the atmosphere, whether as part of a long-term monitoring programme, or for detailed campaign studies of atmospheric processes, show that concentrations vary on time scales from minutes to decades. Some of these changes are clearly related to annual cycles or seasonal changes in the patterns of emission or transport of trace gases, but on a time-scale of days or less, the variability is closely related to the immediate history of the air before arriving at the sampling point. In order to understand the different processes which contribute to the ever-changing mixture of trace constituents of the atmosphere, the first step is often to devise a means of categorizing the data.

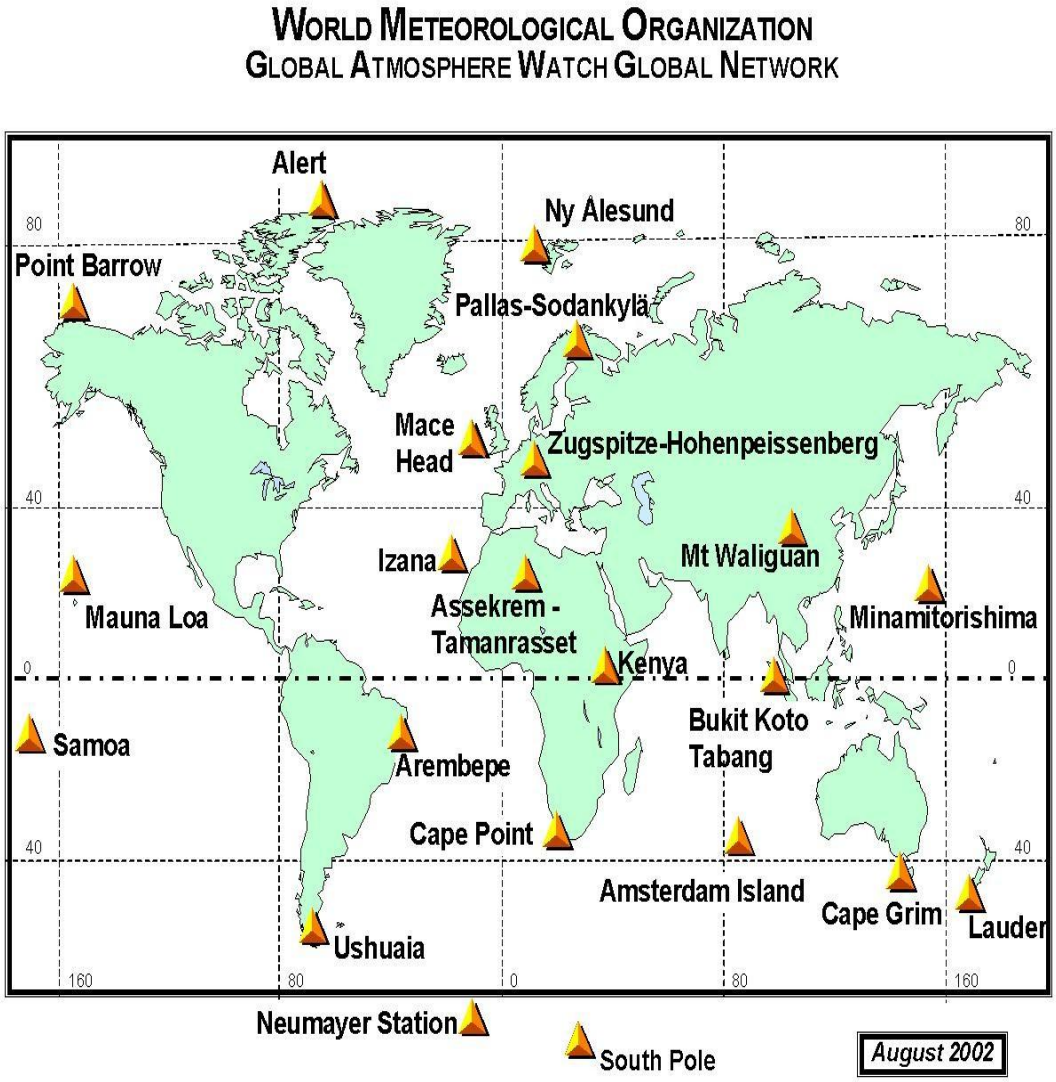

Figure 1.1: The stations of the GAW network (source: http://www.umweltbundesamt.de)

There are two main approaches to this classification of measurement data; first classification is entirely based on the values of trace gas or aerosol data (or related meteorological data) themselves; while the second classification is based on the origin of the sampled air. The former, results from studies of "extreme" events, such as highest and lowest observed concentrations in a given period. The latter approach depends on the measured direction and past history of the air arriving at the site, from relatively simple consideration of the locally measured wind direction to calculated air-mass back trajectories extending over several days. This technique is used when a more general description of the climatology of a site is required [Cape *et al*., 2000].

1.2 Rationale for study

It is the latter approach (described in the previous section) of categorizing back trajectories that is used in this study to provide a greater understanding of the long range transport of trace gases and aerosols to Cape Point to aid in the interpretation of atmospheric measurements.

Air arriving at the south-western part of the Western Cape Province can have a wide range of histories, from clean maritime South Atlantic Ocean air, which may have traces of South American influence still present, to highly polluted air flow from central Africa. There are therefore good *a priori* reasons for attempting some type of geographical classification of the air-mass origins and their transport patterns.

The influence of large-scale circulations on atmospheric transport of trace gases and aerosols has received increasing attention in the past with emphasis on identifying sources and sinks of pollutants. Miller [1981] contributed extensively to the understanding of wind flow climatology by analyzing 5-year back trajectories for Mauna Loa Observatory. Most investigations of long-range transport have been based on case studies. Studies have shown that Saharan dust may be carried to the Caribbean [Prospero *et al.,* 1981; Muhs *et al.,* 1990], the Amazon basin [Swap *et al*., 1992] and Northern Europe and Fennoscandia [Pitty, 1968; Franzen *et al*., 1994]. Transport over long distances of continentally derived particulate carbon in the marine atmosphere was demonstrated quantitatively by Cachier *et al.,* [1986]. Long-range transport studies of aerosols and trace gases associated with biomass burning from southern Africa into the tropical South Atlantic Ocean and south-western Indian Ocean has been reported in the work of authors such as Crutzen and Andreae, [1990], Watson *et al*., [1990], Levine, [1991], and Fishman *et al*., [1991]. During the mid-1990s, the horizontal and vertical transport of air from subtropical southern Africa during the Southern Africa Fire-Atmosphere Research Initiative investigation (SAFARI) was examined in detail [Garstang *et al*., 1996; Swap *et al*., 1996]. More recently, the relationships between the origin of air masses and carbon monoxide measurements at the Cape Point were investigated [Sodemann, 2000].

This study builds on previous research studies of atmospheric transport of trace gases as presented above, to complement several studies of synoptic and long-range transport climatology developed for southern Africa. The Cape Point station was chosen as a receptor site due to its location on the south-western coast which is subjected to maritime air from the South Atlantic and continental air, making it an ideal station for improving the understanding of interactions between the atmosphere, ocean and biosphere.

1.3 Aim

The purpose of this study is to provide climatology of air flow patterns to Cape Point and to determine the meteorological conditions associated with the flow patterns (by means of a cluster analysis based on a three-year database of atmospheric back trajectories). The specific objectives are as follows:

(1) To undertake back trajectory modeling from Cape Point at two different heights, *viz*. 300 m and 5000 m above ground level.

Trajectories from two levels (300 m and 5000 m) are examined to take account of the possible presence of vertical wind shear and to give comprehensive information about the major wind regimes affecting Cape Point. The 300 m level is closer to the surface where impacts of air pollutants are felt, while the 5000 m level is in the upper troposphere were strong horizontal winds occur that can cause trans-boundary transport of pollutants. This analysis also investigates the sensitivity of transport to trajectory altitude and the resulting change in source regions.

(2) To categorize the back trajectories into distinct flow patterns using cluster analysis.

Cluster analysis is performed on trajectories for the period 2001-2003. Inter-annual and seasonal variability is explored by clustering trajectories for each year individually, and for each season. Trajectory classifications based on cluster analysis will be more readily interpretable in terms of synoptic conditions that lead to them, and they will also give much more detailed information about potential source regions affecting Cape Point.

(3) To investigate the influence of meteorological conditions on the flow patterns.

Mean meteorological conditions associated with each of the clusters are examined to determine the influence of circulation patterns on seasonal and inter-annual variability of air flow.

1.4 Study area

The Cape Point station is located in a nature reserve at the southern tip of the Cape Peninsula, South Africa (34.21°S, 18.29°E). The monitoring station is exposed to the sea on top of a cliff 230m above mean sea level (amsl), about 60 km south of the city of Cape Town (Plates 1.1 and 1.2). The sampling air inlet and other pieces of meteorological equipment are mounted on a platform on a 30 m sampling tower. The air sampling regime is representative of the southern mid-latitude oceans.

1.4.1 Topography

The topography of the Western Cape consists of coastal mountains which rise steeply to a height of over 1 km and which act as obstacles to westerly flow in the region. The entire South Africa resembles a dome with a horizontal curvature of about 900 km in radius. The coastal mountains are smoothed-out with the exception of river valleys and these mountains act as barriers. Due to their steep incline and their curved surface, the mountains are able to steer low-level coastal weather efficiently around their periphery [Taljaard, 1972; Reason and Jury, 1990]

Plate 1.1a: Location of the Cape Point GAW station (source: http://gap-vm-pub1.gap.fzk.de).

Plate 1.1b: Cape Point station showing the sampling tower (source: http://gap-vm-pub1.gap.fzk.de).

1.4.2 Typical weather situation

In summer, the Cape south-easter blows strongly for several days with little interruption. The normal south-easter is associated with fine weather. Low clouds during the period in which the south-easter prevails consists of orographic cloud along the mountains with little or no movement or diurnal variation. The south-easter blows when a southerly to northerly pressure gradient is established along the south-western Cape coast. This happens when an anticyclone or a ridge of high pressure extends eastwards south of the Western Cape Province with low pressure over the interior. In winter, the wind is generally strong northerly to north-westerly and usually accompanied by heavy rains [Schulze, 1965].

Berg winds and coastal lows are important features of coastal climates and are associated with large-scale pre-frontal divergence and dynamic warming of subsiding air moving offshore from the plateau [Tyson and Preston-Whyte, 2000]. Berg winds may blow for several days to a few hours, and are most common in late winter and early spring. The strong offshore effect of berg winds on the west coast may transport dust plumes from the coastal plain into the ocean on the west coast [Reason and Jury, 1990; Desmet and Cowling, 1999].

1.5 Scope of the thesis

Chapter 1 gives an overview of the importance of the Cape Point GAW station and the choice of its location on the Cape Peninsula. It gives a detailed account of activities at the station and the history of the station. It further outlines the rationale for undertaking this study and the expected outcome, by detailing a list of objectives that serves as a guide to achieving the goal of this study.

Chapter 2 begins with an introduction of different circulation patterns affecting southern Africa and the frequency of their occurrence. It then gives detailed information about the global circulation systems such as global wind belts, the Walker Circulation and El Niño-Southern Oscillation, and their impact on the flow characteristics of Cape Point. This is followed by a detailed account of the mean circulation patterns over southern Africa and the synoptic circulations affecting the region. Mesoscale and local circulations affecting Cape Point are discussed last.

Chapter 3 describes the data and methodology used in this research. It begins by giving an introduction to trajectory modeling with the aid of mathematical equations, and the advantages and disadvantages of different types of trajectory models. A background to the HYSPLIT model is presented giving details of meteorological data fields used and defining the model's evolution and the recent features added to the model. Source errors encountered in trajectory generation are also discussed. A trajectory database detailing the meteorological data fields used in the computation of trajectories is presented and the choice of using kinematic 3D trajectories as compared to other approaches such as isentropic or isobaric trajectory modeling is justified. A detailed account of the methodology used in calculating the trajectories and the levels and duration of back trajectories chosen for this study is also outlined.

A detailed background of trajectory cluster analysis is given based on the work of several authors. The Ward's method is described in detail to account for the clustering method employed by the HYSPLIT model in trajectory clustering. Finally, the cluster analysis procedure used in this study is explained to give details of how it aids in identifying air flow patterns to Cape Point.

Chapter 4 displays the results graphically, and the observed clusters are discussed, starting with the 3-year cluster means and their membership plots, followed by yearly means, and finally, a discussion of seasonal clusters. The cluster means are also discussed in terms of weather systems affecting southern Africa.

Finally, chapter 5 summarizes the findings based on the objectives outlined in chapter 1.

CHAPTER 2

WEATHER PATTERNS OVER SOUTHERN AFRICA

2.1 Introduction

Southern Africa is situated in the descending component of the Hadley and Ferrel cell circulations (Plate 2.1). The climate in this region is influenced by a great variety of weather systems [Newell *et al*., 1972]. Garstang *et al.* [1996] and Tyson *et al.* [1996a,b] gave detail of how the semi-permanent subtropical anticyclones dominate the lower tropospheric circulation of the region. Other important circulation types (Fig. 2.1) include barotropic quasi-stationary easterly waves, transient ridging anticyclones originating in the midlatitude westerlies, and baroclinic disturbances in the westerlies. Easterly waves were found to dominate in summer, and ridging anticyclones are occurring regularly on an annual basis. Westerly disturbances exhibit a semiannual cycle, peaking in spring and autumn. Continental anticyclones systems occur most frequently in any month from March to September, peaking from April to August than all the other systems combined [Harrison, 1986; Van Heerden, 1987; Taljaard, 1995a; Tyson *et al.*, 1996a]. These weather systems will aid in the interpretation of mean clusters to determine the flow transport to Cape Point.

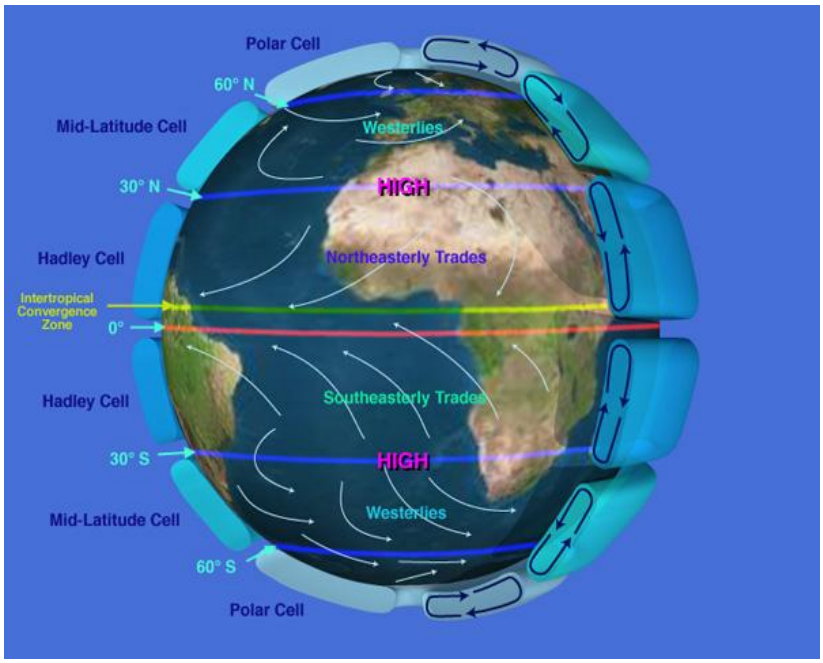

Plate 2.1: Global winds (courtesy of NASA JP: http://sealevel.jpl.nasa.gov)

Weather systems are distinguished by their characteristic scales (ranging from microscale to global-scale) and circulation patterns. The difference in weather patterns are caused by energy imbalances which produce temperature and therefore, pressure variations. Pressure gradients

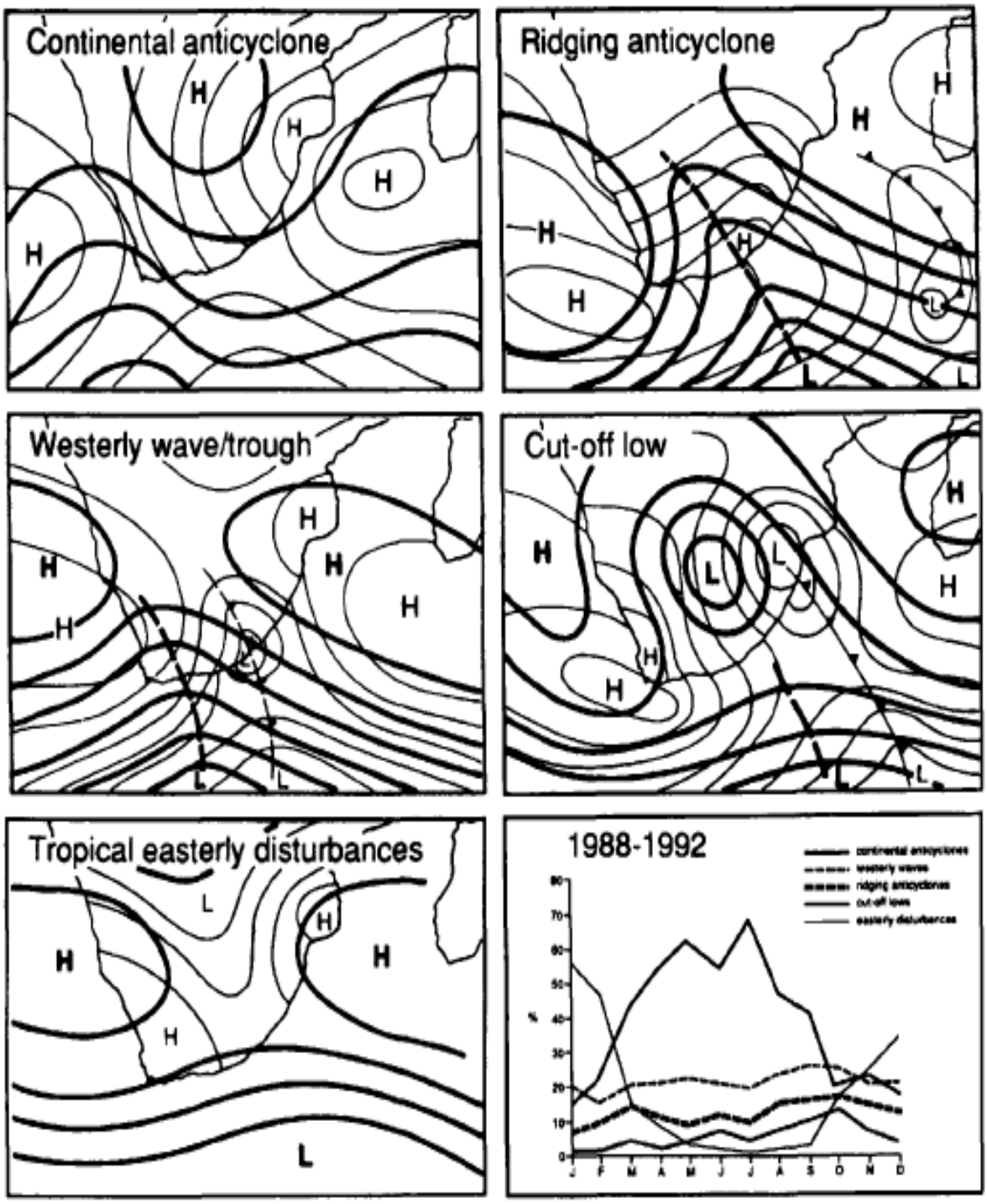

Figure 2.1: Major circulation types affecting southern Africa and their five year monthly frequency (source: Tyson and Preston-Whyte, 2000). Heavy lines represent conditions at 500 hPa; light lines represent conditions at 850 hPa.

generate winds, which in turn are influenced by factors such as the earth's rotation, frictional drag, temperature variations, moisture variations and mountain barriers. The wind systems occur at a variety of scales which are interdependent on each other [Tyson and Preston-Whyte, 2000].

At the microscale, air flow is characterized by small, short-lived, high energy turbulent eddies. These range in size from a few centimeters to a few meters. Near the surface in the boundary layer, they tend to be generated by surface roughness (mechanical turbulence) and heating (thermal turbulence). At the mesoscale level, which ranges from a kilometer to a few hundred kilometers, local wind systems such as land–sea breezes, mountain-valley winds and convective phenomena such as tornadoes and thunderstorms occur due to differential heating and geometry and may persist for several hours in a day [Tyson and Preston-Whyte, 2000]. Synoptic scale circulations, which are smaller macroscale circulations, occur over hundreds to thousands of square kilometers and their life span varies, but they may last for days to even weeks. The largest planetary-scale wind patterns, called macroscale winds, include westerlies and trade winds and these extend over a few hundred to several thousand kilometers [Palmén and Newton, 1969; Chang, 1972; http://wps.prenhall.com].

In this chapter, a detailed description is given of main climatic controls, ranging from those at the global level, through to those at the synoptic scale, and finally to the influence of mesoscale wind systems. Plate 2.2 depicts the area of interest pertinent to this study.

Plate 2.2: South Atlantic Ocean (source: http://go.hrw.com)

2.2 Global atmospheric circulation systems

Seasonal patterns of temperature, precipitation and climate are molded by global winds which also drive surface ocean currents, and provide the setting for all smaller scale wind and weather systems [http://www.sci.ccny.edu]. At the global scale the wind systems (Fig. 2.2) are described by the strength and location of the westerly wind belt in the middle latitudes, the easterly wind belt in the tropical latitudes and the polar easterlies in polar latitudes. The strength of the mean zonal surface winds varies seasonally and are related to the changes in the thickness pattern of the atmosphere, but the patterns of the alternating easterlies and westerlies is present throughout the year, with slight seasonal shifts of the latitudes at which the mean zonal surface winds changes. The ageostrophic mean meridional surface wind is generally weaker than the predominantly geostrophic mean zonal surface wind, and in regions of surface westerlies it is directed poleward, while in regions of surface easterlies it is directed equatorward [Palmén and Newton, 1969; Abraham and Rasmusson, 1970; Chang, 1972; Hastenrath, 1985; Schneider, 2006].

2.2.1 Global wind belts

The Polar cell (Plate 2.1) is a complete circulation that forms when warm air rises and diverges towards the poles at about 60 degrees south or north in the Southern and Northern Hemispheres respectively and once at the poles the air sinks. The Coriolis force then acts on the descending air and deflect it to the right at the surface and force it to move eastwards to create the polar easterlies [Lutgens and Tarbuck, 1979; http://weather.cod.edu]. The Polar front which forms a boundary between the cold air from the polar region and the warm air from the subtropical highs is formed by the convergence of polar easterlies and the westerlies in the mid-latitudes [Henry, 1922; Lutgens and Tarbuck, 1979].

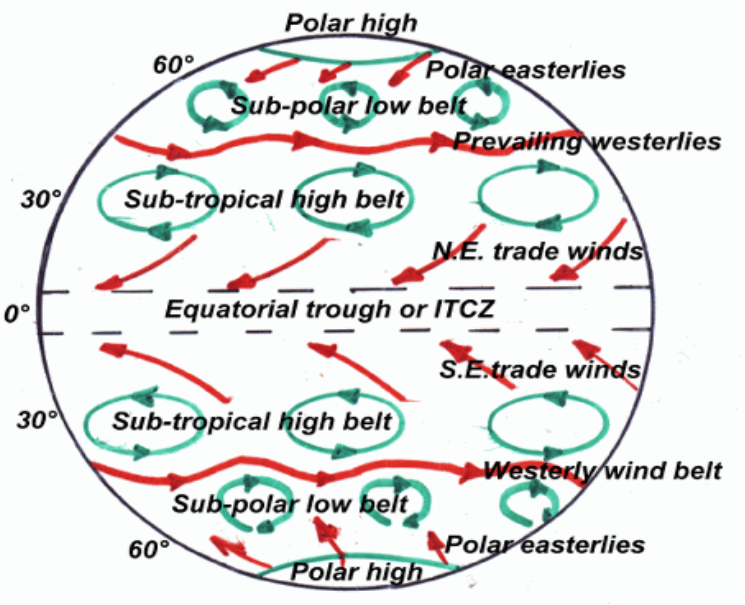

Figure 2.2 : Global winds (source: www.auf.asn.au)

The mid-latitude westerlies (Fig. 2.2) are the circumpolar belts found in both the Northern and Southern Hemispheres in which the west to east motion of the atmosphere dominates. The westerlies are bound by the subtropical high pressure belt on the equatorward site. The westerly belts widens with height, being shallower closer to the surface and encompassing a broader area in the upper troposphere. At sea level the subtropical high-pressure belt in the Southern Hemisphere has a mean position at about 33°S in January and 29°S in July. At the 500 hPa level the equatorward limit of the westerlies varies from about 20°S in January to about 10°S in July. The westerlies in Southern Hemisphere are stronger compared to their Northern Hemisphere counterparts. Embedded in the westerlies are narrow wind currents (jet stream) characterized by strong winds in the upper troposphere in a region between the Hadley and Ferrell cells of the mean meridional circulation. The subtropical jet stream which is strongest near the 200 hPa surface is characterized by strong vertical wind shear in the upper troposphere [Namias and Clapp, 1949; Palmén, 1951; Krishnamurti, 1961; Chang, 1972; Lettau, 1973; Tyson and Preston-Whyte, 2000; Liu and Ren, 2003].

Taljaard [1995a,b,c], in his studies of atmospheric circulation systems found that there are strong westerlies (mean speeds of 30 to 35ms^{-1}) which prevail in winter south of 20°S, decrease to attain mean speeds of 10 to 15m/s from January till March in the zone 20 to 30°S. In summer, a ridge axis, frequented by anticyclones, exists between 15 and 20°S. This ridge provides for predominant light to moderate east winds above the surface Intertropical Convergence Zone (ITCZ), explaining the tendency for low-pressure disturbances to move westward along the ITCZ. At the intermediate levels (700 to 300 hPa) anticyclones predominate over the subcontinent, their centers being displaced step by step northwards and westwards with increasing height [Potgieter, 2006].

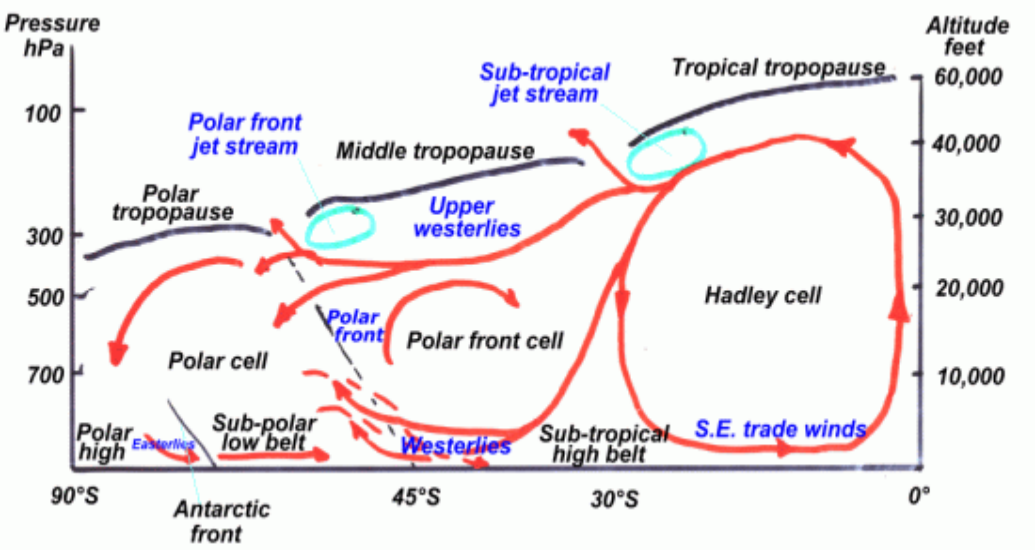

Figure 2.3: Cross-section of tropospheric circulation (source: www.auf.asn.au)

Zonally averaged planetary scale circulation of the tropics consists of an easterly wind regime (trade winds) bounded by the anticyclonic axes of the subtropical highs (Fig. 2.2 and 2.3), and the two thermally direct Hadley cells. In their upstream portion, on the eastern equatorward side of the subtropical anticyclones, the trades are subsiding and divergent. Proceeding downstream,

towards the Equator and the western side of the subtropical anticyclones, divergence gradually gives way to convergence and ascending motion. Surface climate and weather characteristics change accordingly along the trade wind trajectory. A low pressure zone (Inter-Tropical Convergence Zone) is found between two subtropical high pressure belts of the two hemispheres around the globe near the equator. Within this trough of low pressure, the trade wind airstreams from both hemisphere meet, and ascending motion prevail. Over Africa, the Indian Ocean and western Pacific regions the Inter-Tropical Convergence Zone (ITCZ) migrates from the southern to the Northern Hemisphere between January and July. However, over the Atlantic and the eastern Pacific Oceans, the ITCZ remains in the Northern Hemisphere throughout the year [Palmén and Newton, 1969; Newton, 1986; Abraham and Rasmusson, 1970; Chang, 1972; Hastenrath, 1985].

2.2.2 Walker Circulation and El Niño-Southern Oscillation

Ocean-atmosphere research has been undertaken by many meteorologists and oceanographers for well over a century. Walker Circulation (Fig. 2.4) is a term used by Bjerkness [1969] to describe the circulation that occurs due to changes in surface pressure in the east and west of the Pacific Ocean caused by upwelling of cold water in the eastern Pacific. The upwelling cools the air above it, which becomes colder and dense. The air in this region will descend and create a high pressure cell. The western Pacific is characterized by warm wet climate that leads to convective activity in that region. The surface air then flows westward between the two cell circulations of the two hemispheres to the warm west Pacific where it is heated and undergoes a moist-adiabatic ascent, and the air flows eastward in the upper atmosphere to complete the circulation [Julian and Chervin, 1978; Rosenlof *et al*., 1986]. Newell *et al.* [1974] emphasized that the circulation occurs when the wind field decouples from the zonal average. Some authors such as Rosenlof *et al* [1986], Tyson and Preston-Whyte [2000] and Sasamori [1982] described the Walker Circulation as a thermally direct circulation that rises on the western Pacific and has a broad band of subsidence over the eastern Pacific.

[Julian and Chervin, 1978], used the concept of the Southern Oscillation (which refers to the exchange of mass and latent heat along the complete circumference of the globe in tropical latitude) to describe the Walker circulation as the east-west exchange of air covering a little over an earth quadrant of the equatorial belt from South America to the west Pacific. Walker [1923] , Walker and Bliss [1932] and Berlage [1957, 1966] described the Southern Oscillation in terms of changes in pressure due to changes in sea surface temperatures between the Indian and Pacific Oceans and is measured by observing the pressure difference between Tahiti and Darwin. Philander [1983] referred to the Southern Oscillation as the large-scale pattern of climate events over much of the globe. Rasmusson and Carpenter [1982] combined the El Niño and Southern Oscillation concepts to describe the large scale ocean-atmosphere system associated with strong fluctuations in ocean currents and surface temperatures. The entire phenomenon is referred to as the El Niño- Southern Oscillation, or ENSO [Nichols, 1984].

Schumann [1992] emphasized that the core ENSO interactions occur along the equator, and hence the need to identify teleconnections between ENSO and areas remote from the dominant effects in the Pacific region. Shannon *et al*. [1986] was unable to prove effects of ENSO events on the south-west coast of southern Africa, and instead postulated that the less frequent

"Benguela Niño" occurs. However, van Heerden *et al*. [1988] and Lindesay [1990] were able to identify positive correlations between South African summer rainfall and ENSO events, while Walker [1990] identified "Agulhas warm events" outside of the ENSO years.

Shannon *et al*. [1986] and Bakun [1990] (quoted by Schumann [1992]) indicated that little analysis of interannual wind variability has taken place, and that most studies have concentrated on zonal or meridional wind components. Anomalies in winds appear to be primarily zonal, and there is little correspondence between meridional wind changes and the recognized ENSO events [Shannon *et al*., 1986; Tyson and Preston-Whyte, 2000]. Lindesay (quoted in Schumann [1992]) found minimal changes in the mean meridional summer winds (January-March) at Cape Town and along 30°E, but did establish that the zonal winds tended to be more westerly during ENSO events. Jury [1998] stated that a warm sea surface temperature (SST) anomaly observed in the tropical South Atlantic are responsible for disrupting El Niño-induced upper westerly winds over the Atlantic. The warm SST anomaly caused upper easterly winds to oppose the El Niño-induced westerlies.

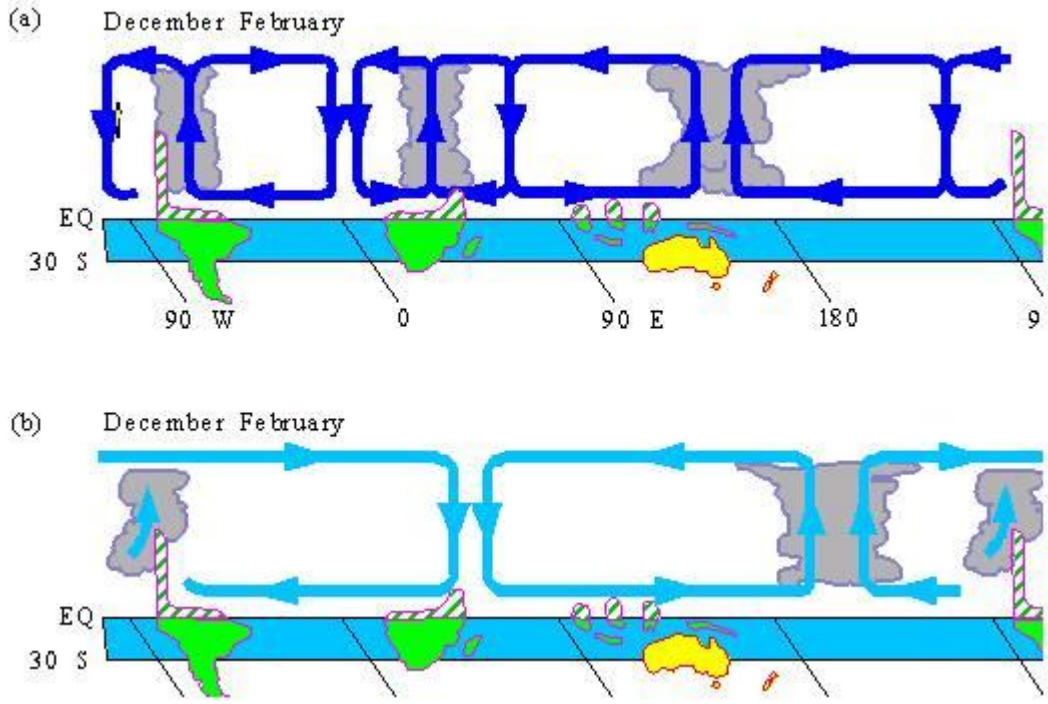

Figure 2.4: The normal mode of the Walker circulation (a), and its breakdown during El Niño years (b) (source: http://eis.jrc.int)

2.3 Mean circulation patterns over southern Africa and the surrounding oceans

It is important to identify the mean circulation patterns over South Africa (Fig. 2.5) and the immediate oceans to be able to establish characteristic air flow patterns. Several studies of climate and weather of southern Africa revealed that they are influenced by the mean circulation of the atmosphere over the subcontinent. Southern Africa's location in the subtropics place it in

the descending component of the Hadley cell circulation (Plate 2.1) where it is affected by circulation systems prevailing in both the tropical latitude to the north and temperate latitudes to the south (Fig. 2.1). It is also dominated by the high pressure systems that on average constitute the semi-permanent subtropical high pressure cells of the general circulation of the Southern Hemisphere [Tyson and Preston-Whyte, 2000; Potgieter, 2006].

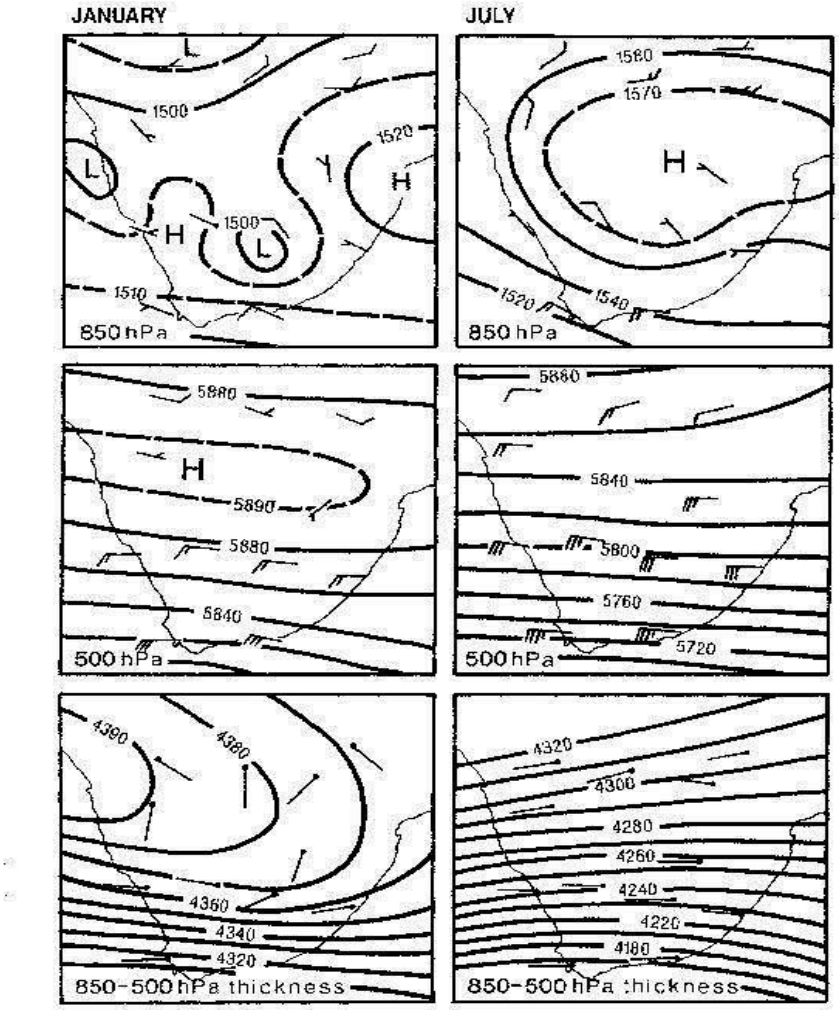

Figure 2.5: Monthly mean winds, contours of the 850 and 500 hPa surfaces (gpm) and 850-500 hPa thickness (source: Taljaard, 1981).

In South Africa, the mean circulation of the atmosphere is anticyclonic and prevails throughout the year, except near the surface where the wind changes due to differences in surface heating. In winter, the mean anticyclone intensifies and moves northward. The easterlies in the upper-level are displaced equatorward due to the expansion of circumpolar westerlies (Fig. 2.5). In summer, there's a trough (at 850 hPa level) extending from northern Namibia across central Botswana to a low over southern Free State and north-east Cape Province. The trough is flanked by a ridge extending eastwards along 30° S from the subtropical Atlantic Ocean and another at 25° S extending westwards from the Indian Ocean to the eastern Mpumalanga Highveld. The minimum

near Windhoek is probably caused by strong heating over the high ground of the Khomas Hochland during summer days [Potgieter, 2006].

The observed semi-permanent ridge over Mpumalanga advects moist tropical air from the Mozambique Channel westwards and then southwards towards the Botswana trough. While the opposite occurs over the west coast where the Atlantic ridge imports very dry subsiding air to the regions west of the Botswana trough. The mean 850 hPa wind observed at Upington is north-westerly whereas it ought to be southerly in accord with to the 850 hPa height distribution. In winter, at the 850 hPa level the heat lows and the trough over Botswana are replaced by mean anticyclonic pressure and wind patterns over the plateau as shown in figure 2.5. The ridge over Mpumalanga indicates a three degrees shift to the north, its axis now being located along 23° S.
In summer, the 500 hPa level indicates a ridging anticyclonic circulation from the west with moderate westerlies and light easterlies. In winter, the westerlies shifts northward and becomes stronger over South Africa. [Potgieter, 2006]

Authors such as Tyson and Preston-Whyte [2000] also described the mean circulation pattern over southern Africa. In general, their account is similar to Taljaard's [1995a, 1995b] description. However, the difference is in the description of the mean 850 hPa circulation during summer, in that the heat low over the Khomas Hochland as described by Taljaard [1995b] is not mentioned in the work of Tyson and Preston-Whyte [2000]. Instead, Tyson and Preston-Whyte [2000] linked the trough over South Africa and Botswana with the tropical low north of Botswana. However, Taljaard [1995b] did not make mention of this tropical low north of Botswana [Potgieter, 2006].

In the Southern Hemisphere, the subtropical anticyclone is the dominant weather system over the subtropical Atlantic Ocean throughout the year. In the summer months (December-March), the ITCZ occasionally affects the northern South Atlantic Ocean with disturbed weather. During the months of May–October, Southern Hemisphere mid-latitude frontal systems influence the southern portions of the region. These frontal systems and the low cloudiness and fog associated with the Benguela Current are the only significant synoptic-scale weather phenomena which affect the region. Winds over most of the region are south-easterly throughout the year, with wind speeds varying from a low of 2.6-7.7 meters/second (m/s) in June to December to a high of 5-10 m/s in June to December. However, between 30°S and 35°S, the distribution is more equal in all directions, with components from the west predominant in the western section of the area, where the wind speeds vary from a low of 5-7.7 m/s in February to May to a high of 5-15 m/s in June to November. Gale force winds equaling or exceeding 18 m/s are a significant problem in the area 30-35°S, during the months of May to October [Schulze, 1965; Hoflich, 1984].

The South Atlantic and Indian Ocean (35°S-50°S and 15°W-60°E) areas are subjected to gale force winds throughout the year. The migratory anticyclones and mid-latitude frontal low centres dominate the weather all months. These systems are most intense and travel farthest north through the area during the austral winter. Winds in the area (35°S-50°S and 15°W-20°E) are predominantly westerly with coastal summer season directions mainly south to south-west. Over the Indian Ocean (20°E-60°E) the roaring forties are the predominant winds in this region [Schulze, 1965].

2.4 Synoptic scale circulation

Hewitson and Crane [2002] gave a brief history of synoptic classification; the historic development of synoptic-scale atmospheric circulation can be traced back to the late 19th century (Köppen, 1874; Abercromby, 1883, 1887 cited in Hewitson and Crane [2002]). Barry and Perry [1973] in their publication of 'Synoptic climatology: methods and applications', described synoptic climatology as sub-field of climatology, where they investigated the relationships of weather elements individually or collectively to atmospheric processes.

Crane, 1978; Yarnal 1984; Wigley and Jones, 1987 (quoted in Hewitson and Crane, 2002) examined the interactions or relations between the circulation and local environmental parameters in using synoptic classification as a data reduction tool. Lamb [1950], employed manual classification in defining synoptic types; although his approach was very effective, it was however extremely time consuming. Yarnal [1993], summarized the basic characteristics of synoptic classification technique based on procedures involving correlation, clustering, and/or eigenfunction analysis.

Weather systems or circulation types over southern Africa have been identified and described by several authors of which the work of Taljaard [1995a], Harrison [1984] and Tyson [1986] are the most widely used. The classification methods used by these authors differ. Taljaard [1995a] described the circulation types that occur over southern Africa in summer and winter. He identified all the typical surface pressure distribution patterns as well as upper air pressure distributions, and specific examples were used in explaining these systems. He used the location, intensity, temperature and certain structural features of cyclones, anticyclones, troughs and ridges to aid his classification. This classification can be regarded as one of the most complete classifications of the different circulation patterns that occur over southern Africa. He also constructed the synoptic climatology for January and July over South Africa. Harrison [1986] focused on identifying summer rain-producing circulation types. He employed statistical methods combined with satellite imagery. Tyson [1986] divided his classification into a few categories. He described the weather systems in terms of the easterlies and the westerlies influencing South Africa's weather (Fig. 2.6). He described typical weather systems that are associated with fine or mildly disturbed conditions and he also described systems that can lead to pollution transport over the country [Tyson and Preston-Whyte, 2000; Potgieter, 2006].

South Africa is located between 22° and 35° S (Fig. 2.7) and lies astride the subtropical high pressure belt which is centered at about 30° S and within a zone that is critically affected by seasonal meridional shift in the Indian Ocean high [Taljaard, 1953]. The South African weather is primarily seasonal and is dominated by a few large scale synoptic circulations such as the South Indian Anticyclone which is responsible for transporting moist air from the Indian Ocean into the interior of South Africa, the continental high which is largely responsible for warm dry conditions usually experienced over the interior of the country, and the South Atlantic Anticyclone which is mainly responsible for south easterlies blowing south of South Africa. All

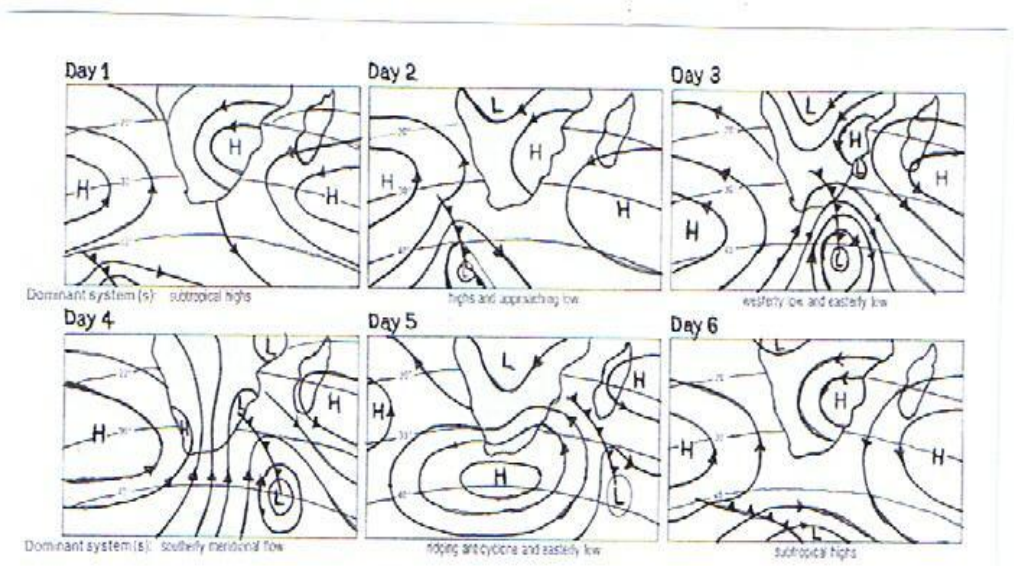

Figure 2.6:(a)-Weather disturbances over southern Africa (Day 1, subtropical highs; Day 2, highs and approaching lows; Day 3, westerly and easterly lows; Day 4, southerly meridional flow; Day 5, ridging anticyclone and easterly low; Day 6, subtropical highs.(Source: Tyson and Preston-Whyte, 2000).

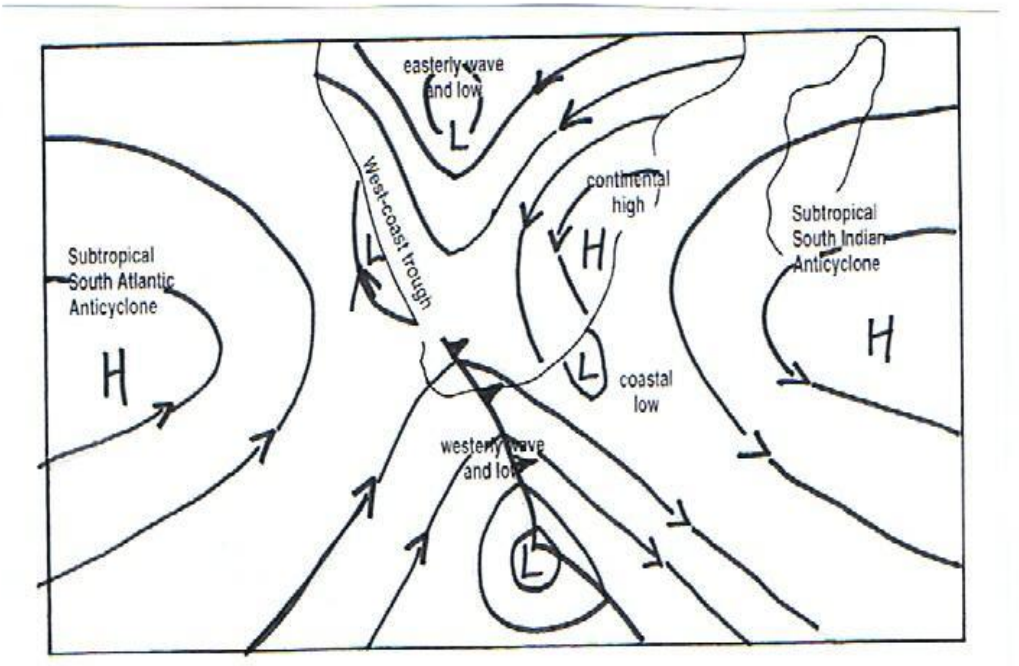

Figure 2.6(b)-Surface atmospheric circulation over southern Africa (Source: Tyson and Preston-Whyte, 2000).

these systems are the elements of the high-pressure belt that circles the southern hemisphere at about 30°S [Tyson and Preston-Whyte, 2000]. The pressure distributions and the wind regime over southern Africa are completely different in summer and winter [Triegaardt and Landman, 1992]. The subtropical high-pressure belt at sea level is displaced northwards by almost five degrees of latitude from summer to winter on both sides of the land [Tyson and Preston-Whyte, 2000; Potgieter, 2006].

2.4.1 Subtropical anticyclones

The intensity and position of the South Atlantic, Indian and South Pacific Ocean highs vary extremely during the entire year in the Southern Hemisphere. The subtropical highs are closest to the Equator during winter and are displaced poleward in summer (Fig. 2.7). The South Atlantic and Indian highs are shifted further west during the Southern Hemisphere winter [Palmén and Newton, 1969; Chang, 1972; Hastenrath, 1985]. The subtropical anticyclones are deep and are tilted upward from the surface towards the north-west in the upper level. They are associated with divergence in the near-surface wind field, strong subsidence throughout a deep layer, the occurrence of inversions, fine clear conditions and little or no rainfall [Tyson and Preston-Whyte, 2000].

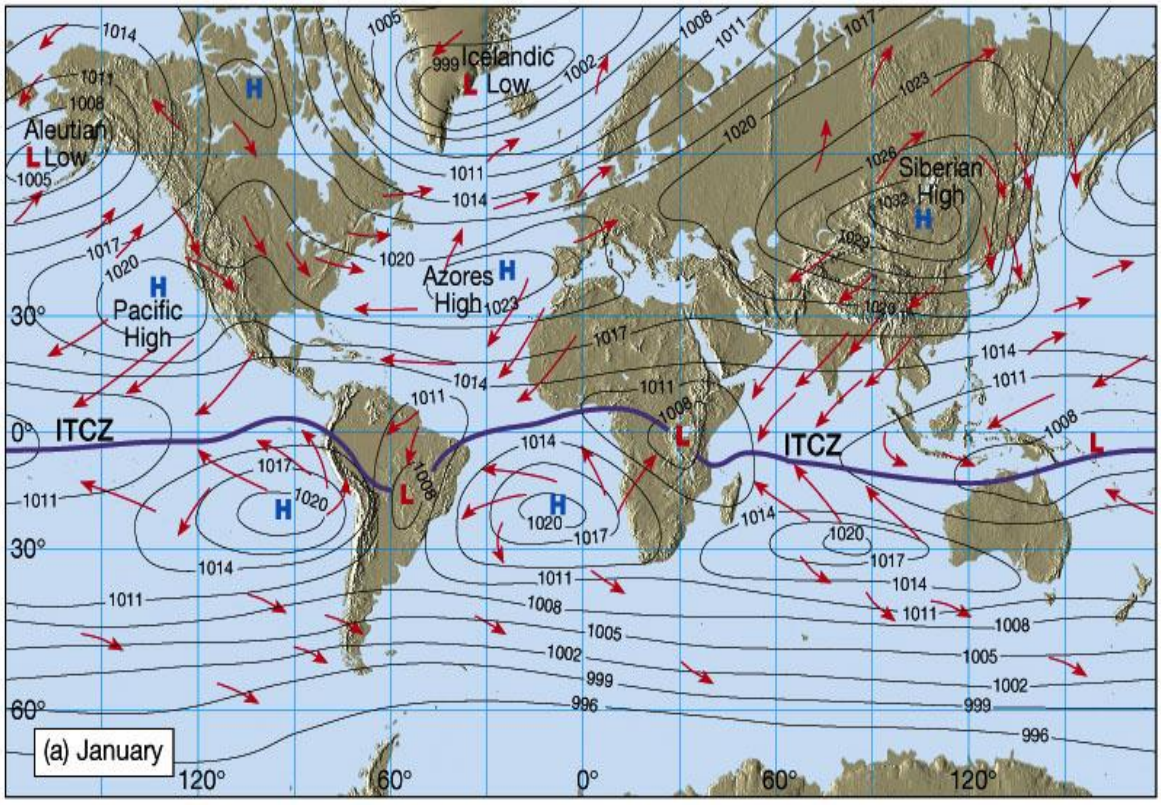

Figure 2.7: a) Southern shift of ITCZ in January (source: Lutgens and Tarbuck,2001)

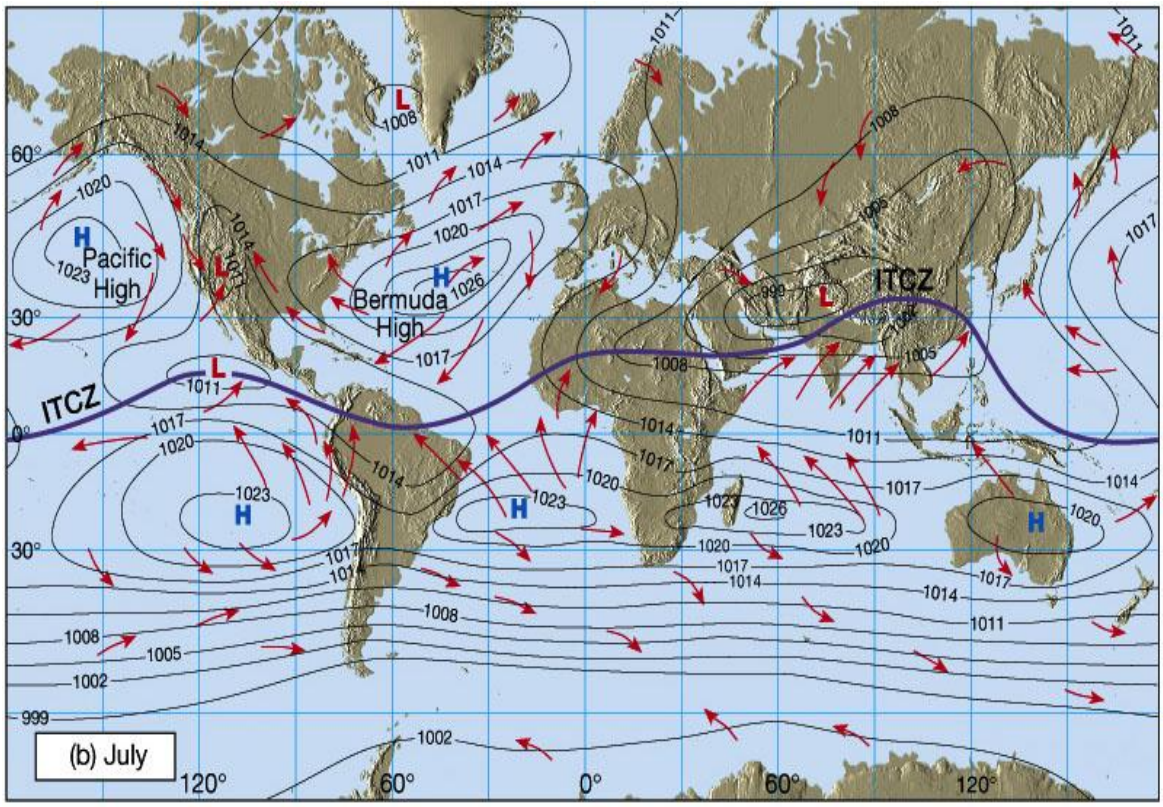

Figure. b) Northern shift of ITCZ in July. (source: Lutgens and Tarbuck,2001).

The continental highs are deepest and strongest in winter (June-July), during which they occur with a frequency of more than 70 per cent. In summer (December-January) their frequency falls to below 20 per cent. Secondly, Transient mid-latitude ridging anticyclones originate on the southern margin of the South Atlantic anticyclone and ridge to the east over the southern parts of southern Africa in the wake of traveling westerly disturbances. Their variability is minimal throughout the year and may occur with a frequency of 10-15 per cent, with slight maximum in the austral spring (September-October). When both types of anticyclonic circulation are averaged together, the high pressure cells are found to prevail on more than 80 per cent of all days in July [Tyson and Preston-Whyte, 2000].

In his comparison of the circulations of the hemispheres, Gibbs [1953] found significant differences in the distributions of cyclones and anticyclones. These differences are detailed in the results of Taljaard [1967], who described in detail the behavior of Southern Hemisphere synoptic systems. Southern Hemisphere anticyclones are more concentrated in subtropical latitudes at about 36°S in summer, 32°S in winter and 34°S in the intermediate seasons with smaller frequencies of closed anticyclones in higher latitudes. Cyclone centers are most numerous at 62-64°S. In summer peak frequencies occur at 22.5°S and 62.5°S, the former being due to heat lows over the land areas and tropical lows over the Pacific and Indian Oceans. The cyclones of the west wind belt move, on the average, towards east-southeast [Palmén and Newton, 1969; Hastenrath, 1985; Van Loon, 1965].

2.4.2 Westerly waves and cut-off lows

Westerly baroclinic disturbances may occur in the form of traveling Rossby waves or, more occasionally, cut-off lows. They exhibit little seasonal variation with a combined frequency of 20-30 per cent, showing a spring (October) maximum of occurrence, when the frequency reaches 40 per cent. In the region of southern Africa the passage of westerly wave disturbances occurs with a quasi-regular period of about 6 days [Tyson and Preston-Whyte, 2000].

Wave perturbations are important features of the westerlies and have been studied extensively [Tyson and Preston-Whyte, 2000]. Two major classes may be distinguished: large-scale semi-stationary forced waves tend to exhibit a barotropic structure and transient baroclinic disturbances are somehow steered by the semi-stationary waves and large-scale flow. These transient disturbances in the westerlies are responsible for most of the high frequency atmospheric variability over southern Africa [Kelbe, 1988].

Perturbations in mid-latitude westerly flow to the south of the subcontinent constitute the strongest regularly occurring disturbances affecting circulation over southern Africa. Westerly Rossby waves are always deep and tend to disturb the general anticyclonic circulation over the interior plateau, with an average height of about 1500 m. They often disturb the entire troposphere over the region. Cut-off lows are stronger and deeper and always perturb the troposphere from the upper westerlies down to the surface. All westerly disturbances are associated with steep pressure gradients and strong winds (Fig. 2.8), [Tyson *et al.*, 1996a; Taljaard, 1995a; van Heerden, 1987]. The westerly waves transecting the southern Africa subcontinent diminish in intensity as they propagate toward the north-eastern regions of South Africa [Kelbe, 1988; Tyson and Preston-Whyte, 2000].

The typical synoptic sequence associated with the development, maturity and decay of cut-off low systems (Fig. 2.9) has been described by Potgieter [2006]. They identified several stages during the life cycle of a typical cut-off low system. In the first stage a moderate upper air trough is situated just west of southern Africa with the high-level winds (300 hPa) all slightly north-westerly over South Africa. Over the ocean two surface systems are of importance. Firstly, a stronger than normal high pressure system typically situated south-west of the country, more or less located near Gough Island. Secondly, a cold front is typically nearing Cape Town. Over the land a trough or closed low is indicated over the western part of the plateau by the 850 hPa contours. Relatively warm, moist air flows from the north over the central and eastern parts. Along the coast, pressure falls significantly ahead of the cold front and rise to its rear. Light to moderate and at times heavy rainfall can occur along the south coast as onshore flow commences in the wake of the cold front.

The second phase is characterized by the intensification of the upper air trough. Over the western part of South Africa, winds in the upper-level are south-westerly while the winds elsewhere become north-westerly. At the surface the Atlantic high pressure system advances east-south-eastwards through 10 degrees of the longitude and cold air is advected in over the south western part of the country.

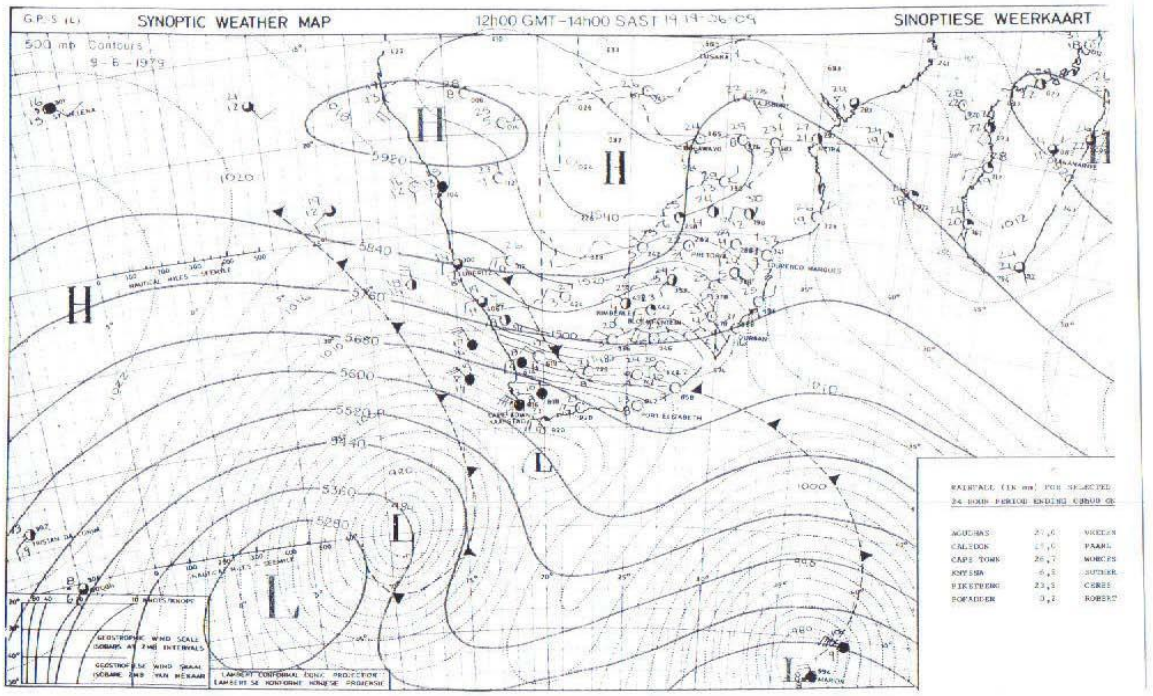

Figure 2.8: Typical westerly wave and a low type. Dotted lines indicate isobars at mean sea level (hPa) over the oceans and contours of the 850 hPa surface over land; heavy lines show contours of the 500 hPa surface (source: van Heerden,1987).

Strong west north-westerly to north-westerly winds occur over the northern parts of the country while south-easterly to north-easterly winds occur south of the centre of the cut-off low during its mature stage. Tyson *et al.* [1996a] showed that insignificant amount of air is transported from the interior of South Africa into the Atlantic Ocean by these systems; only recirculated air is transported to the west from the interior.

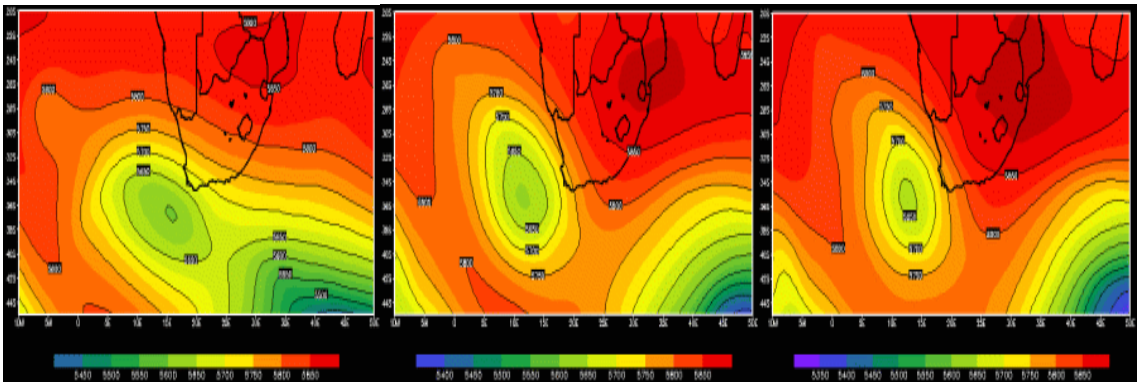

*Figure 2.9: Development of a cut-off low (source: **http://www.myweather.co.za**)*

2.4.3 Easterly waves

Easterly waves (Fig. 2.10) over southern Africa are barotropic semi-stationary waves [Tyson and Preston-Whyte, 2000]. An increase in intensity of the easterly flow must prevail throughout the entire troposphere for them to develop [Riehl, 1954]. This condition is seldom attained over the south-west Indian Ocean [Padya, 1984] because of the intrusion of westerly flow at upper levels [Lindesay and Jury, 1991]. Hence, the easterly waves over the south Indian Ocean are only a summer phenomena which occurs when the upper westerlies are situated further poleward [Potgieter, 2006]. Therefore, it is a disturbance in the tropical easterly flow which is driven largely by thermal heating of the continent and it is associated with the ITCZ, warm humid easterly flow, and an easterly jet. Over southern Africa they tend to be semi-stationary during summer occurring as open waves or closed lows [Tyson and Preston-Whyte, 2000].

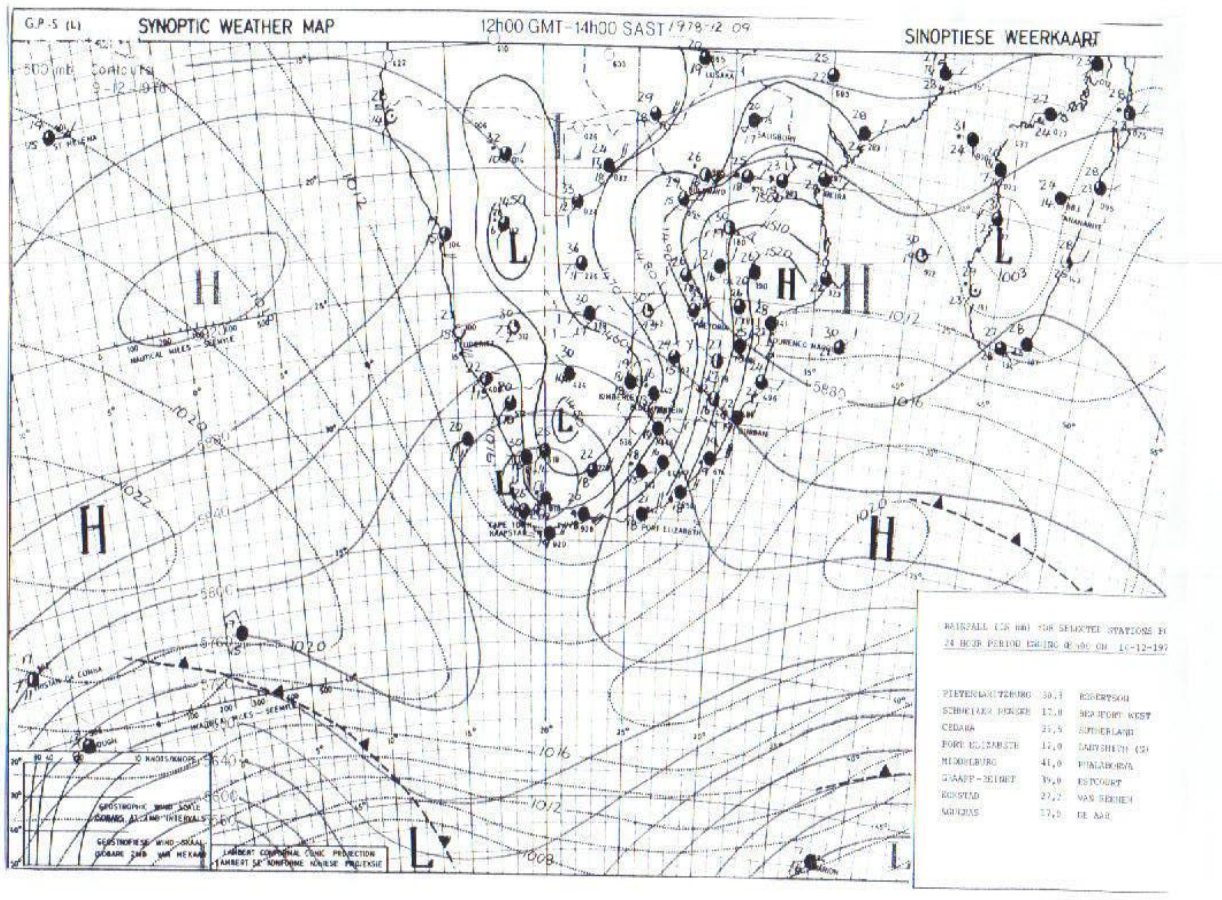

Figure 2.10: Typical easterly wave and an easterly low. Dotted lines indicate isobars at mean sea level (hPa) over the oceans and contours of the 850 hPa surface over land; heavy lines show contours of the 500 hPa surface (source: van Heerden,1987).

The warm Indian Ocean acts as moisture source. Convergence to the east of the trough produces strong uplift and good rains usually as thunderstorms. Divergence to west produces subsidence and no rain. The attenuation of transport is rapid. Only 8 percent of the air reaches 10° W at 850 hPa after 8.4 days. Easterly waves are strongly seasonal; absent in winter and peak between December and February, during which they strongly control precipitation over the interior of the country [Tyson *et al*., 1996a; http://www.myweather.co.za]. Some of the eastward flowing air recirculates back into the tropics in the tropical westerlies at about 5° S. Most of the recirculated air recurves anticyclonically to the south such that about 20 percent is transported in a westerly mean into the mid-latitudes across south-west South Africa [Tyson *et al*., 1996b].

2.4.4 Coastal lows and Berg winds

The coastal lows occurring over southern Africa (Fig.2.11) are shallow, mesoscale low-pressure disturbances that propagate eastwards around the subcontinent and whose distinct features arise from the interaction between the atmospheric stratification, the synoptic weather patterns and the topography of the region [Reason and Jury, 1990].

Coastal lows and Berg winds usually occur together and contribute significantly to the characteristic features of coastal and inland climates. Coastal lows owe their origin to the generation of cyclonic vorticity with the eastward movement of air off the high interior plateau. They are usually initiated on the west coast bringing north-westerly winds from the Western Cape Mountains to the south-western coast of the Western Cape Province [Tyson and Preston-Whyte, 2000].

Van Rooy [1936] and Jackson [1951] used weather elements such as temperature, pressure and humidity to aid them in identifying Berg winds, which they described as subsiding air moving off-shore that is associated with large-scale circulations. The winds are most common in late winter and early spring, and result in high temperatures being recorded in winter at coastal stations [Tyson and Preston-Whyte, 2000]. The easterly flow off Cape Point associated with a coastal low creates an alongshore gradient in wind flow which perturbs the atmospheric and oceanic thermal fronts from coastal alignment [Jury, 1987]. Behind the coastal low a strong onshore flow often develops. Such flow is generally west to south-west on the south-west coasts (e.g. Cape Point). These winds are often associated with rapid development of low clouds and fog. The temperature falls rapidly when the Berg winds are replaced with onshore flow [Hayward and Steyn, 1967; Schulze, 1965].

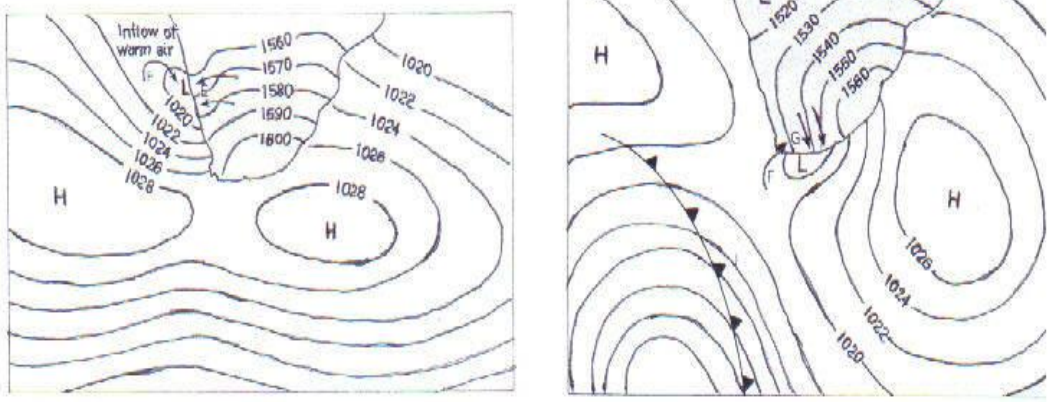

(a) Development of coastal low. *(b) Two days after the formation of low.*

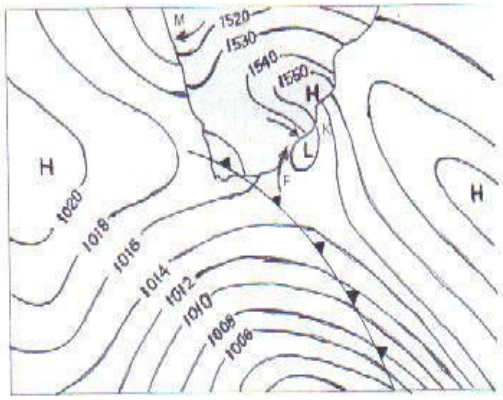

(c) Four days after the formation of low.

Figure 2.11: Basic movement of a coastal low (source: van Heerden, 1987).

2.5 Mesoscale and local wind circulations

Discontinuities in energy-balance or regimes lead to the generation of local winds. These discontinuities are often experienced along the shorelines of lakes or seas, between sloping surfaces and the air beyond, or between mountains and valleys [Tyson and Preston-Whyte, 2000]. The wind experienced at a particular site is influenced by a variety of factors at various times and geographical scales. Orographic effects, friction and pressure gradients play an important role in generating local winds [Hsu, 1988; Hunter, 1988; Schumann and Martin, 1991].

Mesoscale winds prevail in the form of land/sea breeze, mountain and valley breezes, anabatic winds, and katabatic winds. Differential heating is the root cause of land breezes and sea breezes. 0When the land is heated more intensely during the daylight hours than the adjacent body of water, it will result in the expansion of air above it, creating an area of low pressure. A sea breeze then develops, blowing cooler air off the water and onto the land. At night, the reverse may take place; the land cools more rapidly than the sea and a land breeze develops. The scale of land and sea breezes depends upon the location and the time of year [Jackson, 1954; Lutgens and Tarbuck, 1979; Bonnardot *et al*., 2005]. The wind speed and the inland penetration of cool marine air have significant impacts on coastal ocean currents, wind energy, as well as air pollution [Jury *et al*., 1993].

Land and sea breezes (Fig. 2.12) are a significant feature of the atmospheric circulation in sub-tropical latitudes and they may be the dominant winds. In the Cape Peninsula the strength of the sea breeze depends on the topography and the trend of the coastline; a light westerly breeze, not usually felt beyond ~8km from the shore, develops on the Atlantic side, while on the shores of False Bay an easterly breeze strengthens the south-easterlies (Fig. 2.13b). The Land breeze is characterized by north-easterly winds (Fig. 2.13a) in the morning [Jackson, 1954]. Bonnardot *et al* [2005] analyzed surface wind data for the Stellenbosch and Drakensberg districts in February, 1996-1998, which revealed that 30 to 64% of the wind directions, depending on the locations, were of maritime origin in the afternoon.

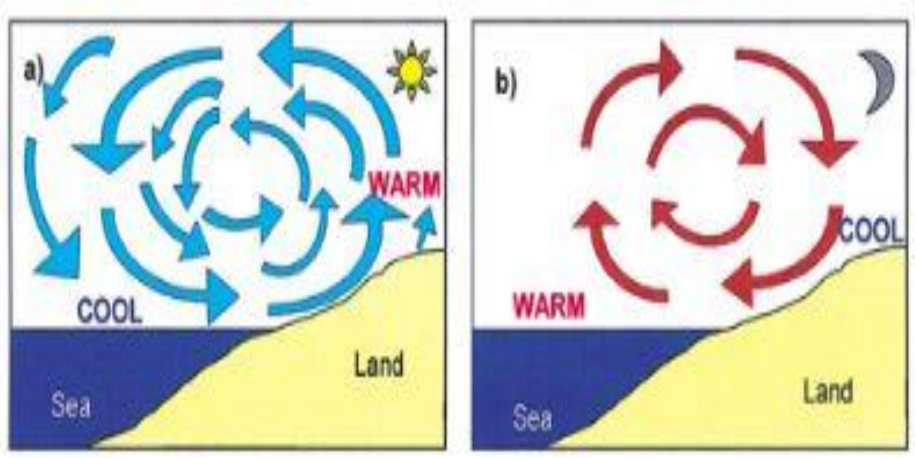

Figure 2.12 Sea (a) and land (b) breeze circulations (source: Bonnardot et al, 2005).

There was also a sudden change in direction from predominantly north and north-east (land origin) at night to predominantly west to south-west (sea origin) in the afternoon, accompanied by increase in wind velocity.

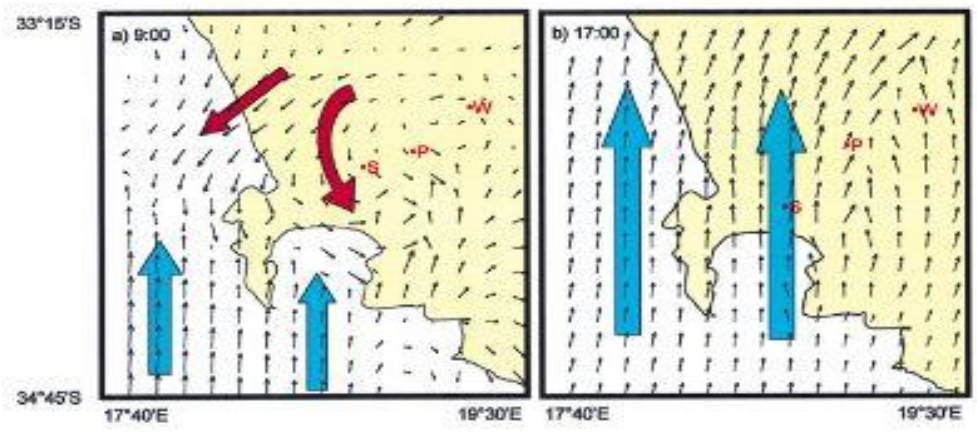

Figure 2.13 Surface wind vectors during February 2000 at (a) 09:00 and (b) 17:00 over the Cape (source: Bonnardot et al, 2005).

Varying conditions of topography produce a large variety of local winds. In mountainous areas, wind flows in response to temperature distribution and gravity. An anabatic wind is one that blows up an incline, usually as a result of surface heating [Lutgens and Tarbuck, 1979; Tyson and Preston-Whyte, 2000; http:/www.irbs.com].

2.5.1 Seasonal wind variation

The Western Cape experiences strong winds during the period from December to February. Over the Cape Peninsula and adjoining areas, south to south-east winds blow 60 per cent of the time, day and night. The wind speed and direction are modified by the topography. From False Bay to Cape Flats the wind direction is almost due south-east and veers more southerly in Cape Town. The south-easters are at times very strong and gusty. Inland, the winds are lighter and the directions are more variable than at the coast.

The period from March to May is a relatively calm season in most areas of the Western Cape region, except the Cape Agulhas which usually experiences strong winds at the beginning of autumn. Over the interior, winds are light in the morning but fresh in the afternoon, west and south-west are the main wind directions

From June to August the winds are influenced by the passage of frontal systems traveling eastwards. In the extreme south-western Cape the prevalent winds are strong north-westerly winds accompanied at times by low cloud and rain. Frequently, they reach gale force that can cause disasters.

The Cape Town weather is influenced by southerly to south-easterly winds in September to November, with wind speeds peaking during November [Schulze, 1965].

2.6 Summary

Chapter 2 provided a detailed literature review on weather patterns over southern Africa. It outlined types of weather systems affecting southern Africa ranging from global circulation systems to mesoscale and local circulations. These systems are responsible for transporting

different pollutants throughout the entire tropospheric column. Hence, a trajectory model will be used in trying to simulate air mass transport to the receptor site. The trajectories will then be clustered and the resulting cluster means will be used to interpret the reviewed weather systems.

CHAPTER 3

DATA AND METHODOLOGY

3.1 Introduction

This chapter expounds the general principles of trajectory modeling and provides details on the HYSPLIT model in particular which is used in trajectory calculations in this study. Model parameters and input and output data are also discussed. The chapter also outlines the trajectory cluster method and cluster analysis used in this study.

3.2 Trajectory Modeling

Trajectories simulate the paths followed by air parcels with time. Trajectory modeling is a useful tool for understanding the three-dimensional transport of airborne material in the atmosphere. It has been used in monitoring of long-range movement of natural aerosols, atmospheric pollutants and trace gases. Backward trajectories are particularly useful in tracing the origin of gaseous and particulate matter back in time and space [D'Abreton, 1996]. Air particle transport is more difficult to model in the boundary layer (BL) than in the upper troposphere or stratosphere due to significant amounts of moisture and the diabatic factors driving the growth and dissipation of the BL itself [http://www.arl.noaa.gov]. Three main methods are employed in the calculation of air parcel trajectories (kinematic, isentropic and isobaric approaches) [D'Abreton, 1996].

The kinematic approach uses the observed three dimensional wind velocity components to trace the movement of air parcels. The mass continuity is used when calculating the vertical velocity. Kinematic trajectories constructed in this way usually exhibit greater vertical displacements and undergo greater diabatic rates than is synoptically acceptable. Kinematic trajectory model uses terrain-following routine to overcome topographic obstacles. Depending on the type of meteorological data used, such as the European Center for Medium Range Weather Forecasts (ECMWF), kinematic trajectories were found to perfectly represent large-scale atmospheric motion. The kinematic model uses the explicit integration defined by:

$$x(t + \Delta t) = x(t) + V[x(t)]\,\Delta t \qquad (1)$$

where $x(t + \Delta t)$ is the new three dimensional parcel position at $t + \Delta t$. $x(t)$ is the old position and $V(t)$ is the parcel velocity vector [D'Abreton, 1996].

The isentropic approach uses the same methodology as its kinematic counterpart. The vertical velocity is replaced by potential temperature when constructing isentropic trajectories. The potential temperature is then conserved to compute the pressure (and hence height) field of the air parcel. Subsequently, the two-dimensional adiabatic flow comprises of the vertical motions that normally would have been calculated separately. The same initial conditions as in kinematic trajectories are used in the interpolation of isentropic trajectories. The potential temperature (θ) is calculated from equation 2 below

$$\theta = T(1000/P)^{0.286} \quad (2)$$

where T is the interpolated temperature at selected start pressure P. The parcel is advected along the isentropic level using equation (1).

The isentropic approach has major limitations in that it operates on the assumption that the atmosphere is cloud and rain-free. Hence the model is best suited for use over subtropical southern Africa during the dry, cloud-free winter months and must be used with caution at all times [D'Abreton, 1996].

The isobaric approach ignores the vertical direction that an air parcel movement can take. The model assumes that air particle motions take place on surfaces of constant pressure. The horizontal levels are interpolated to the prescribed pressure levels. Under a strongly baroclinic condition, the model gives large errors that are not encountered in three dimensional models [Lee *et al.*, 1997].

3. 3 HYSPLIT model

3.3.1 Background

Trajectory models are mathematical tools used in studying relations between source and receptor locations [Collett and Dyuyemi, 1997; Zannetti and Puckett, 2004]. Among them, the Hybrid Single-Particle Lagrangian Integrated Trajectory (HYSPLIT) [Draxler and Hess, 1998] model is a commonly used air transport modeling program that is capable of constructing the air mass pathways from one region to another. The HYSPLIT model is a (hybrid between the Lagrangian approach which considers moving frame of reference as the air parcel moves from its initial location and Eulerian approach in which the three-dimensional is used as a frame of reference) complete system that is designed to compute a wide range of simulations related to the regional or long-range transport, dispersion, and deposition (wet and dry) of air pollutants [Anastassopoulos *et al*, 2004]. The HYSPLIT model output varies from simple air parcel trajectories to complex dispersion and deposition simulations [NOAA, 1999]. The trajectory calculation (which forms the basis of this study) is achieved by time integration of the position of an air parcel as it is transported by the 3-D winds [Draxler and Hess, 1997]. Source locations can be identified by analyzing air mass back trajectories arriving at a receptor site at a particular time [Poissant, 1999; Hsu *et al*., 2003; Anastassopoulos *et al*., 2004].

The use of HYPSLIT as operational tool can be a time-intensive and resource-intensive, therefore, the air transport modeling remains a combination of human operator effort (e.g., manual model setup and input) and computer processing effort. The analysis of graphical trajectory plots generated by HYSPLIT's trajectory module is basically a manual operation. It is therefore of importance to limit the number of modeling runs to a value that will achieve satisfactory and statistically significant results; since a lower modeling resolution (i.e. fewer runs) translates directly into potential time and money savings [Anastassopoulos *et al*., 2004].

In air transport climatology, meteorological data are used in combination with an analysis model to further interpolate data over time and space to model air mass transport. The HYSPLIT model was chosen as an analysis tool to be used in this research project because of its ability to model long-range transport of air particles. The model is available for online use through the NOAA website (http://www.arl.noaa.gov/ready/hysplit4.html), using archived meteorological data or through a PC downloadable version, which allows a user to perform more advanced and more configurable analysis [http://www.env.wustl.edu].

3.3.2 Meteorological data fields

The HYSPLIT model cannot directly use the meteorological data recorded across the globe. Meteorological models are then used to interpolate the data into grids. The modeled meteorological data are created at various degrees of resolution to maintain a larger degree of flexibility within the trajectory model. The meteorological data files are then used as input to an internal trajectory model terrain-following (σ) coordinate system [NOAA, 1999; http://www.env.wustl.edu],

$$\sigma = (Z_{top} - Z_{msl}) / (Z_{top} - Z_{gl}), \quad (3)$$

where the heights are expressed relative to mean-sea level and the top of the trajectory model coordinate system is denoted by Z_{top}. The internal heights (within the model) above ground level are chosen at any interval, however a quadratic relationship between height (z) and model level was specified, such that each level's height with respect to the model's internal index, k, [NOAA, 1999] is defined by

$$z = ak^2 + bk + c, \quad (4)$$

where a=30, b=-25, and c=5. Equation 4 results in diminishing resolution away from the surface, with the first level (k=1) at 10 m, the second level at 75 m, the third at 200 m, while by the 20^{th} level, at 11500 m, with the difference between levels being about 1200 m. The user can specify the vertical resolution which depends on the constant in Eq. (4) [NOAA, 1999].

Taylor [1997] deduced that the trajectory model's horizontal grid system is designed to be identical to that of the meteorological data. He used a set of universal mapping transformation routines to project Polar Stereographic, Mercator and Lambert Conformal maps.

Meteorological data fields are provided in four different vertical coordinate systems depending on the type of operation undertaken such as pressure-sigma, pressure-absolute, terrain-sigma, or a hybrid absolute-pressure-sigma. These operations are carried out at ECMWF (European Centre for Medium-Range Weather Forecasting). The minimum requirements for the model are U, V (the horizontal wind components), T (temperature), Z (height) or P (pressure), and the pressure at the surface, P_0. There are optional parameters such as moisture and vertical motion. However, the vertical motion is computed based upon the type of vertical coordinate chosen [NOAA, 1999].

The model can also run with multiple nested grids and there is a utility program that can be used to display and manipulate the meteorological data. There's a built-in software designed for converting MM5 (The Fifth-Generation Mesoscale Model), RAMS (Radiation Measurement System), COAMPS (Coupled Ocean Atmosphre Mesoscale Prediction System) and other data into a format suitable for input to HYSPLIT model [http://www.arl.noaa.gov].

3.3.3 Model definition

The HYSPLIT model has evolved over several stages since its inception in 1982. During its early stages, only rawinsonde observations were used with the assumption that a uniform mixing exist during the day and no mixing at night [Draxler and Taylor, 1982]. Draxler and Stunder, [1988] modified the model by replacing the rawinsonde meteorological input data with gridded meteorological data from either analyses or short-term forecasts from routine numerical weather prediction models. All the equations used in the computation of the vertical mixing height have been revised in recent literature [HYSPLIT_3 - Draxler, 1990; 1992]. The model has recently been modified to include features such as terrain correction for starting heights above mean sea level, mixed layer depth computed from minimum temperature, integrated solution of the source-receptor matrix and automated source attribution configuration from measured data.

An air mass trajectory can be thought of as a path along which an air particle traveled through space. The path is then plotted on the map as a series of joined points with known X and Y coordinates along the longitude and latitude lines. The time intervals between the points is fixed and it indicates either forward or backward motion. The particle's movement in space is calculated by averaging the three-dimensional velocity vectors for an initial position P(t) and the first-guess position P'(t+Δt) [Draxler and Hess, 1997; 1998]. The differential trajectory equation is given by

$$dP/dt = V[P(t)]. \quad (5)$$

Expanding P(t) in a Taylor series about $t = t_0$ evaluated at $t_1 = t_0 + \Delta t$; and about $t = t_1$ evaluated at $t = t_0$ [Draxler and Hess, 1997; 1998], results in the first-guess position given by

$$P'(t+\Delta t) = P(t) + V(P,t)\,\Delta t \quad (6)$$

and the final position is

$$P(t+\Delta t) = P(t) + 0.5[V(P,t) + V(P', t+\Delta t)]\,\Delta t. \quad (7)$$

Equation (7) gives inaccurate results when applying higher order methods. Hence, the second order method is employed to give accurate results.

3.3.3.1 Auto Trajectory Generator (ATG)

A Visual Basic program (Auto Trajectory Generator) is built within the trajectory model to automate the creation of HYSPLIT trajectory output files. The HYSPLIT trajectory modeling executable is fast and stable, however, the user interface is very complicated. The inflexibility of the output format and the inability to generate a large number of trajectories at once limit the HYSPLIT model's performance [NOAA, 1999; http://www.env.wustl.edu].

3.3.3.2 Automatic Trajectory Generation

The HYSPLIT model's current version is designed to create single to multiple simultaneous trajectories. The Auto Trajectory Generator (ATG) affords the user an option to choose from different approaches such as isentropic, isosigma, isobaric and isopycnic. The model can also output meteorological variables along the trajectory path [NOAA, 1999; http://www.env.wustl.edu; http://www.arl.noaa.gov].

3.3.3.3 Output Formats

The text output file created by the HYSPLIT trajectory model can be used as an input file (text delimited) to ArcCatalogue to create maps using ArcMap [NOAA, 1999]. The maps can then be exported as jpeg as was the case in this study.

3.3.4 Trajectory Robustness Analysis

The error associated with current HYSPLIT trajectory generation is in the range of 15-30% and depends on the distance the trajectory traversed. The model's inability to highlight the relative error associated with each trajectory generated, limits the user from drawing stronger conclusions from analysis of results.

3.4 Trajectory database

Backward air trajectories arriving at Cape Point were calculated using the Web version of the Hybrid Single Particle Integrated Trajectory (HYSPLIT-4) model (http://www.arl.noaa.gov/ready/open/traj.html). This model is employed in the computation of air mass trajectories and complex dispersion and deposition simulations [Draxler and Hess, 1997, 1998]. Meteorological data fields to run the model are available from archives. In this study, 5-day back trajectories were calculated at two different heights (300 and 5000 agl) using reanalysis data from the National Center for Environmental Prediction (NCEP) and the National Center for Atmospheric Research (NCAR) available from National Oceanic and Atmospheric Administration's (NOAA) Air Resources Laboratory (ARL) archives. The reanalysis data covers the globe from 1948 to the present with a horizontal resolution of about 2.5 x 2.5 degrees latitude-longitude and with an output every 6- hours.

Several authors such as Kahl and Samson [1986], Haagenson *et al.* [1987] and Draxler [1987] investigated uncertainties in trajectory models due to interpolation of sparse data. The main errors were due to the numerical inaccuracies during computation (integration error), data's misrepresentation of the atmosphere (resolution error) and the measurement error encountered when creating the meteorological model data. Kahl *et al*. [1997] also encountered model errors such as the observational or analysis errors and the bias that can result from the trajectory model's approximation of the real atmosphere.

Kinematic 3D trajectories were employed in this study following the suggestion of several authors about the major accuracy of these trajectories in comparison to all the other approaches (isentropic, isobaric) when accurate fields of vertical wind are available [Martin *et al*. 1990; Draxler, 1996; Stohl and Seibert 1998]. A recent review on computation and applications of trajectories was provided by Stohl [1998]. The length of the back trajectories depends entirely on the distances between source regions and the receptor location. The arbitrary choice of 5-day back trajectory duration is a compromise between the ambition to identify distant source and sink regions and to limit the uncertainties in the trajectories. Stohl [1998] affirmed that errors of 20% of the distance traveled seem to be typical for trajectories computed from analyzed wind fields. Freiman and Piketh [2003] in their study of 4-day backward trajectories to determine air transport into and out of the industrial Highveld region of South Africa, found four major transport pathways originating from the Atlantic Ocean, the Indian Ocean, subtropical Africa, and over southern Africa.

In this study, an attempt was made to describe the flows reaching the middle troposphere, the low free troposphere and the upper boundary layer by computing 5-day, 300- and 5000-agl kinematic back trajectories for Cape Point once a day (12:00 UTC~14:00 SAST) for the period 2001-2003. The average station height at Cape Point is 230m above mean sea level, so tropospheric transport in a climatological sense should be well represented by trajectories at these levels. The 5-day trajectory duration was chosen to facilitate the identification of potential upwind source regions. In total, 6% and 8% of the trajectories (300- and 5000 agl respectively) were unavailable for analysis or were incomplete because of gaps in the meteorological data archive or due to trajectories leaving the model domain. Model parameters and a summary of the trajectory data base are given in Tables 3.1 and 3.2 below.

Table 3.1 Model parameters used for all runs

MODEL PARAMETER	SETTING
Meteorological dataset	NCEP/NCAR 2.5 degree latitude-longitude
Trajectory direction	Backward
Total run time (trajectory duration)	120hr
Start point	Cape Point (34.21ºS, 18.29ºE)
Start time	12:00 UTC (14:00 SAST)
Start height1	300m agl (~ 975 hPa)
Start height2	5000m agl (~ 550 hPa)

Table 3.2 Summary of 5-Day, Once-Per Day Back Trajectory Data Used

Year	300m-agl Back Trajectories		5000m-agl Back Trajectories	
	N	% Availability	N	% Availability
2001	325	89	337	92
2002	351	96	334	92
2003	356	98	335	92
	Total=1032	**Average=94**	**Total=1006**	**Average=92**

Missing data are due to gaps in the meteorological data archive or trajectories leaving the model domain. N is the number of trajectories available for clustering.

3.5 Trajectory clustering analysis

3.5.1 Background

Anderberg [1973], Everitt [1980] and Harris [1992] defined cluster analysis as a multivariate statistical technique designed to explore the structure within a dataset. It is often described as an objective classification method, however, Stohl [1998] found this to be untrue since the selection of the clustering algorithm, the specifications of the distance measure and the number of clusters used are subject to user's specification [Stohl 1998]. With the existence of many different clustering algorithms, there is also much variation in the computational requirement for interpretation of the data. Historically, the wind sector approach was employed in the construction of long-range transport climatologies in which trajectories are grouped according to compass sector [Miller, 1981]. This method proved to be unsatisfactory in that the groupings are arbitrarily chosen and also because trajectory curvature is ignored. Traditional synoptic classification schemes used for transport climatology studies also fall short because they are unable to account for the time evolution of the wind field, information which is contained within the trajectory data [Yarnal, 1993; Kahl *et al*., 1997].

Cluster analysis emerged towards the end of the 1980s as a valuable mathematical tool to be applied to meteorological data [Kalkstein *et al*., 1987]. Moody [1986] and Moody and Galloway [1988] were the first to perform studies using cluster analysis with atmospheric trajectories. They applied clustering techniques to interpret trajectory and precipitation chemistry data. Several authors applied the same technique to analyze the influence of atmospheric transport patterns on pollutant concentrations applying trajectory clusters [e.g., Moody and Samson 1989; Moody *et al*., 1995; Dorling *et al*. 1992a, b; Dorling and Davis 1995; Brankov *et al*., 1998; Avila and Alarcón 1999; Cape *et al*., 2000]. In principle, cluster analysis results are similar to those of flow climatology, but the former technique is more objective and accounts for variations in transport speed and direction simultaneously, yielding clusters of trajectories that have a similar length and curvature [Stohl 1998]. Harris and Kahl [1990] and Harris [1992] derived flow climatology for the Mauna Loa Observatory in Hiloa, Hawaii, and the South Pole, respectively, clustering a large

number of back trajectories. Calvo [1993] and Petisco and Martín [1995] developed synoptic climatology by clustering surface pressure and constructing geopotential maps. Ribalaygua and Borén [1995] obtained a synoptic classification by clustering precipitation patterns. Martín-Vide [2001] found some weakness in the methodology used by Jenkinson and Collison [1977] and Spellman [2000] in their attempt to automate synoptic classification.

3.5.2 Cluster method

In this study cluster analysis was performed using the HYSPLIT_4 model (windows-based HYSPLIT). The model uses Ward's method described by [Romesburg, 1984], Moody and Galloway [1988] and Stunder [1996]. Sodemann [2000] normalized three-dimensional trajectory position prior to clustering, and Eneroth *et al*. [2003] used the spherical distance between trajectory points.

The Ward's method is described as follows. The trajectory endpoints in Ward's method are used as cluster variables representing wind speed and direction. If N represents the number of trajectories, then each trajectory will initially be defined with a zero spatial variance, where the cluster spatial variance is the sum of the squared distances between the trajectory endpoints. The aim of this process is to combine the neighboring clusters that will result in the minimum increase in total spatial variance (TSV), where TSV sums all the cluster spatial variances. This process continues until all trajectories have merged into one cluster [Stunder, 1996].

The TSV increases sharply in the initial stages of clustering, and then the rate of increase drops until it becomes constant (at a point called a breaking point) before it starts to rapidly increase again. The sudden increase in TSV is an indication that dissimilar clusters are being combined. Hence, the clustering process should be terminated at that point [Stunder, 1996].

There are few selectors that limit the number of clusters per run. The meteorology also plays an important role in selecting the number of clusters. A minimum value should be set to limit the number of clusters from declining to one. The number of trajectories being clustered should not be too small to avoid TSV scatter with no defined break point. Hence, the resulting numbers of clusters L are kept if the following criteria are met: $3< L<10$, at least 30 trajectories are clustered, and the rate of increase of the percent change in TSV at the break point must be at least 30%. The upper limit of 10 clusters may be too high for a small sample size, that is, near the lower limit of 30, but these criteria give quite reasonable results [Stunder, 1996].

3.5.3 Cluster analysis

When performing cluster analysis, it is necessary to decide how many clusters are needed to adequately describe the data. The criteria for this decision depend on the analysis goal. When long-range transport climatology is the ultimate goal, as is the present study, cluster analysis may be used as an analysis tool to provide a descriptive summary of a trajectory data set [Harris and Kahl, 1990]. With this goal, a robust method for determining the optimal number of clusters is unnecessary. Rather, only a specific number of clusters which can reveal the meaningful structure (i.e., coherent patterns) in the data will be chosen.

The goal of previous meteorological studies in which cluster analysis was employed [Fernau, 1988] has largely been to search for "natural' clusters in the data, a procedure demanding rigorous validation of the data and a robust method for determining the true number of clusters. In this study there is a related but different purpose of providing a descriptive climatology of a 3-year data set, using cluster analysis as a tool to discover meaningful structure in the data. Ward's method was used to help in deciding the number of trajectory clusters to create. This procedure indicated that airflow characteristics to Cape Point may be best described by two to five clusters. Five clusters were chosen for each set of model runs because this number was sufficient to identify all major flow patterns, as well as several less common but nonetheless important patterns.

Once the number of clusters had been decided, Quick Cluster (Run) was chosen as the technique to produce clusters for the total data set. Quick Cluster has the advantage that cluster membership can change, allowing the cluster centres to migrate to a locally optimal solution. A practical advantage of Quick Cluster is its ability to accommodate a large volume of data.

The variables clustered were the latitude and longitude of trajectory segment endpoints at 12-hour intervals along each 5-day back trajectory. Thus each data vector, or case, consisted of 40 elements: 20 consecutive latitude and longitude pairs that describe the wind speed and direction along the full extent of each trajectory.

To summarize the air flow climatology to Cape Point, all 5-day back trajectories were clustered for the years 2001-2003 at once. The procedure was performed separately for 300 m and 5000 m trajectories. Cape *et al*. [2000] emphasized that the analysis of the 3-year data can conceal significant differences in the pattern of clustering as a function of season and year. Hence, the above cluster analysis was repeated for each year independently, and for each of the four composite seasons using data over the full 3-year period. Seasons were defined as: December-February (summer), March-May (autumn), June-August (winter) and September-November (spring).

In this procedure, individual trajectories were averaged to produce "cluster-mean" trajectories. Thus the large data base was reduced to a number of cluster-mean plots that can be interpreted in terms of known weather systems. For each cluster, ensemble plots of all individual trajectories belonging to that cluster were produced. These ensembles or "cluster membership" plots were used to validate the mean and to assess the variability within the cluster itself.

Trajectory analysis is used as an indication of the general airflow rather than the exact pathway of an air parcel. Hence, a large number of trajectories were analyzed to reduce the effects of individual errors so that a reasonable representation of airflow to Cape Point is presented.

CHAPTER 4

RESULTS AND DISCUSSION

4.1 Introduction

This chapter presents the results obtained by applying Ward's method of trajectory clustering to the trajectory database with back trajectories originating at 300 and 5000 m agl. The clustering method produced a cut-off of 5 clusters at each level. The cluster results are summarized in Tables 4.1 and 4.2. The results are discussed as follows. Firstly, the identified flow patterns for the entire record at both levels are characterized, followed by the inter-annual patterns and lastly the seasonal patterns. Then the flow patterns are analyzed to establish their relationship to weather patterns over southern Africa.

Table 4.1a: Number of trajectories within each cluster[a] for the total data period, individual years and seasons.

Cluster Number	2001-3	2001	2002	2003	DJF 2001-3	MAM 2001-3	JJA 2001-3	SON 2001-3
1	249	104	86	106	101	91	61	42
2	146	56	70	102	60	76	63	87
3	219	75	45	47	40	34	56	66
4	323	61	60	83	13	29	62	31
5	186	29	90	18	24	40	24	32
Total	1123	325	351	356	238	270	266	258

[a]5-day back-trajectories at 300m agl at Cape Point (34.21S, 18.29E). DJF (Summer), MAM (Autumn), JJA (Winter) and SON (Spring)

Table 4.1b: Percentage of trajectories within each cluster[b] for the total data period, individual years and seasons.

Cluster Number	2001-3	2001	2002	2003	DJF 2001-3	MAM 2001-3	JJA 2001-3	SON 2001-3
1	24, N	32, W	24, SW	30, NW	42, W	33, W	23, SW	16, NW
2	14, SE	17, NE	20, SW	29, S	25, SE	28, NE	24, W	34, SW
3	21, NW	23, SW	13, NW	13, NE	17, W	13, SW	21, NW	26, SW
4	23, SW	19, SE	17, SW	23, SW	6, SW	11, SE	23, NE	12, SE
5	18, SW	9, W	26, SE	5, SW	10, SE	15, SW	9, SE	12, SW

[b]5-day back-trajectories at 300m agl at Cape Point (34.21S, 18.29E), with source direction indicated as (N, NW, NE, SW, SE, S, and W). DJF (Summer), MAM (Autumn), JJA (Winter) and SON (Spring)

Table 4.2a: Number of trajectories within each cluster[c] for the total data period, individual years and seasons.

Cluster Number	2001-3	2001	2002	2003	DJF 2001-3	MAM 2001-3	JJA 2001-3	SON 2001-3
1	196	80	101	93	79	36	59	88
2	262	85	90	92	62	71	65	70
3	274	109	43	47	34	32	59	29
4	154	23	75	31	39	62	28	42
5	120	40	25	72	41	51	39	20
Sum	1006	337	334	335	255	252	250	249

[c]5-day back-trajectories at 5000m agl at Cape Point (34.21S, 18.29E). DJF (Summer), MAM (Autumn), JJA (Winter) and SON (Spring)

Table 4.2b: Percentage of trajectories within each cluster[d] for the total data period, individual years and seasons.

Cluster Number	2001-3	2001	2002	2003	DJF 2001-3	MAM 2001-3	JJA 2001-3	SON 2001-3
1	20, W	24, W	30, NW	28, NW	31, NW	14, W	24, NW	35, NW
2	26, W	25, NW	27, NW	27, NW	24, NW	28, N	26, NW	28, NW
3	27, NW	32, NW	13, W	14, NW	13, N	13, NW	24, NW	12, NW
4	15, NW	7, W	22, NW	9, N	16, W	25, NW	22, W	17, NW
5	12, W	12, N	8, NE	22, W	16, W	20, NW	15, NW	8, W

[d]5-day back-trajectories at 5000m agl at Cape Point (34.21S, 18.29E), with source direction indicated as (N, NW, NE, SW, SE, S, and W). DJF (Summer), MAM (Autumn), JJA (Winter) and SON (Spring)

4.2 Cluster Characterization

Cluster analysis has established five principal patterns of air flow features to Cape Point. Five clusters were chosen because it was a 'break point' selected by the HYSPLIT model based on the total data set, and any number above five would combine dissimilar clusters. The cluster mean plots contain the following information: (1) the mean trajectory for each cluster with a square, circle or arrow signs indicating 12-hour upwind intervals which are also indicated at the bottom of the figures; (2) the colour coding representing different clusters are; red (cluster1), blue (cluster2), light green (cluster3), turquoise (cluster4) and pink (cluster5) . The cluster numbers are used for identification purposes only and have no inherent significance. Tables 4.1 and 4.2 show the number of trajectories clustered and the percentages within each cluster, for the 300 and 5000 m heights respectively. The descending plot at the bottom of the cluster means plot indicates the average trajectory height above ground level (agl) at each time step. The cluster means represent the average flow of the complete back trajectory group. Therefore, a general description of the main transport features of a cluster can be achieved by examining its mean

[Jorba *et al*, 2004]. The cluster membership plots show all trajectories within each cluster mean, and indicate the variability within a given cluster.

4.3. Cluster analysis results for the entire data record (2001-2003)

4.3.1 300 m level mean trajectories

Figure 4.1 shows cluster means at 300 m agl while Figure 4.2a-e shows cluster membership plots at the same level determined from kinematic trajectories for the three year period of study (2001-2003). The dominant 300 m transport regimes from January 2001 to December 2003 include south-easterly flows (cluster 2) originating in the south-west downwind with moderate wind speeds, southerly flows (cluster 4) also with a south-westerly origin and moderate wind speeds, south-westerly flows with fast moving winds (cluster 5), westerly flows (cluster 3) with a north-westerly origin and moderate wind speed, and slow moving north-westerly flows (cluster 1). The slow moving mean cluster (cluster 1) requires consideration of the corresponding membership plots (Fig.4.2). These flows are mainly regional recirculations over a relatively limited area. Cyclonic conditions can cause air masses to recirculate over a zone for several days [Millán *et al*, 1997].

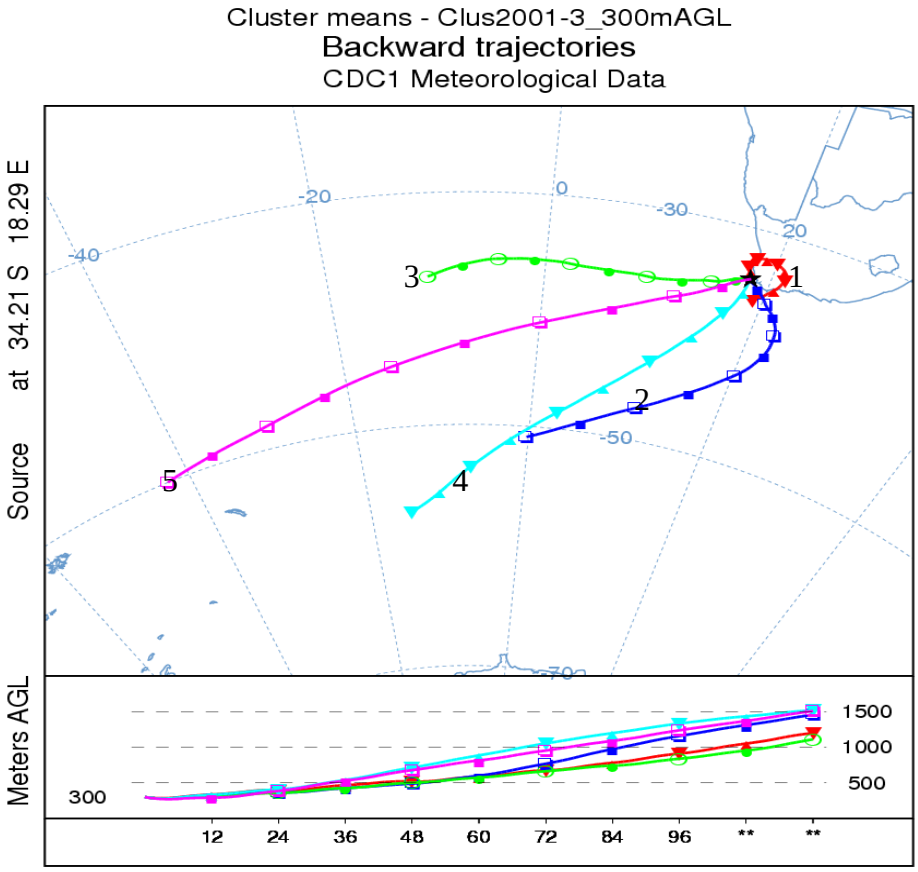

Figure 4.1: Cluster mean plots at 300 m for 2001-2003

Table 4.1a shows the number of trajectories in each cluster obtained with Ward's method, with a cut off size of 5 clusters. Table 4.1b presents the corresponding percentages in each cluster for the three year back trajectory database. The anticyclonic flows (cluster 1) account for 24% of the data, representing 5-day transport well within the southern Africa region as shown in the cluster membership plot (Fig. 4.2a). This transport regime was recognized by Tyson *et al* [1996] using forward trajectories to illustrate scales of recirculation occurring at different levels from different localities of origin. There are three clusters originating from the south-west (clusters 2, 4, and 5). These clusters account for a total of 55% of the data. The westerly flow (cluster 3) accounts for 21% of the total data. Cluster 2 occurs with a frequency of 14%, and approaches the measuring site from the south-east with slow moving winds. Cluster 3 with 23% of the trajectories approaches Cape Point from the south. And finally, cluster 5 presenting 18% of the trajectories approaches from the south-west with moderate wind speeds.

All clusters show a similar arrival height below 500 m agl within the 24 hour period prior to arrival. Differences are noted 48 hours downwind where clusters 1, 2 and 3 are at 500 m agl and clusters 4 and 5 are at about 700 m agl. Cluster 2 deviates in height from both cluster 1 and 3 from 60 hours downwind and starts aligning to clusters 4 and 5 from 96 hours downwind. Clusters 2, 4, and 5 originate at about 1500 m agl, with cluster 4 at a slightly higher level than cluster 5 followed by cluster 2. Cluster 1 originates at about 1250 m agl while cluster 3 shows an origin of about 1100 m agl (Fig. 4.1).

Cluster-membership plots Figure 4.2 a-e corresponding to cluster means 1 to 5 (Fig. 4.1) were examined to establish the variability within each cluster. The membership plots clearly indicate substantial variability within each cluster. The cluster means show a clear representation of the individual trajectories irrespective of their variability. The solid line enveloping the cluster-membership plots indicates the geographical area traversed by the individual trajectories.

Figure 4.2a indicates widespread slow moving back trajectories traversing over countries in southern Africa and the South Indian and South Atlantic Oceans. These trajectories can transport a mixture of clean air from the ocean and polluted air from the main land. Figure 4.2b shows cluster membership trajectories with moderate wind speed veering from the south-west to the south-east of Cape Point. Cluster-membership trajectories in Figure 4.2c veer from westerly to north-westerly direction and approaches the Cape Point with moderate wind speed, while those depicted in Figure 4.2d veer from south-westerly to south south-westerly. Finally, Figure 4.2e depicts fast moving cluster-membership trajectories from the south-westerly.

Figures 4.2a, b and e indicate great variability of trajectory movement as compared to Figures 4.2c and e which indicate moderate wind variability.

Figure 4.2a: Cluster 1 membership plots at 300m for 2001-2003

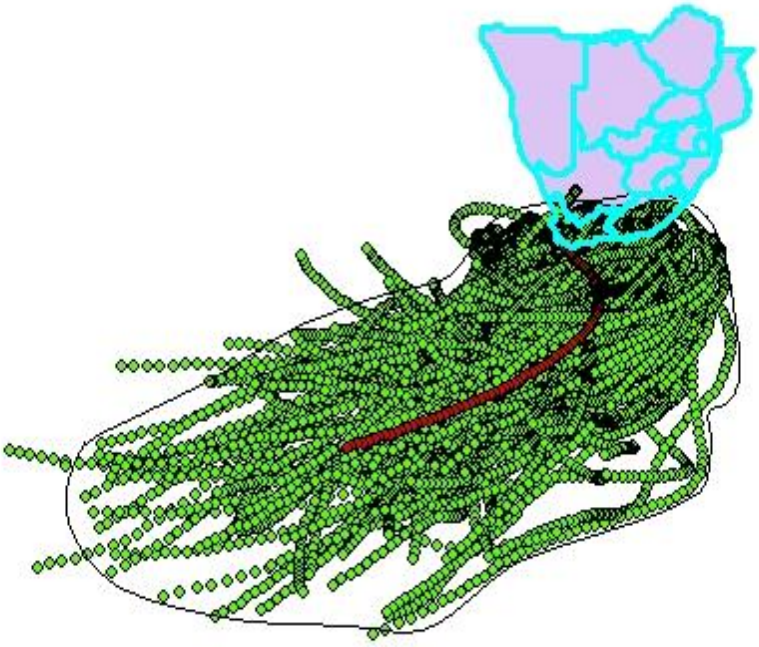

Figure 4.2b: Cluster 2 membership plots at 300m for 2001-2003

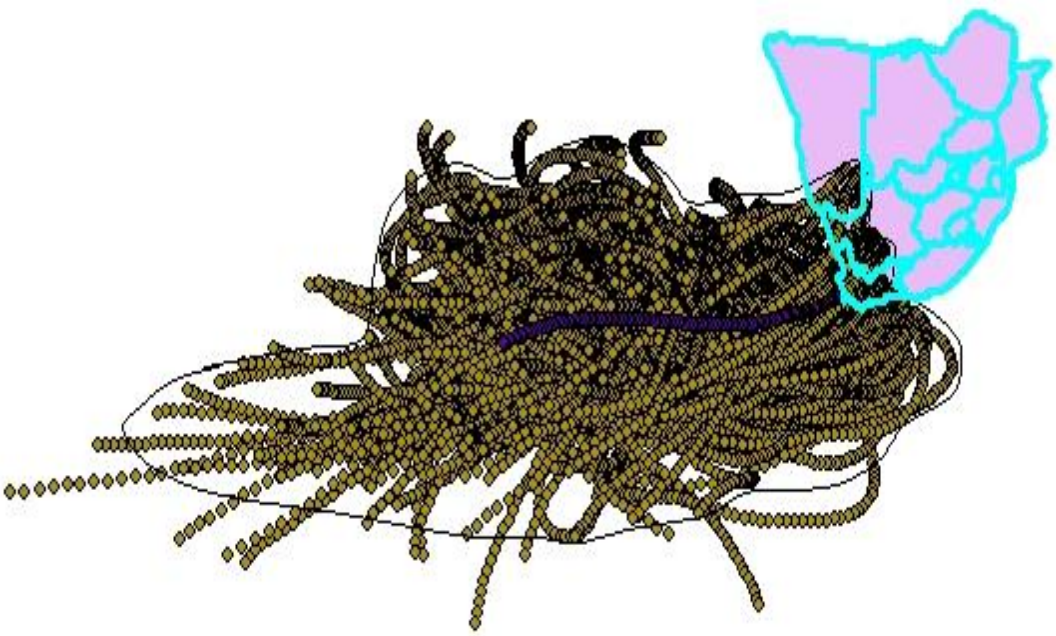

Figure 4.2c: Cluster 3 membership plots at 300m for 2001-2003

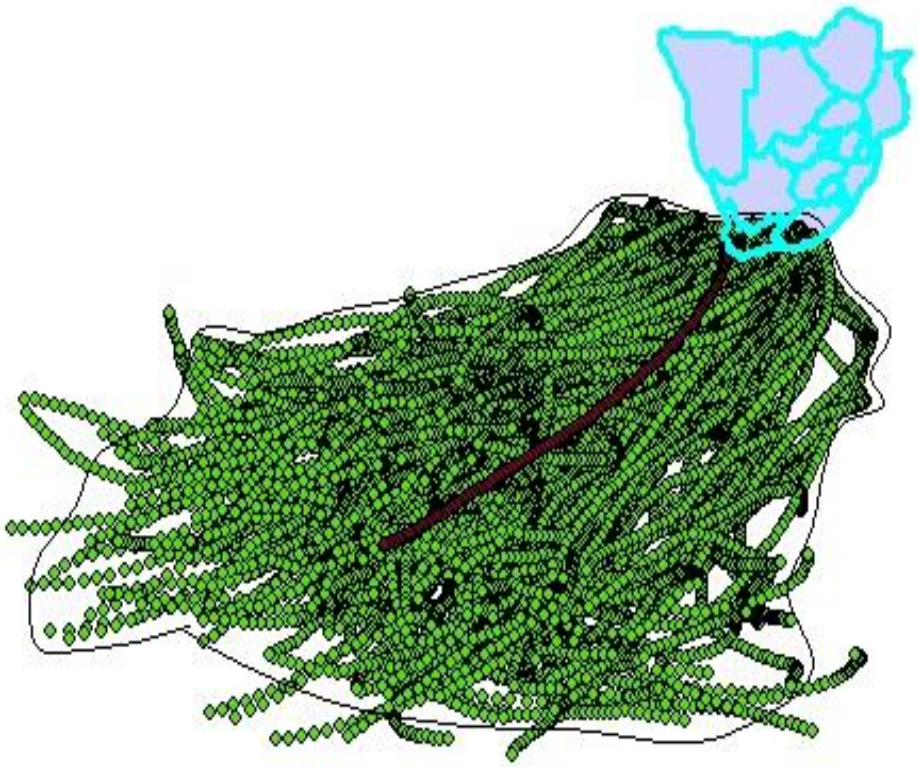

Figure 4.2d: Cluster 4 membership plots at 300m for 2001-2003

Figure 4.2e: Cluster 5 membership plots at 300m for 2001-2003

4.3.2 5000 m level mean trajectories

Figure 4.3 shows the cluster means arriving at 5000 m agl for the three year period (2001-2003). Table 4.2a shows the number of trajectories within each cluster obtained with Ward's method, with a cut off size of 5 clusters. Table 4.2b gives the corresponding percentage frequencies in each cluster for the three year back trajectory database. The dominant transport regimes to Cape Point at 5000 m agl during the three year period include clusters from the west (clusters 1, 2, 3 and 4). These westerly originating clusters account for 88% of the data. Cluster 5 with slow moving winds accounts for only 12 % of all trajectories in the entire period of study. This type of transport pattern can be attributed to regional recirculation due to the reasons given in Section 4.3.1, as shown in Figure 4.4e (membership plots). Clusters 1 and 2 with relatively high wind speeds originate in the southern South Pacific and South America (Argentina) respectively. The westerly cluster also contains trajectories approaching Cape Point from the north-westerly direction (cluster 3 and 4) with moderate wind speeds. The cluster means at 5000 m height indicates stronger wind speeds as compared to their counterparts at 300 m level.

All clusters indicate different arrival heights 12 hours before reaching Cape Point. Clusters 1, 2, and 4 indicate descending air flow, with cluster 1 descending from a higher altitude followed by clusters 2 and 4 respectively. Cluster 3 approaches at a constant altitude of about 5000 m agl 36 hours prior to arrival, while cluster 5 indicates ascending air flow 36 hours prior to arrival. Clusters 2 and 4 originate at an altitude of about 4500 m and 4300 m agl respectively and slowly

ascend to an altitude of about 6000 m and 5500 m respectively before descending to 5000 m. Cluster 1 originates from just above 5500 m and ascends to a level of about 6750 m before a sharp descent to the arrival point. Cluster 3 originates at a height of about 6000 m and gradually descends to 5000 m 36 hours prior to arrival. And lastly, cluster 5 originates from a level of about 5200 m and slowly descends to 5000 m 60 hours downwind, then moves along that height until it starts to ascend 36 hours prior to arrival. The 5000 m height cluster means show variability in arrival height closer to the arrival point, while those at the 300 m level indicate descending flow throughout.

The cluster-membership plots at 5000 m level are depicted in Figures 4.4a-e. The membership trajectories in Figure 4.4a-d indicate high wind speeds with trajectories originating from South America and the South Pacific. Figure 4.4e depicts trajectories with moderate wind speed from southern Africa and the surrounding Oceans. The envelope around trajectories in Figures 4.4a, b and d indicate moderate variability with trajectories veering from the west to north-west of the arrival point. A great variability is observed in Figures 4.4 c and e with trajectories indicating a cyclonic behavior over the Atlantic Ocean.

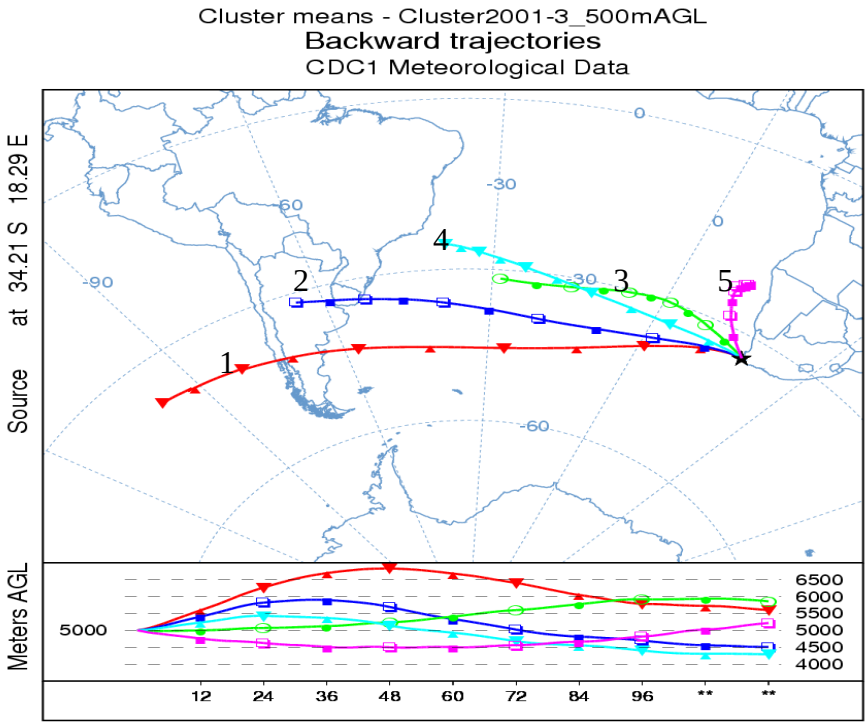

Figure 4.3: Cluster mean plots at 5000 m for 2001-2003

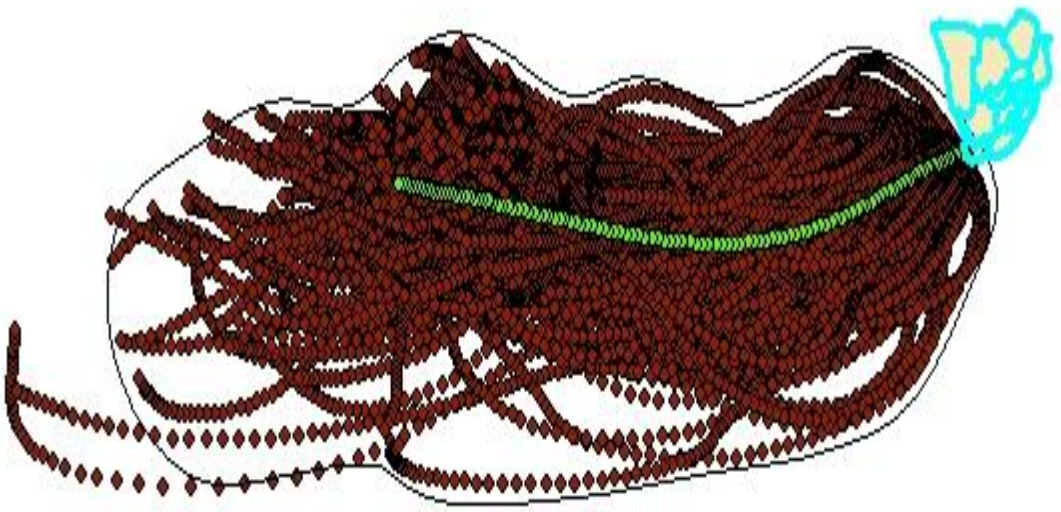

Figure 4.4a: Cluster 1 membership plots at 5000 m for 2001-2003

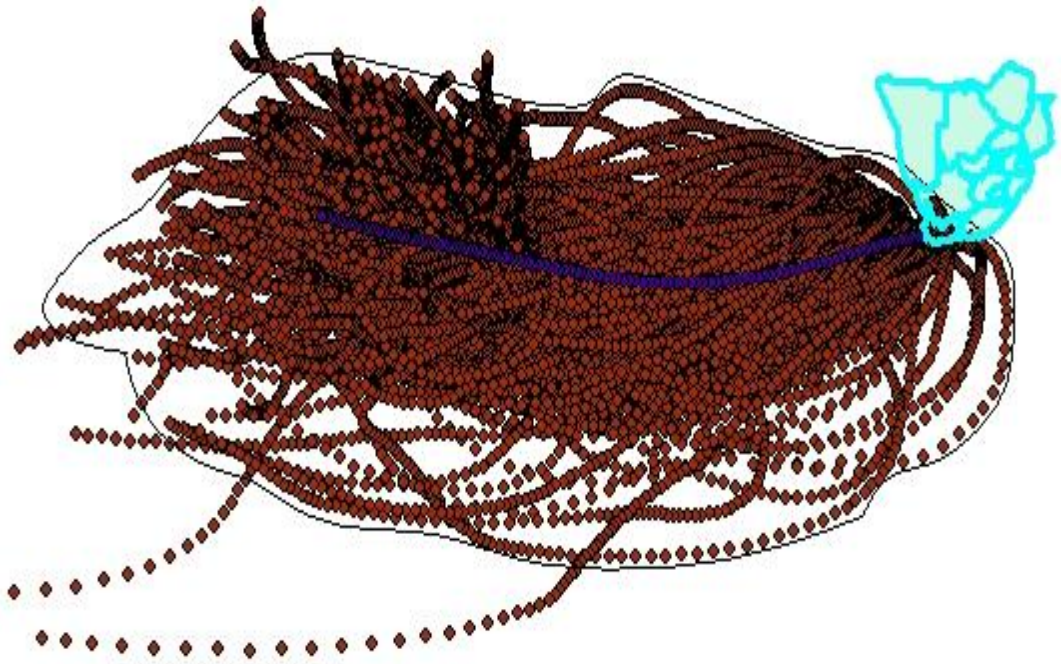

Figure 4.4b: Cluster 2 membership plots at 5000 m for 2001-2003

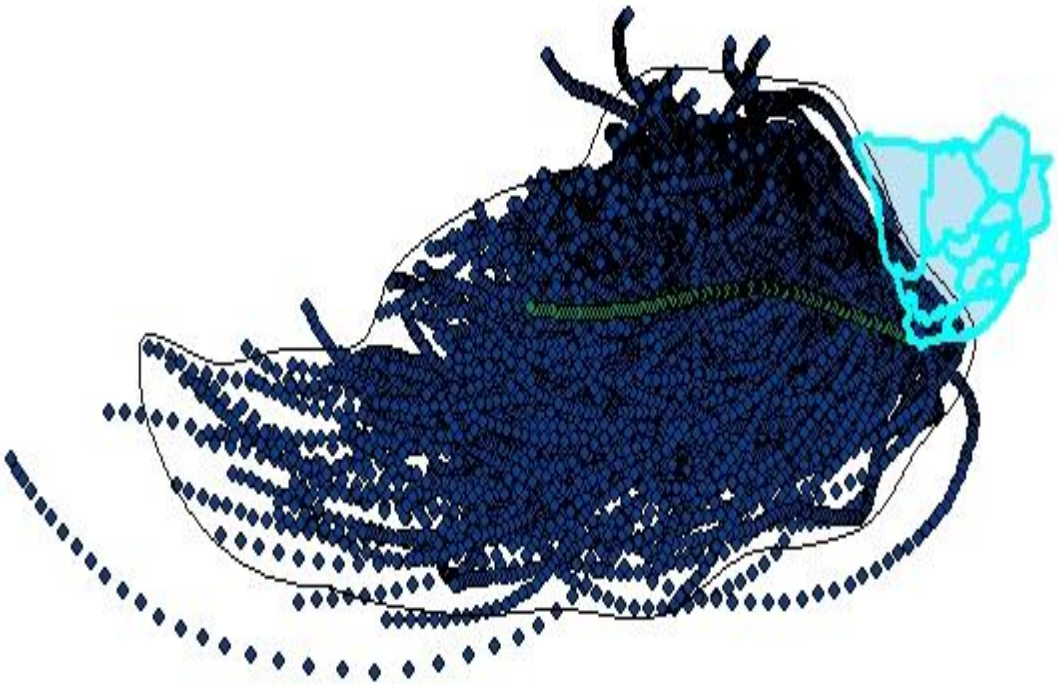

Figure 4.4c: Cluster 3 membership plots at 5000 m for 2001-2003

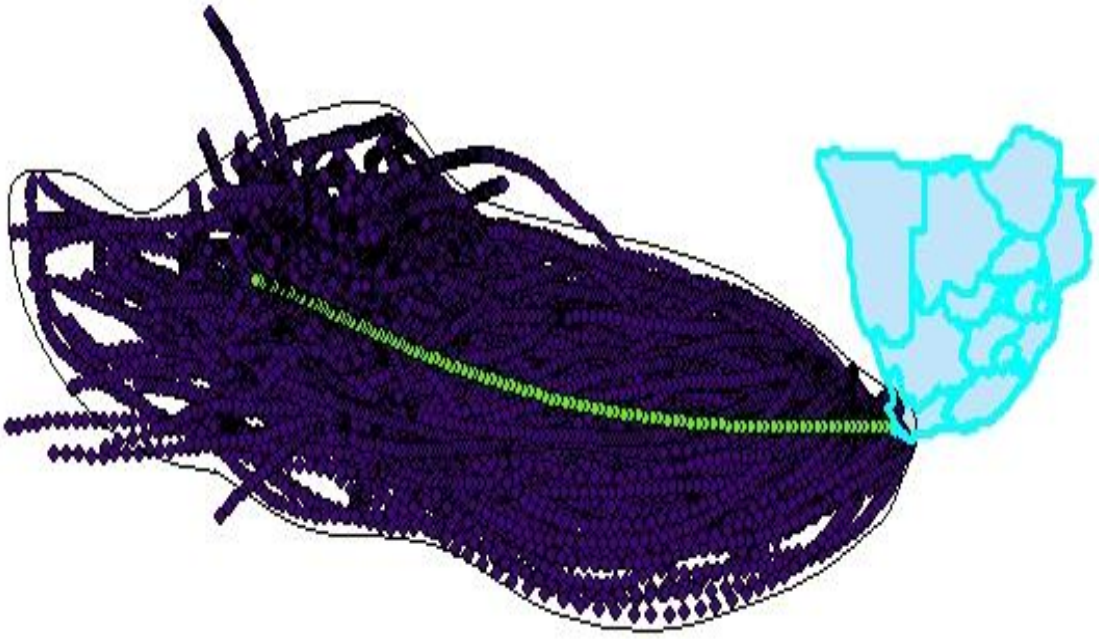

Figure 4.4d: Cluster 4 membership plots at 5000 m for 2001-2003

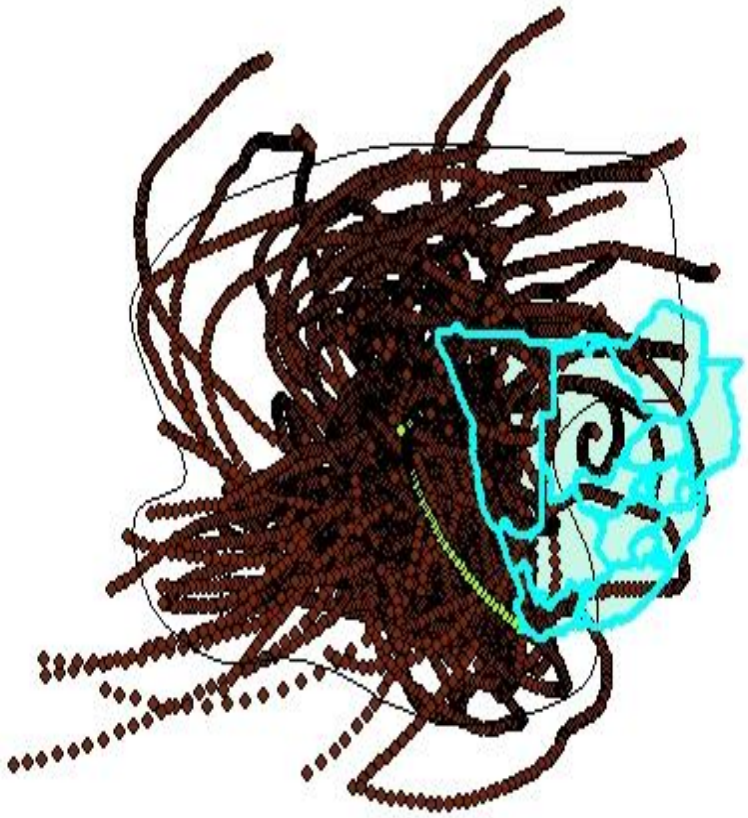

Figure 4.4e: Cluster 5 membership plots at 5000 m for 2001-2003

4.4 Cluster analysis results for individual years

Cluster results may show variability from one year to the next. In this section the results of individual year-to-year data are explored to determine the variability in atmospheric transport to Cape Point. The results were also summarized in Table 4.1.

4.4.1 300 m level mean trajectories

Cluster mean plots for each year are shown together with the means over the whole 3-year period for comparison in Figure 4.5. In 2001 (Fig.4.5b), a north-easterly flow (cluster 2) is observed which accounts for 17% of the total trajectory data . This cluster originates in the south-east and approaches Cape Point from the north-easterly direction. Clusters 3 and 5 in the 3-year mean (Fig.4.5a) are combined to give a moderate and fast moving westerly clusters 1 and 5 in 2001 with 32% and 9% of the trajectories respectively. South-westerly flow (cluster 3) with moderate to fast moving wind speed is observed and accounts for 23% of the total trajectory data. A moderate moving flow (cluster 4) originating in the south-west and approaching Cape Point from the south-east is also observed and accounts for 19% of the total data. All trajectories show similar arrival heights 36 hours prior to arrival at Cape Point. Clusters 1, 2, and 5 originate at

about 1000 m agl while clusters 3 and 4 originate at about 1500 m agl; this is a clear indication of subsidence (Fig 4.5b).

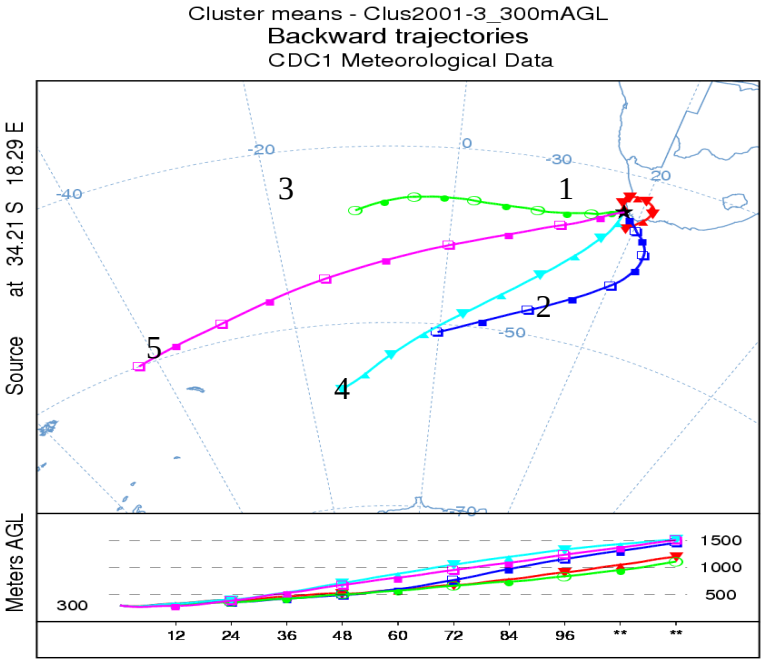

Figure 4.5a: 2001-2003 cluster means at 300 m

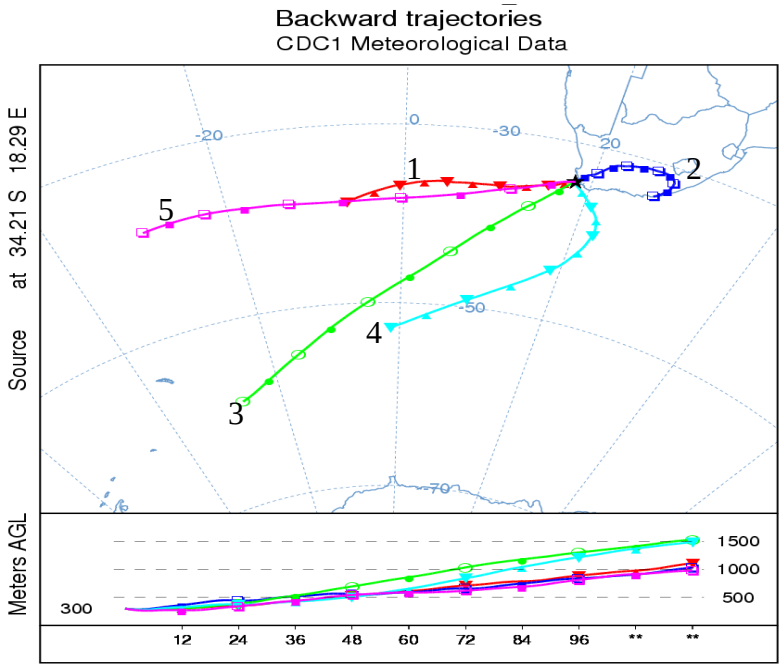

Figure 4.5b: 2001 cluster means at 300 m

Figure 4.5c shows mean trajectories for 2002. An easterly flow (cluster 5) originating in the south-west, now approaches Cape Point from the south-east as compared to north-east in 2001, this regional flow pattern accounts for 26% of the total trajectory data. A westerly cluster 3 with moderate wind speeds accounts for 13% of the total clustered trajectories. Two south-westerly clusters 1 and 2 with fast and moderate flows respectively are observed and account for 24 and 20% of total data respectively. A south-south-westerly cluster 4 with moderate wind speeds is also observed and represents 17% of clustered trajectories. All clusters indicate similar arrival height of about 400 m agl 12 hours before arriving at the measuring site. However, variability in height is observed from 36 hours downwind. Cluster 1 originates at about 1700 m above the surface, with clusters 2 and 4 originating at about 1500 m agl. Cluster 5 originates at a level closer to 1250 m above the surface. Lastly, cluster 3 originates at a level lower than the rest of the trajectory means at a level of about 900 m. All the flow patterns in 2002 indicate subsidence from their point of origin.

Figure 4.5d shows cluster means for 2003. Easterly zonal flows (cluster 3) account for 13% of the data. This cluster with slow wind speeds originates from the interior of South Africa and approaches Cape Point from a north-easterly direction. Three westerly flow categories are observed. These flows are grouped into moderate westerly flow (cluster 1) with a 30% of occurrence, fast south-westerly flows (cluster 4) accounting for 23% of the total data, and moderate south south-westerly flows (cluster 2) representing 25%. Cluster 5 originates from the south and approaches Cape Point from the south-west with moderate wind speed and accounts for 10% of the total trajectory data. Similarity in height below 500 m agl is observed 24 hours downwind on all trajectories. Cluster 1 is still below the 500 m level 60 hours downwind where it starts to ascend until a point of origin at about 1100 m agl. Cluster 2, 3, and 4 originate at a level of about 1500 m and they descend at the same rate till they reach the arrival point. Cluster 5 originates at 1100 m agl and ascends to a level of about 1300 m then starts to descend to the arrival point 72 hours downwind.

There were some similarities observed in the inter-annual clusters and the 3-year mean clusters. The first similarity is observed in clusters 2, 5 and 3 in 2001, 2002 and 2003 respectively, where the cluster is seen to veer from a north-westerly direction in 2001 to south-westerly in 2002 and back to north-westerly in 2003. This cluster is also depicted in the 3-year mean clusters (cluster 1) with an anticyclonic curvature. Clusters 1, 3 and 1 in 2001, 2002 and 2003 are also similar, with winds veering from westerly in 2001 to north-westerly in both 2002 and 2003, and it resembles cluster 3 in the 3-year means. Clusters 5, 1 and 4 in 2001, 2002 and 2003 resembles cluster 5 the 3-year cluster means with fast moving winds veering south-westerly and westerly between the years. Cluster 4 in 2001 and clusters 2 and 5 in 2003 resembles cluster 2 the 3-year cluster means. However, cluster 5 originates from the south (near Antarctica), while the other clusters indicate a south-westerly origin. Cluster 4 in the 3-year means is comparable to clusters 3 and 4 in 2001 and 2002 respectively, with cluster 3 in 2001 indicating strong winds.

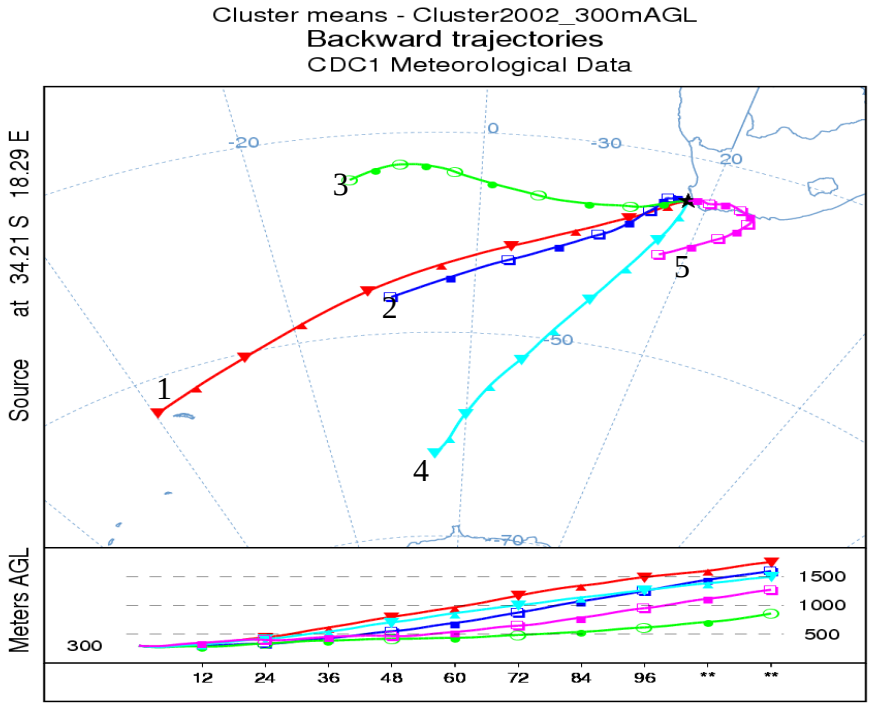

Figure 4.5c: 2002 cluster means at 300 m

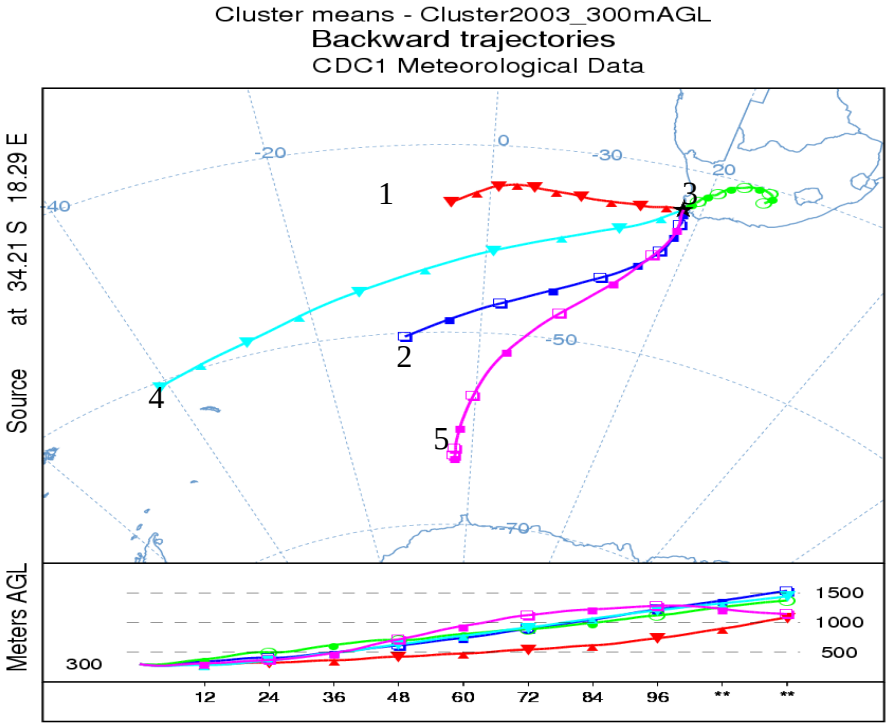

Figure 4.5d: 2003 cluster means at 300 m

4.4.2 5000 m level mean trajectories

Cluster mean plots for each year are shown together with the means over the whole 3-year period for comparison in Figure 4.6. The 3-year mean trajectories (Fig.4.6a) are shown for comparison. The 2003 cluster means (Fig. 4.6d) are remarkably similar to the 3-year ensemble cluster means, and therefore are not discussed here. In 2001 (Fig. 4.6b) the main difference from the 3-year means is that the two cluster means (clusters 1 and 4) combine to form a strong westerly flow with a percentage frequency of 31%, and there is a flow (cluster 2) extending to southern Brazil with a percentage frequency of 25%. In 2002 (Fig. 4.6c), the main difference from the 3-year means is that two clusters (4 and 5) originate from the South Pacific with a combined percentage frequency of 35%. Cluster 1 with 30% of the total data originating from the southern coast of Brazil is observed in 2002. Lastly, a northerly to north-easterly cluster 5 with slow moving winds recirculates air over the north-western parts of southern Africa. Arrival and source heights of the individual years display similar flow height characteristics as those in the 3-year period (section 4.3.2).

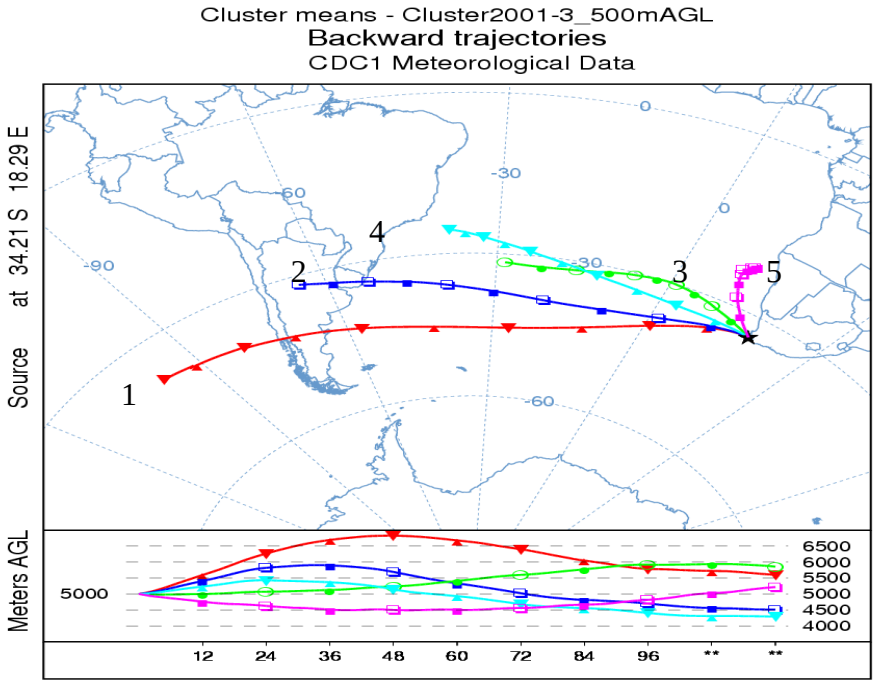

Figure 4.6a: 2001-2003 cluster means at 5000 m

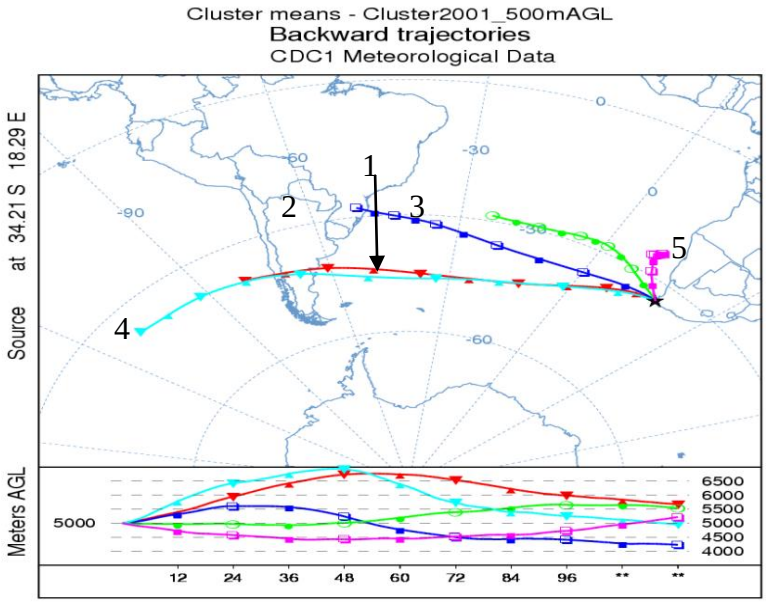

Figure 4.6b: 2001 cluster means at 5000 m

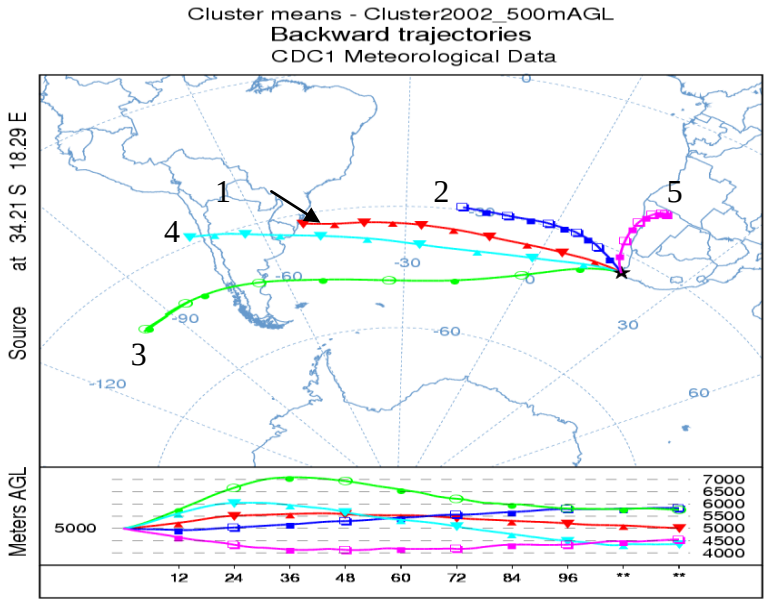

Figure 4.6c: 2002 cluster means at 5000 m

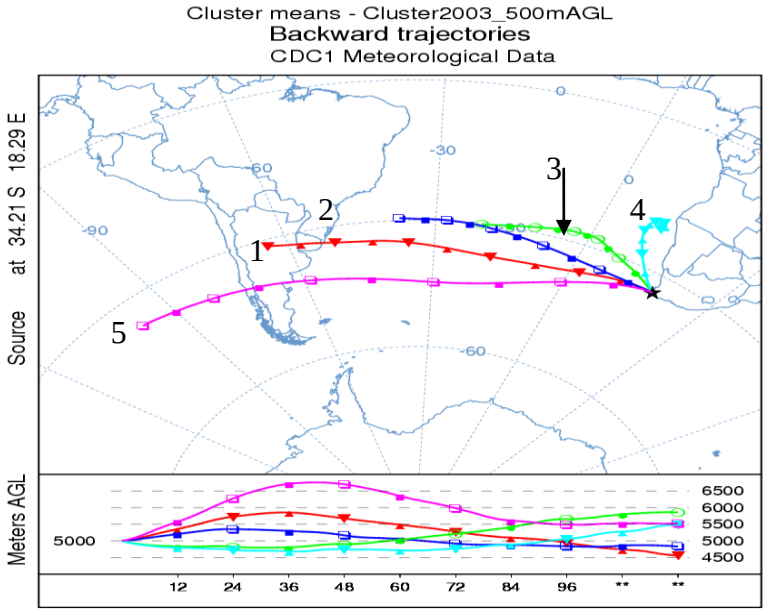

Figure 4.6d: 2003 cluster means at 5000 m

4.5. Cluster analysis results for seasonal trajectories

4.5.1 300 m levels mean trajectories

The 5-day mean upwind trajectories for the primary transport patterns in each season are shown in Figure 4.7 (a-d). Figure 4.7a represents summer (DJF) cluster means for the 3-year period of study. Two easterly clusters (2 and 5) and three westerly to south-westerly clusters (1, 3, and 4) are observed. Westerly flow (cluster 1) with moderate wind speeds accounts for 42% of the data. Westerly to south-westerly flow (cluster 3) with fast moving wind speeds accounts for 17%, and southerly to south-westerly flow (cluster 4) with moderate wind speeds approaches Cape Point with a percentage frequency of 6%. All cluster means indicate similar arrival height below the 500 m level within 24 hours prior to arrival. The difference in height is observed 36 hours downwind with clusters 3 and 4 showing strong subsidence followed by clusters 1 and 2. Cluster 5 show subsidence 84 hours downwind. Clusters 1, 2, and 4 originate at a height of about 1400 m level, while cluster 3 originates at a higher level of approximately 1800 m. Cluster 5 originates at a level of about 1000 m.

Figure 4.7b shows cluster means for autumn (MAM) for the 3-year period of study. As in DJF, there are two easterly clusters and three westerly to south-westerly clusters. The main difference from DJF is that there are clusters with fast moving southerly flow (cluster 5) approaching Cape Point from the south-west with a percentage frequency of 15%. Cluster 4 which is similar to cluster 2 in DJF has shifted southerly and approaches from the south-east, with moderate wind speeds and a percentage frequency of 11%. Cluster 2 with slow moving wind speeds approaches Cape Point from the north-east and accounts for 28% of the data. Arrival heights for all trajectory means are similar to those in DJF in the first 24 hours prior to arrival. Beyond the 24 hour period, clusters 3 and 5 couple in height and indicate strong subsidence followed by cluster

4. Clusters 1 and 2 show weak subsidence beyond 48 hours downwind of Cape Point. Cluster 3 indicates a source level of just above the 2000 m level. Clusters 4 and 5 originate at a level between 1500 and 2000 m with cluster 5 originating a little higher than cluster 4. Clusters 1 and 2 originate from a level of about 1000 m.

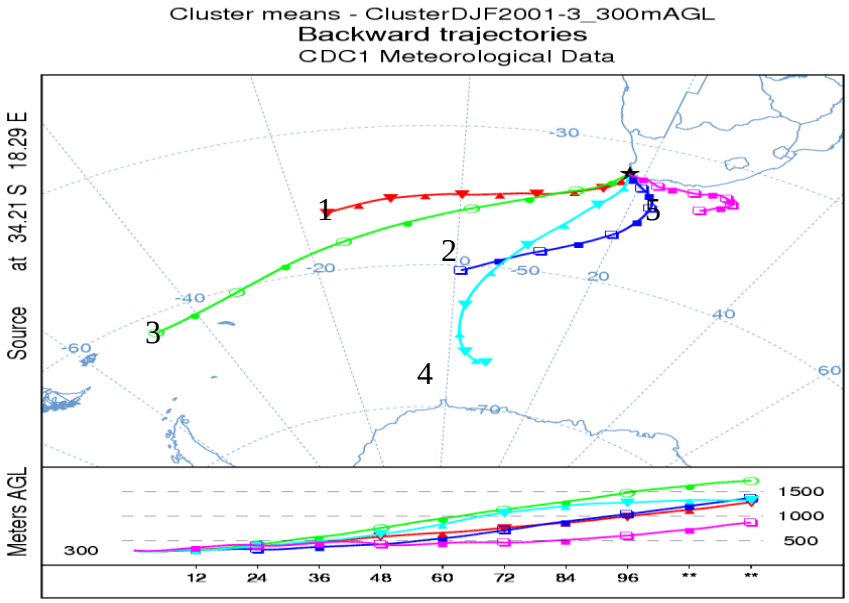

Figure 4.7a: 2001-2003 summer cluster means at 300 m

Winter clusters (JJA) are depicted in Figure 4.7c. There are north-easterly flows (cluster 4) with slow moving winds indicating circulation over southern Africa and extending to the Atlantic Ocean with a percentage frequency of 23%. The remaining clusters are similar to those in MAM, except that cluster 5 accounting for 9% of the total data shows a stronger south-easterly winds and cluster 1 with 23 % of total data indicates weaker wind speeds compared to winds in depicted by cluster 5 in MAM. An arrival height closer to 300 m agl is observed for all clusters 12 hours before arrival. Cluster 4 indicates a weak subsidence 84 hours downwind and originates at about 600 m agl. Cluster 2 with a percentage frequency of 23% originating at a level of about 2000 m agl with cluster 1 from a level of about 1500 m agl and accounting for 24% of the total data. Clusters 3 and 5 originate from a height of about 1100 m agl.

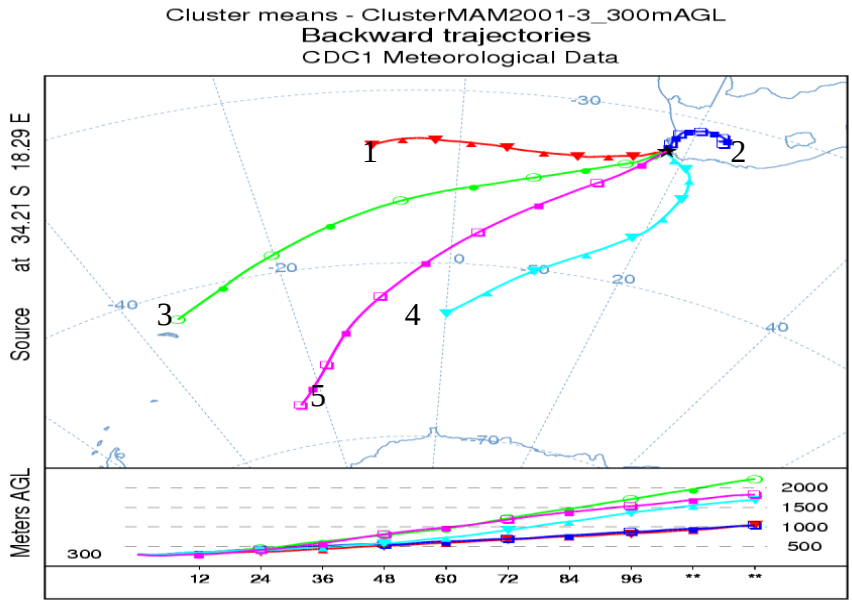

Figure 4.7b: 2001-2003 autumn cluster means at 300 m

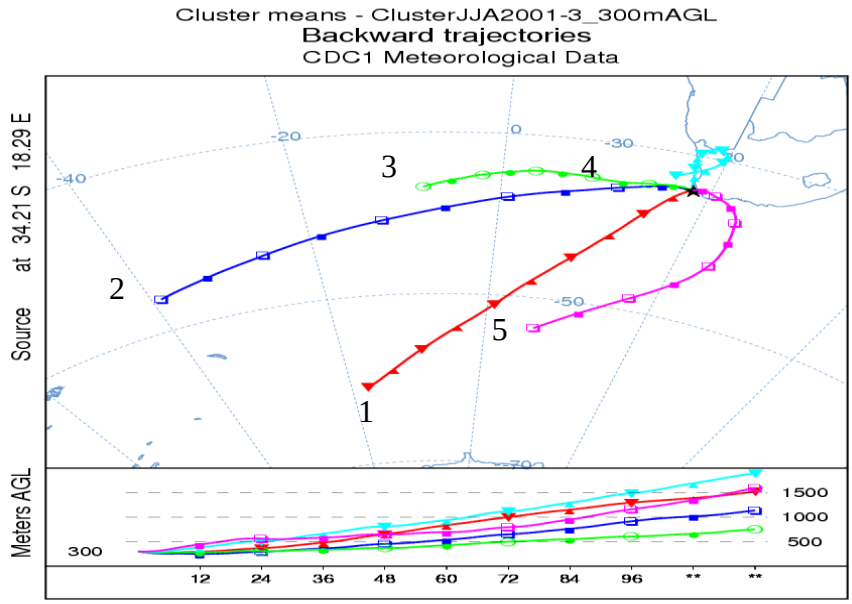

Figure 4.7c: 2001-2003 winter cluster means at 300 m

Figure 4.7d depicts spring (SON) trajectory means for the whole data set (2001-2003). There are four westerly to south-westerly flows (clusters 1, 2, 3 and 5) and a south-easterly flow (cluster

4). Cluster 1, 5 which account for 16 and 12% of the data respectively are common in all seasons, cluster 2 with 24% of the trajectories is similar to cluster 1 in JJA. Cluster 4 accounts for 12% of the total data and resembles cluster 5 in DJF. A south-westerly flow (cluster 3) with relatively slow wind speeds is observed in spring with a percentage frequency of 26%. This cluster is not observed in other seasons. All clusters indicate an arrival height closer to 300 m at 12 hours downwind and the difference in height is experienced 24 hours downwind. Cluster 4 moves along the 300 m level within the 84 hour prior to arrival and beyond that it shows weak subsidence that originates from a level about 500 m. Cluster 3 which originates from a 1000 m level, subsides to a level just above 300 m level 48 hours downwind and reaches 300m level 36 hours before arrival. Cluster 5 has the same source height as cluster 3 and moves along the 1000 m level until it reaches the 84 hour mark downwind where it gradually subsides to the 300 m level 12 hours before arrival. Cluster 1 indicates a source height of about 1400 m and descends steeply to a level of 750 m at 84 hours downwind where is starts a gradual descent to the 300 m level 12 hours prior to arrival. Lastly, cluster 2 with a source height of about 1700 m descends to 1400 m 84 hours downwind where it begins a steep descent to the 300 m level 12 hours before arriving at Cape Point.

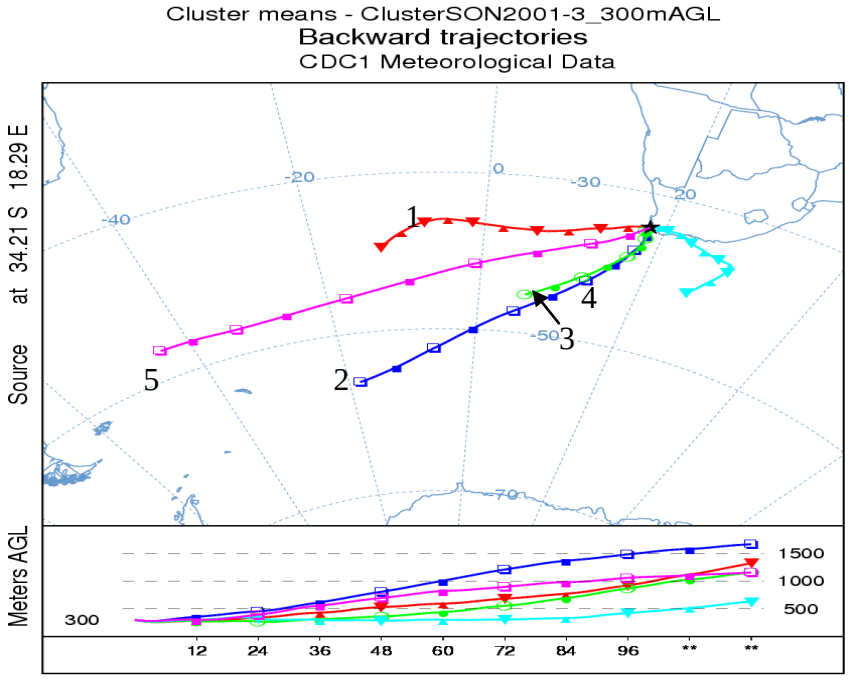

Figure 4.7d: 2001-2003 spring cluster means at 300 m

4.5.2 5000 m levels mean trajectories

Figure 4.8(a-d) shows seasonal cluster means at 5000m agl. Summer mean trajectories (DJF) for the period 2001-2003 are depicted in Figure 4.8a. The figure indicates that there are three westerly clusters (1, 2, 4 and 5), and a northerly cluster 3. Cluster 1 shows southern Brazil as a source region and approaches Cape Point from a north-westerly direction with fast wind speeds and a percentage frequency of 31%. There are also westerly flows (cluster 2) with moderate wind speeds accounting for 24% of the total data and the trajectories approach the arrival point from a north-westerly direction. There are strong westerly flows (clusters 4 and 5) approaching Cape Point from a westerly direction with a combined percentage frequency of 32%. Cluster 3 indicates slow moving flows originating from the north-west and arriving at Cape Point from a northerly direction with a percentage frequency of 13%. Cluster 1 with a source height of 4500 m ascends to a level of 6000 m at 24 hours downwind and starts to descend to the arrival point of 5000 m. Cluster 3 descends from approximately 5600 m to reach about 4600 m at 36 hours downwind where it starts to ascend to the arrival point. Cluster 5 slowly descends from a source level of about 6100 m to 6000 m where at 96 hours downwind it starts a gradual ascent to the 6100 m level, followed by a steep ascent 84 hours downwind and a steep descent 48 hours prior to arrival. Cluster 2 originates from a level of about 6300 m, gradually descends to the 5000 m level 24 hours before arrival and moves along that level until it reaches the arrival point. Cluster 4 with a source height of 1900 m, moves along the same level until it starts a steep descent to the arrival point 60 hours downwind.

Figure 4.8b shows autumn trajectory means (MAM) for the entire period of study. Clusters 2 and 4 with moderate and fast wind speeds respectively approach the arrival point from the north-west and account for 53% of the total data. Strong westerly flows (clusters 1 and 5) account for 34% of the total data. Cluster 3 which accounts for 13% of the data is similar to cluster 3 in DJF. There are similarities in arrival height 12 hours prior to arrival between clusters 1 and 5. Cluster 1 with a source height at the 6000 m level ascends to about 6600 m and moves along that level 72 hours downwind until descending steeply 36 hours prior to arrival at CapePoint. Cluster 3 indicates a source height of 5500 m and descends to 4600 m two days prior to arrival. 12 hours later it again starts to ascend to the arrival point of 5000 m. Cluster 2 has a source height of about 5400 m and moves along that same height until it starts descending 72 downwind to the arrival

point. Cluster 4 ascends gradually to 5500 m 60 hours downwind and descends a day before arrival until reaching the arrival point. Finally, cluster 5 with the same source height as cluster 4 starts a steep ascent 96 hours downwind until it finally starts to descend to the arrival point 36 hours downwind.

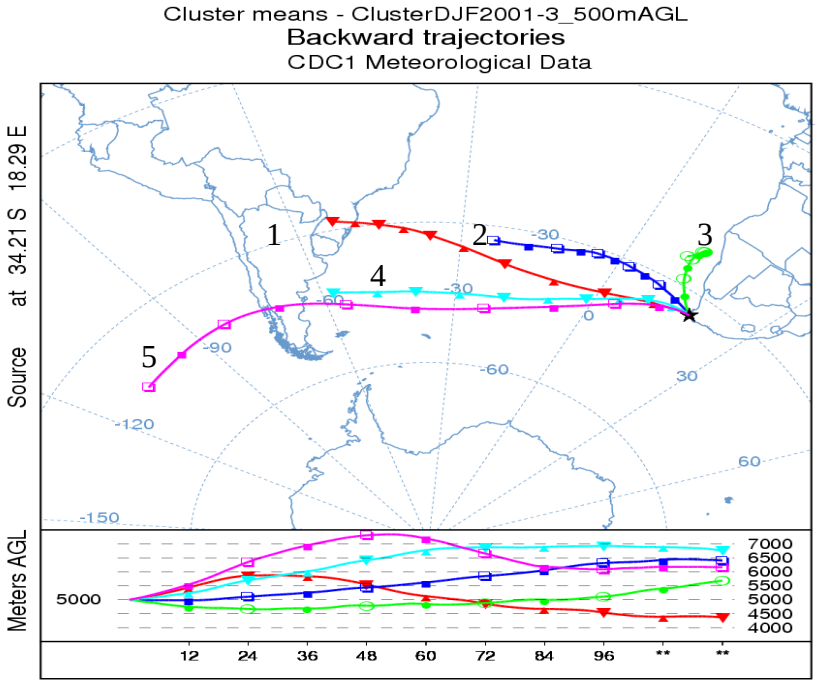

Figure 4.8a: 2001-2003 summer cluster means at 5000 m

Winter trajectory means (JJA) are depicted in Figure 4.8c. All clusters indicate a westerly origin. Clusters 2 and 3 with slow and moderate winds approach Cape Point from the north-west with a combined percentage frequency of 50%. Strong westerly clusters (1, 4 and 5) account for 50% of the total data. Cluster 1 indicates a flow originating from a level of about 3800 m and moving along that level until it starts to ascend 84 hours downwind. It then starts to descend to the arrival point 2 days prior to arrival. Cluster 2 with a source height of about 4250 m displays the same pattern as cluster 1. However, it only rises to a level of about 5100 m before descending to the arrival point 2 days prior to arrival. Cluster 3 indicates a descending flow from the 6000 m level to about 4500 m 48 hours downwind. Clusters 4 and 5 with source heights of 4600 and 5000 m

respectively indicate flows with ascending motion. Cluster 4 starts to descend after reaching the 7000 m level 48 hours downwind, while cluster 5 descends after reaching the 6000 m at the same time.

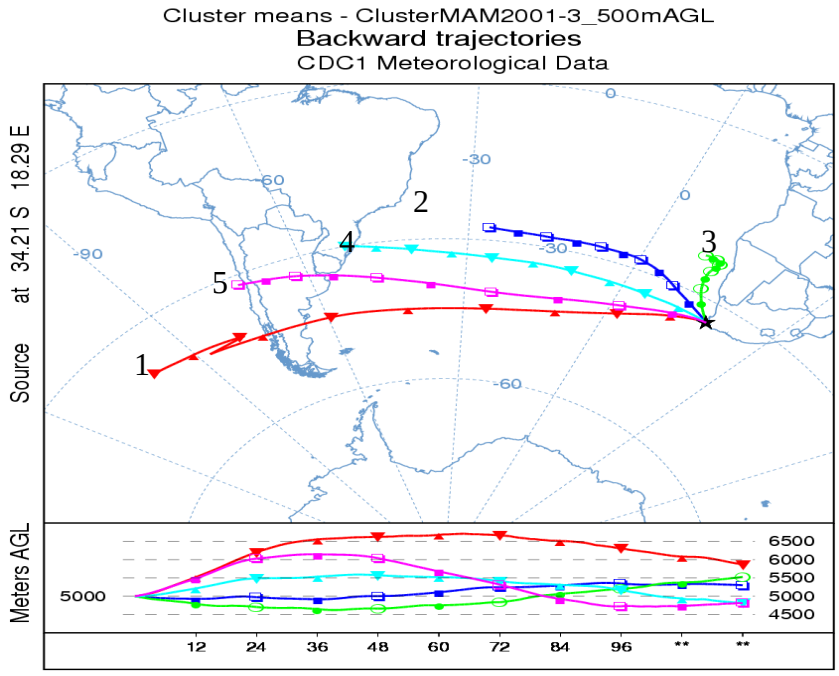

Figure 4.8b: 2001-2003 autumn cluster means at 5000 m

Figure 4.8d shows spring trajectory means (SON) for the same period as in the other seasons discussed above. Cluster 2 with moderate winds accounts for 28% of the total data and arrives at Cape Point from the north-west. There are three westerly clusters (1 and 5 with fast moving winds and 3 with moderate wind speeds) with a combined percentage frequency of 57%. Cluster 4 which is similar to cluster 3 in DJF and MAM accounts for 17% of the total trajectory data.

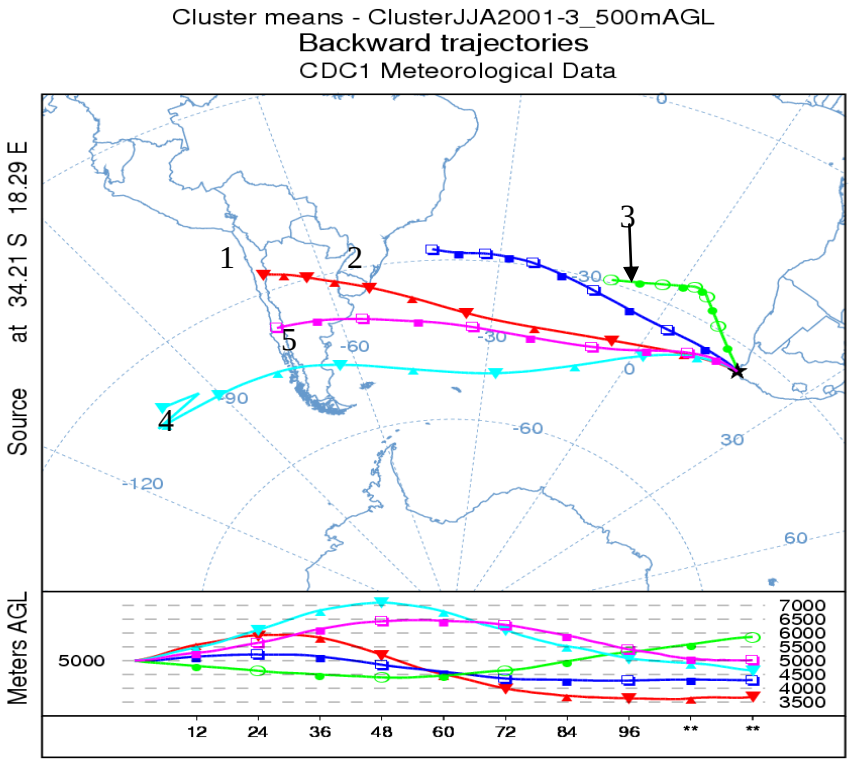

Figure 4.8c: 2001-2003 winter cluster means at 500 m

Cluster 1 shows flows ascending from a level of 5000 m 5 days downwind to a level of 6100 m 36 hours before arrival and then descend to the arrival point thereafter. Cluster 2 with a source height of about 4600 m displays the same flow height pattern as cluster 1, but only reaches the 5000 m level. Cluster 3 has a source height of about 5600 m and ascends from that level to 7000 m between 84 and 96 hours downwind before descending to the 5000 m level a day before arrival, and continuing at that level to the arrival point. Cluster 4 with the same source height as cluster 2 moves closer the 4500 m level and starts ascending to the arrival point 36 hours downwind. Finally, cluster 5 with same source height as cluster 3, gradually ascends to about 7100 m 36 hours downwind before descending to the arrival point.

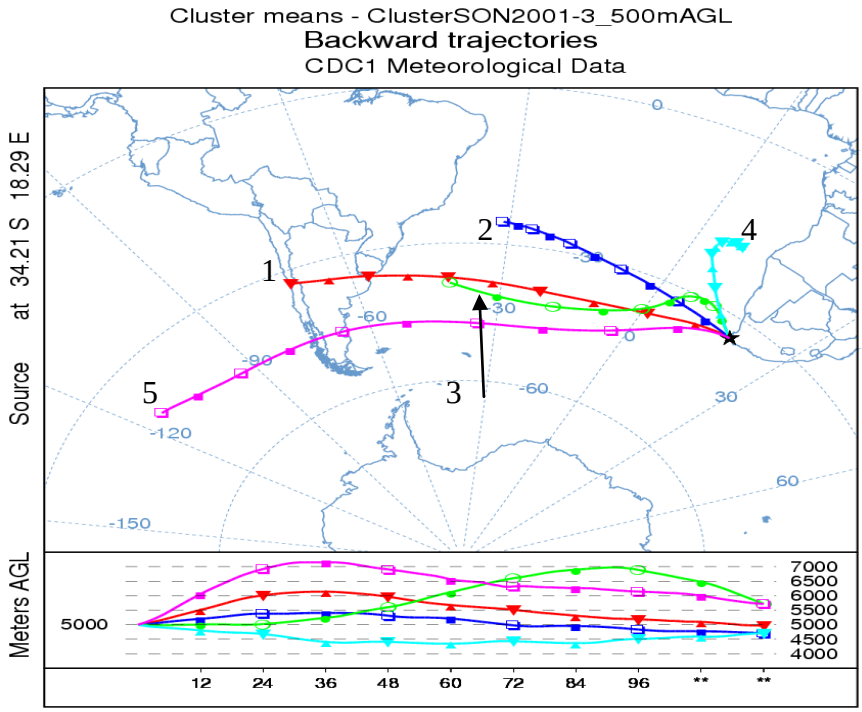

Figure 4.8d: 2001-2003 spring cluster means at 5000 m

4.6 Analysis of results

4.6.1 Whole data sets

Figure 4.1 shows dominant 300 m agl transport regimes for the entire period of study (2001-2003). Cluster 1 indicates slow-moving anticyclonic flow over the interior of the country. This cluster contains a population of trajectories (Fig.4.2a) from southern Africa and the surrounding oceans which clearly indicates regional recirculation over southern Africa and the surrounding oceans. This type of cluster can be associated with anticyclonic circulations ridging over the west and south coasts of South Africa coupled with continental highs. Cluster 2 with south-easterly to south-westerly flows is representative of southerly ridging anticyclones. The southerly ridging anticyclones are westerly disturbances associated with steep pressure gradients, strong winds and diminished atmospheric stability. The easterly component of cluster 2 is attributed to south-east trade winds which are associated with the South Atlantic anticyclone. Cluster 3 is associated with westerly flows generated at the base of the South Atlantic high ridging over the south-west coast of South Africa. Clusters 4 and 5 are the results of westerly waves which are the strongest occurring disturbances affecting circulation over southern Africa. Westerly waves are responsible for rapid transport of air masses from South America to South Africa due to strong winds.

Clusters 2, 4 and 5 have the same source height of about 1500 m agl and all originate from the south-west of the Cape Point, while clusters 1 and 3 originates at lower level than the other three. All these clusters confirm the assertion by Garstang *et al* [1996a] that South Africa and the

adjacent Atlantic and Indian Oceans are located in the region of large-scale subsidence occurring between the Hadly and Ferrel cells of the southern hemisphere general circulation. Figure 4.2 displays mean transport patterns at 5000 m agl, with cluster 5 depicting a north-westerly flow with a north-easterly origin. This cluster transports air under weak easterly wave conditions that occur at levels between 700 and 500 hPa. This type of cluster was also observed by Tyson *et al* [1996a]. Clusters 1 and 2 indicate the existence of strong westerlies in the region between 33º and 45º S, while clusters 3 and 4 indicate moderate westerly winds in the region between 25 and 33º S. The broadening of the westerly wind belts in the mid to upper troposphere resulted in the dominance of westerly transport to Cape Point .

The observed variability in source height of the westerlies is a clear indication that pollutants can be transported from different levels of the atmosphere to the receptor site. This was also noted by Taljaard [1953] who observed that the variation in wind speed and direction at different levels is instrumental in superposing air masses from different source regions and in producing stable or unstable stratification.

4.6.2 Year to year variability

It is well known that cluster results may show variability from one year to the next [Jorba *et al.*, 2004]. Cluster mean plots for each year were shown in Figure 4.5 (b-d). The pie charts (Fig. 4.9) indicate the percentage of trajectories in each cluster. In 2001, westerly flow (clusters 1 and 5), south-westerly flow (cluster 3) and south-easterly flow (cluster 4) are similar to the 3-year clusters shown in Figure 4.5a. A north-easterly flow (cluster 2) indicates regional flow due to ridging anticyclones on the south and south-east coasts of South Africa; the slow moving winds are due to the varying topography of the Western Cape which ranges from 1000 m to about 1500 m with mountains rising to about 3000 m, this variation in height will cause surface drag that will result in reduced wind speed. Cluster 4 in 2002 and 2003 indicates the influence of southerly meridional flow on the west coast of South Africa. This type of flow is discussed in Tyson and Preston-Whyte [2000]. Perturbation in the mid-latitude westerly flow to the south of southern Africa constitude the strongest regularly occurring disturbances that results in generation of southerly to south-westerly clusters 1, 2 and 4 in 2002 and clusters 4, 2 and 5 in 2003. Cluster 5 in 2002 and cluster 3 in 2002 result from southerly ridging South Atlantic anticyclones.

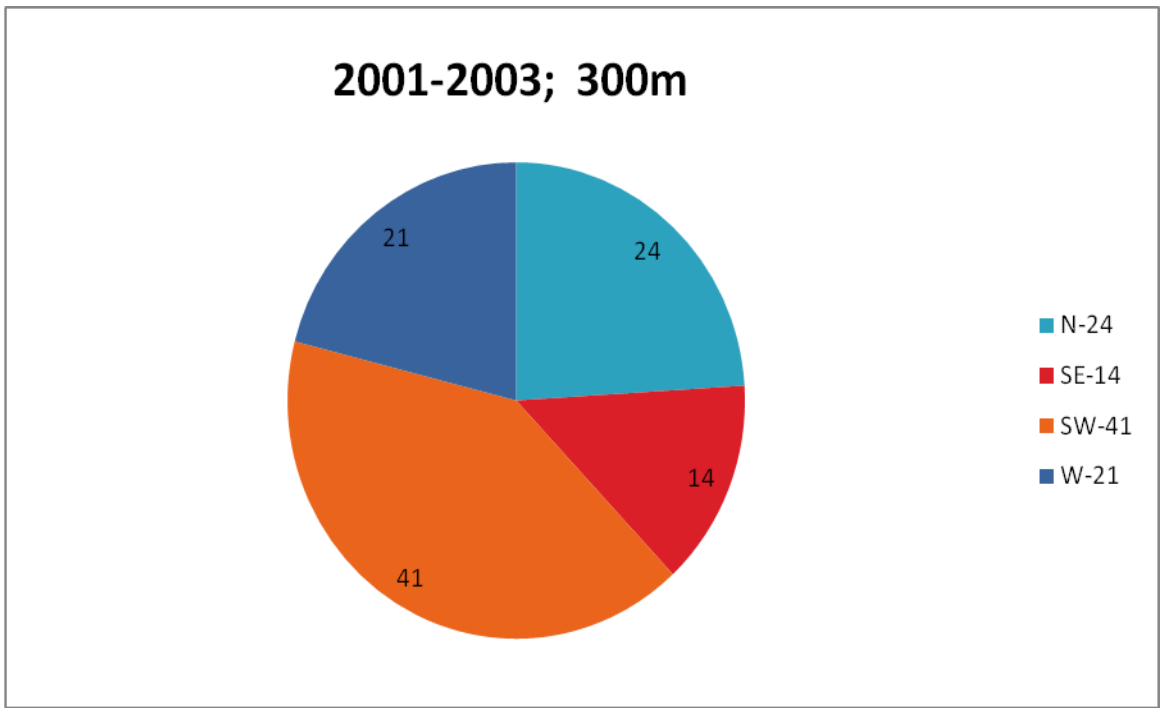

Figure 4.9a: 2001-2003 pie chart indicating trajectory source percentages

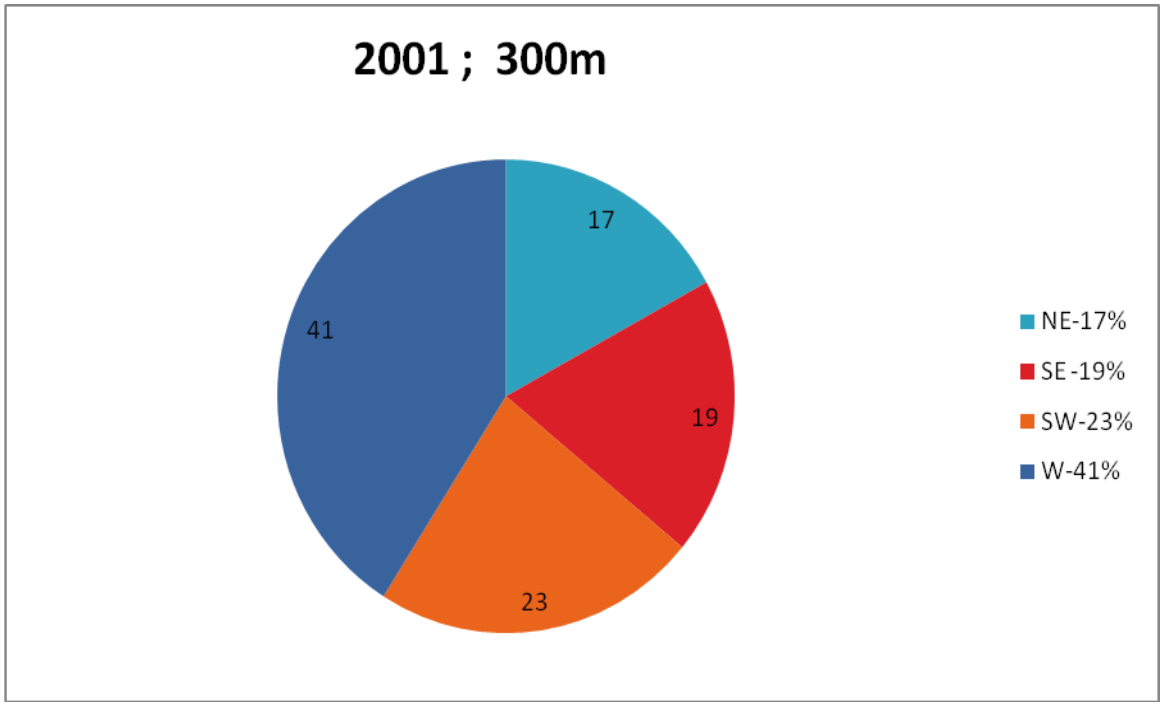

Figure 4.9b: 2001 pie chart indicating trajectory source percentages

The main difference between the 2001 and the 3-year mean clusters arise because clusters 1 and 5 combine resulting in a higher percentage of westerly clusters as compared to the 3-year means. There is also a north-westerly cluster 3 with slow moving winds observed in 2001 as compared to the recirculation (cluster 1) observed in the 3-year means. The 2002 and 2003 clusters show similarity in terms of percentage distribution of south-westerly clusters which are higher than in 2003. The westerlies are dominant in 2001 at 41% followed by 2003 at 30% with 2002 at 13 %. A cluster with a north-easterly component observed in 2001 at 17 % and 2003 at 26% approaches Cape Point from south-easterly direction in 2002 at 13%. The weak 2002-2003 El Niño may be responsible for the variation in percentage distribution of clusters, in that zonal winds along the west coast tend to be more westerly during ENSO events . However, other meteorological factors such as the variation in intensity and position of the transient mid-latitude ridging anticyclones and the semi-permanent subtropical anticyclones are also responsible for the variation. The observed difference in source direction and height due to decoupling of the atmosphere were also observed by Garstang *et al.*, [1996a].

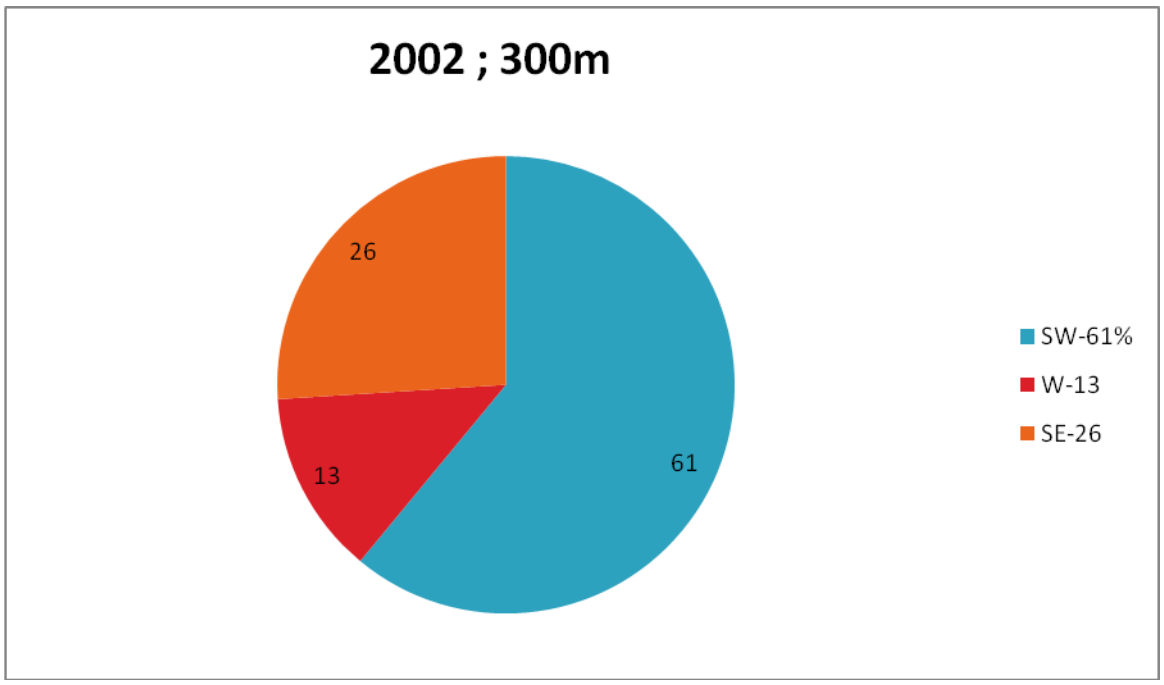

Figure 4.7c: 2002 pie chart indicating trajectory source percentages

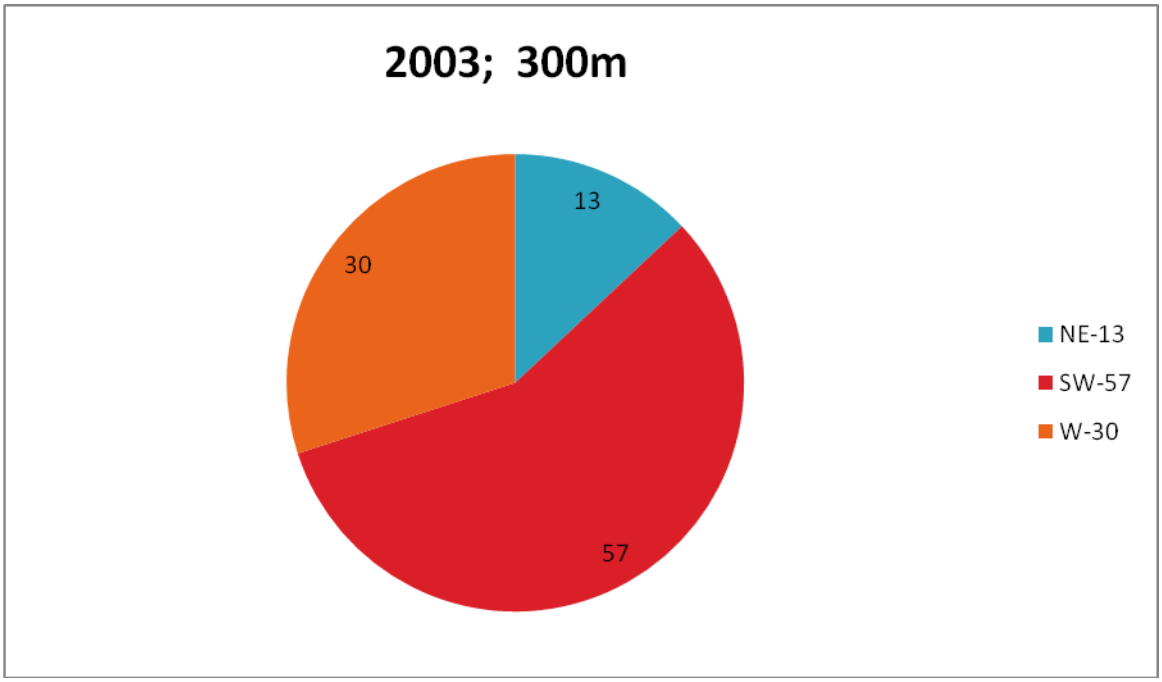

Figure 4.7d: 2003 pie chart indicating source percentage

Figure 4.6 showed yearly cluster means at 5000 m agl. Table 4.2b displayed percentages of trajectories within each mean cluster. The overall pattern of clusters in the 3 years is similar to that depicted in the 3-year mean clusters (Fig. 4.6a) with clearly defined westerly, north-westerly-westerly, north-westerly, northerly and north-easterly clusters. In 2001, transport with westerly origin comprise 88% and only 8% shows regional transport from the north. In 2002, westerly transport accounts for 92%, while in 2003 it accounts for 91%. A north-easterly cluster with 8% is observed in 2002 as compared to the 9% of north-westerlies observed in 2003. This clearly indicates that the yearly patterns are similar to the 3-year means. The variability in source direction and height for individual years is similar to the 3-year means.

4.6.3 Seasonal differences

Brankov *et al.* [1998], emphasized that care should be taken to include seasonal clusters when constructing cluster analysis of trajectories because of strong variations in weather system activity of different times of the year. Figure 4.7 depicted seasonal cluster means at 300 m agl. The seasonal clusters over the 3-year period showed variation in the wind flow to Cape Point. The dominant overall features are the westerlies and recirculation. The pattern of westerlies and strong westerlies veering to south-westerlies are present in varying degrees during all seasons and are related to the annual cycle of intensification and migration of the South Atlantic anticyclones..

In summer, transient mid-latitude ridging anticyclones originate on the southern margin of the South Atlantic anticyclone and ridge to the south-western, south and east coasts of South Africa [Tyson and Preston-Whyte, 2000; Jackson, 1951]. Schulze [1965] found that south to south-east winds to the Western Cape blow 60 per cent of the time, with south-easters being particularly strong at times. Hence, the observed westerly, south-westerly and south-easterly trajectories during this season.

In autumn, the westerly cluster 1 in summer veers to a north-westerly direction and the south-easterly cluster 5 in summer veers to a north-westerly direction. There is also a cluster (cluster 4 in summer and cluster 5 in autumn) originating in the south that is observed in both seasons. This cluster indicates the southerly meridional flow from the south of the subcontinent that brings cooler temperatures to the west and east coast of South Africa.

In winter, a cluster (4) showing regional recirculation is observed. This type of recirculation results from continental high pressure systems dominating over southern Africa during the period June-August.

Schulze [1965] observed that the south-easterlies peak during the spring season. Clusters in figure 4.7d (spring) are similar to the ones in summer except that there is a cluster originating in the south during summer that is absent in spring. Clusters with westerly components account for 65% in summer, 61% in autumn, 68% in winter and 88% in spring, while those with an easterly component accounts for 35%, 39%, 32% and 12% in summer, autumn, winter and spring respectively.

Figure 4.8a-d depicted seasonal cluster means at 5000 m agl. The same pattern of clusters is observed in each season, although there are some differences. All seasons indicate strong westerly flows. In winter there is no cluster representing an easterly flow, but there is a north-westerly flow with slow moving winds. There is a north to north-easterly cluster that approaches Cape Point at a lower level observed in summer, autumn and spring. This type of trajectory was also observed by Tyson *et al* [1996a] and results from zonal transport in the easterly and westerly directions.

CHAPTER 5

CONCLUSIONS

This study focused on the geographical classification of the air-mass origins and their transport patterns to Cape Point. The main objectives of this research were to use a database of 5-day back trajectories computed at different levels (300 m and 5000 m) twice a day for the 3-year period 2001-2003 to identify major transport patterns to Cape Point and to investigate the source receptor relations. Inter-annual and seasonal variabilities were examined, as well as the differences in flow patterns between the two levels and the sensitivity of transport to trajectory height. The influence of meteorological conditions on flow patterns was also investigated.

The 5-day back trajectories were computed using the HYSPLIT-4 model. The trajectories were then grouped into 3-year, yearly and seasonal trajectory databases. A multivariate statistical procedure known as cluster analysis was used to group similar trajectories into distinct transport regimes. The cluster analysis was performed for all 3-year, yearly and seasonal trajectories at both 300 and 5000 m above ground levels. The dominant features were summarized as follow:

- Seven flow patterns to Cape Point were identified (northerly, north-westerly, north-easterly, south-easterly, southerly, south-westerly and westerly cluster means).
- Cluster analysis identified similar year to year gross features of atmospheric transport patterns to Cape Point at 5000 m, however, variability is observed at 300 m.
- Both spring and summer mean clusters exhibit a south-easterly transport associated with trade winds, while autumn and winter show recirculation associated with anticyclones dominating over the interior of South Africa during this period.
- The 300 m level show subsiding air prior to arrival at Cape Point while the 5000 m level show both subsidence and uplift of air prior to arrival point, this clearly indicates shear winds between 300m and 5000m levels.
- South-easterly and southerly transport associated with trade winds, ridging anticyclones and southerly meridional flow is observed at 300m level, whereas at 5000m level only strong westerly flow and moderate north-westerly flow originating over South America are dominating, the flow patterns are associated with westerlies generated by South Atlantic Anticyclones, indicating the sensitivity of transport to trajectory altitude.
- The 300m level exhibit both southerly and south-westerly clusters associated with southerly meridional flow and ridging anticyclones.
- Air mass transport to Cape Point with northerly to north-easterly direction indicates recirculation over southern Africa at both levels. This type of transport could be responsible for transporting high concentration of air pollutants to Cape Point.
- The strong westerly flow at both levels may be responsible for transporting a broad range of pollutants from South America to Cape Point. This may occur when surface level emissions and the resulting photochemical pollutants undergo a process of up-lift from

the continental boundary layer to upper troposphere via convection and large-scale advection before being transported across the South Atlantic to Cape Point.

- The weak 2002/2003 ENSO caused insignificant changes to the flow characteristics.

This study demonstrated that the cluster analysis technique is a powerful tool to establish air transport climatology. It contributes to the description of the flow affecting Cape Point, and new approach to dynamic climatology of the Cape Point. The absence of significant transport from highly polluted industrial Highveld region of South Africa confirms the choice of Cape Point GAW station as a background monitoring of the atmosphere. The results show that easterly waves have insignificant role in air transport to Cape Point as compared to all other circulation systems affecting southern Africa. The frequency of occurrence of each class determines the percentage of each transport pattern. The results of this study can also be used to facilitate the interpretation of the influence of atmospheric transport patterns on pollutant concentrations at Cape Point.

Future climatology studies using cluster analysis should consider clustering seasonal trajectories month-wise (e.g. 3-years of January trajectories, etc.) as suggested by Harris and Kahl [1990], rather than seasonally (e.g. December-February, March-May, etc.) as was the case in this study, suggested by Cape *et al* [2000]. This procedure may generate significant differences in flow patterns between seasons and may also clearly indicate the influence of ENSO events on flow patterns. The study should also focus on the relationship between intercontinental transport patterns and chemical constituents measured at the surface. Lastly, shorter (2-day) back trajectories should also be run to investigate the influence of mesoscale weather phenomena on regional transport to Cape Point that cannot be clearly revealed by long-range transport.

REFERENCES

Abraham, H. O. and E. M. Rasmusson, 1970: On the annual variation of the monthly mean meridional circulation. *Monthly Weather Review*. **98**, (6), 423-442.

Anastassopoulos, A., S Nguyen and X. Xu, 2004: On the use of HYSPLIT model to study air quality in Windsor, Ontario, Canada. *Environ. Inform. Arch.* **2**, 517-525.

Anderberg, M. R., 1973: Cluster analysis for applications. Academic Press, San Diego, California, 359pp.

Avila, A. and M. Alarcón, 1999: Relationship between precipitation chemistry and meteorological situations at a rural site in NE Spain. *Atmos. Environ*., **33**, 1663-1677.

Barry R.G., and Perry A.H., 1973: Synoptic climatology; methods and applications. Metheun & Co Ltd, London.

Berlage, H. P., 1957: Fluctuations of the general atmospheric circulation of more than one year, their nature and prognostic value. *Mededel. Verhandel*., **69**, Kon. Ned, Meteor. Inst., 152pp.

Berlage, H. P., 1966: The southern oscillation and world weather. *Mededel. Verhandel*. **88**, Kon. Ned, Meteor. Inst., 152pp.

Bjerkness, J., 1969: Atmospheric teleconnections from the equatorial pacific. *Monthly Weather Review*. **97**, 163-172.

Bonnardot, V., O. Planchon and S. Cautenet, 2005: Sea breeze development under an offshore synoptic wind in the South-Western Cape and implications for the Stellenbosch wine-producing area. *Theor. Appl. Climatol*. **81**, 203-218.

Brankov, E., S. T. Rao and P. S. Porter, 1998: A trajectory-clustering-correlation methodology for examining the long-range transport of air pollutants. *Atmos. Environ*. **32**, 1525-1534.

Cachier, H. P., P. Buat-Menard, M. Fontugne and P. Chesselet, 1986: Long-range transport of continentally-derived particulate carbon in the marine atmosphere; Evidence from stable carbon isotope studies. *Tellus*, **38(B)**: 161-177.

Calvo, J., 1993: Flow classification at 500hPa for the Iberian Peninsula. Tech. Note **32**, Service of Numerical Weather Prediction, Instituto Nacional de Meteorología, Madrid.

Cape, J. N., J. Methven and L. E. Hudson, 2000: The use of trajectory cluster analysis to interpret measurements at Mace Head, Ireland. *Atmos. Environ*. **34**, 3651-3663.

Chang, J., 1972: Atmospheric circulation systems and climates. The Oriental Publishing Company. 71pp.

Collett, R. S. and K. Dyuyemi, 1997: Air quality modeling; a technical review of mathematical approaches. *Meteorol. Appl*., **4**, 235-246.

Crutzen, P. J. and M. O. Andreae, 1990: Biomass burning in the tropics; impact on atmospheric chemistry and biochemical cycles. *Science*, **250**, 1669-1678.

D'Abreton, P. C, 1996: Lagrangian kinematic and isentropic trajectory models for aerosol and trace gas transport studies in southern Africa. *J. Geophys. Res*., **92**, 157-160.

Desmet, P.G., and R.M. Cowling, 1999: The climate of the Karoo- a functional approach. The Karoo: Ecological patterns and processes. Cambridge University Press. 3pp

Dorling, S. R., T. D. Davies and C. E. Pierce, 1992a: Cluster analysis; a technique for estimating the synoptic meteorological controls on air and precipitation chemistry-methods and applications. *Atmos. Environ*. **26A (14)**, 2575-2581.

Dorling, S. R., T. D. Davies and C. E. Pierce, 1992b: Cluster analysis; a technique for estimating the synoptic meteorological controls on air and precipitation chemistry- results from Eskdalemuir. *Atmos. Environ*., **26B (14)**, 2583-2602.

Dorling, S. R. and T. D. Davies, 1995: Extending cluster analysis- synoptic meteorology links to characterize chemical climates at six north-west European monitoring stations. *Atmos. Environ*. **29(2)**, 145-167.

Draxler, R. R., 1990: The calculation of the low-level winds from the archived data of a regional primitive equation model. *J. Appl. Meteorol*., **29**, 240-248.

Draxler, R. R., 1992: Hybrid single-particle Lagrangian integrated trajectories (HYSPLIT): Version 3.0—user's guide and model description. NOAA Tech. Memo. *ERL ARL*-**195**, 26pp.

Draxler, R.R, 1996: Boundary layer isentropic and kinematic trajectories during the August 1993 North Atlantic regional experiment intensive.

Draxler, R. R. and A.D. Taylor, 1982: Horizontal dispersion parameters for long-range transport modeling. *J. Appl. Meteorol*., **21**, 667-372.

Draxler, R.R., 1987: Sensitivity of a trajectory model to the spatial and temporal resolution of the meteorological data during CAPTEX. *J. Clim. Appl. Meteorol*. **26**:1577-1588.

Draxler, R. R. and B. J. B. Stunder, 1988: Modeling the CAPTEX vertical tracer concentration profiles. *J. Appl. Meteorol*. **27**, 617-625.

Draxler, R. R. and G. D. Hess, 1997: Description of HYSPLIT_4 modelling system. NOAA technical memorandum *ERL ARL*-**224**, 24pp.

Draxler, R. R. and G. D. Hess, 1998: An overview of the HYSPLIT_4 modelling system for trajectories, dispersion and deposition. *Australian Meteorological Magazine*, **47**, 295-308.

ECMWF, 1995: The description of the ECMWF/WCRP level III-A global atmospheric data archive. European Centre for Medium-Range Weather Forecasts (ECMWF). Reading, Berkshire, England.

Eneroth, K., E. Kjellström, and K. Holmén, 2003: Interannual and seasonal variations in transport to a measuring site in western Siberia and their impact on the observed atmospheric CO_2 mixing ratio. *J. Geophys. Res*., **108**, 4660-4673.

Everitt, B., 1980: Cluster analysis. Halstead, New York, 136pp.

Fernau, M.E, 1988. Use of cluster analysis to define periods of similar meteorology and precipitation chemistry in eastern North America, PhD thesis, 330 pp., Univ. of Mich., Ann Arbor.

Fishman, J., K. Fakhruzzaman, B. Cros and D. Nganga, 1991: Identification of widespread pollution in the southern hemisphere deduced from satellite analyses. *Science*, **252**, 1693-1696.

Franzen, L. G., M. Hjelmroos, P. Kållberg, E. Borstom-Lunden, J. Juntto and A. Sarolainen, 1994: A case study of long-range transport of soil, pollen and stable organic compounds. *Atmos. Environ*., **28**, 3587-3604.

Freiman, M. T. and S. J. Piketh, 2003: Air transport into and out of the industrial Highveld region of South African. *S. Afr. J. of Sci*. **98**: 527-540.

Garstang, M., R. Swap, M. Edwards, P. Kållberg, and J. A. Lindesay, 1996: Horizontal and vertical transport of air over southern Africa. *J. Geophys. Res*., **101(D19)**, 23721-23736.

GAW, 2002: GAW Report No. 143; Global Atmosphere Watch Measurements Guide.

Gibbs, W. J., 1953: A comparison of hemispheric circulations with particular reference to the western Pacific. *Q. J. R. Meteorol. Soc*. **79**, 131-136.

Haagenson, P.L., Y. H. Kuo, M. Skumanich and N. L. Seaman, 1987: Tracer verification of trajectory models. *J. Clim. Appl. Meotorol*. **26**, 410-426.

Harris, J. M. and J. D. Kahl, 1990: A descriptive atmospheric climatology for the Mauna Loa Observatory, using clustered trajectories. *J. Geophys. Res*. **95**, 13651-13677.

Harris, J. M., 1992: An analysis of 5-day midtropospheric flow patterns for the South Pole; 1985-1989. *Tellus*, **44**, 409-421.

Harrison, M. S. J., 1984: The annual rainfall cycle over the central interior of South Africa, *S. Afr. J. Sci*., **75**, 1-8

Harrison, M. S. J., 1986: A synoptic climatology of South African rainfall variations. Unpublished PhD Thesis, University of the Witwatersrand, 341 pp.

Hastenrath, S., 1985: Climate and circulation of the tropics. Kluwer Academic Publishers' Group.

Hayward, L. G., and E. E. Steyn, 1967: Aeronautical climatological summaries; Descriptive memoranda for five South African airports, *WB* 31. Weather Bureau, Dept. of Transport, Pretoria, 73pp.

Henry, A. J, 1922: J. Bjerknes and H. Solberg on the life cycle of cyclones and the polar front theory of atmospheric circulation. *Monthly Weather Review*. 468-473.

Hewitson, B. C., and R. G. Crane, 2002: Self-organizing maps; application to synoptic climatology. *Clim. Res*. **22**: 13-26.

Hoflich, O., 1984: Climate of the South Atlantic Ocean. Climates of the oceans [H. van Loon, ed.] Vol IV, Elsevier Publishing Company, Amsterdam. The Netherlands, 1-191.

Hsu, S. A., 1988: Coastal Meteorology, Academic Press, San Diego.

Hunter, I. T., 1982: The coastal wind field of the southern Cape, in coastal studies off Natal, Lect. Notes coastal estuaries stud. **26**, edited by E. H. Schumann, pp 81-100, Springer-Verlag, New York.

Jackson, S. P., 1951: A preliminary study of the atmospheric circulation over South Africa. Unpublished PhD Thesis. University of London. 228pp.

Jackson, S. P., 1954: Sea breeze in South Africa. *S. Afr. Geogr. J*. **36**, 13-23.

Jenkinson, A. F., and B. P. Collison, 1997: An initial climatology of gales over the North Sea. *Synop. Climatol. Branch Memo*. No **62**, Meteorological Office, London, 18pp.

Jorba, O., C. Pérez., F. Franscesc. and J.M. Baldasano, 2004: Cluster analysis of 4-day back trajectories arriving in the Barcelona area (Spain) from 1997-2000. *J. Appl. Meteorol*. **43**. 6: 887-901.

Julian, P. R. and R. M. Chervin, 1978: A study of the Southern Oscillation and the Walker circulation phenomena. *Monthly Weather Review*. **106**, 1433-1451.

Jury, M. R., 1987: Air observations of meteorological conditions along Africa's west coast between 30°-35°S. *J. of Clim. and Appl. Meteor*. **26**, 1540-1552.

Jury, M. R. 1998: Global significance of climate variability in the tropical South Atlantic; modulation of the ENSO circulation. Presented at the Symposium on Environmental Variability in the South Atlantic. Swakopmund, Namibia. March 30 to April 4.

Jury, M. R., R. D. Diab and M. Schormann, 1993: An aircraft study of mesoscale wind patterns and associated meteorological conditions over Cape St. Francis, South Africa. *Amer. Meteorol. Soc*. **32**, 1647-1655.

Kahl, J. D. and P. J. Samson, 1986: Uncertainty in trajectory calculations due to low resolution meteorological data. *J. Clim. Appl. Meteorol*. **25**, 1816-1831.

Kahl, J. D. W., J. H. Harris, G. A. Herbert and M. P. Olson, 1998: Intercomparison of three long-range trajectory models applied to Arctic haze. *Tellus,* **41B**, 524-536.

Kahl, J.D.W., D. A. Martinez, H. Kuhns, C. I. Davidson, J. Jaffrezo and J. M. Harris, 1997: Air mass trajectories to Summit, Greenland; A 44-year climatology and some episodic events. *J. Geophys. Res*., **101 (C12),** 26,861-25875.

Kalkstein, L. S., G. Tan and J. A. Skindlov, 1987: An evaluation of three clustering procedures for use in synoptic climatological classification. *J. Clim. Appl. Meteor*., **26**, 717-730.

Kelbe, B., 1988: Features of westerly waves propagating over southern Africa during summer. *Bull. Amer. Meteor. Soc.* **116**, 60-70.

Krishnamurti, T.N, 1961: The subtropical jet stream of winter. *J. Meteorol*. **18**, 172-191.

Lamb, H.H., 1950: Types and spells of weather around the year in the British Isles; annual trends, seasonal structure of the year, singularities. *Q. J. R. Meteorol Soc*. **76**: 393-429.

Lee, T., S. Park and S. Kim, 1997: Dependence of trajectory accuracy on the spatial and temporal wind densities. *Tellus* B, **49**, 199-215.

Lettau, B, 1973: Pressure-wind relationships in the equatorial surface westerlies. *Monthly Weather Review*, **102**: 202-218.

Levine, J. S., 1991: Global biomass burning; atmosphere, climate and biospheric implications, MIT Press, Cambrdge, Mass., 551pp.

Lindesay, J. A. and M. R. Jury, 1991: Atmospheric circulation controls and characteristics of a flood event in central South Africa. *Int. J. Climatol*. **11**, 609-627.

Liu, Y., G. Wu and R. Ren, 2003: Relationship between the subtropical anticyclone and diabatic heating. *J. Climate*, **13**, 682-698.

Lutgens, F. K. and E. J. Tarbuck, 1979: The atmosphere 'an introduction to meteorology'. Prentice-Hall, Inc, Englewood Cliffs, New Jersey. 152pp.

Lutgens, F.K and E. J. Tarbuk, 2001 : *The Atmosphere, 8th edition*

Martin, D., G. Bergametti and B. Strauss, 1990: On the use of the synoptic vertical velocity in trajectory model; validation by geochemical tracers. *Atmos. Environ*., **24A**, 2059-2069.

Martín-Vide, J., 2001: Limitations of an objective weather-type system for the Iberian Peninsula. *Weather*, **56**, 248-250.

Millán, M.M., R. Salvador, E. Mantilla and G Kallos, 1997: Photooxidant dynamics in the Western Mediterranean basin in summer. *J. Geophys. Res*., **102**, 8811-8823.

Miller, J. M., 1981: A five-year climatology of five-day back trajectories from Barrow, Alaska. *Atmos. Environ*., **15**, 1553-1558.

Moody, J. L., 1986: The influence of meteorology on precipitation chemistry at selected sites in the Eastern United States. Ph.D. dissertation, University of Michigan, Ann, Arbor, 176 pp.

Moody, J. L. and J. N. Galloway, 1988: Quantifying the relationship between atmospheric transport and the chemical composition of precipitation on Bermuda. *Tellus*, **40**, 463-479.

Moody, J. L. and P. J. Samson, 1989: The influence of atmospheric transport on precipitation chemistry at two sites in the Midwest United States. *Atmos. Environ*., **23**, 2117-2132.

Moody, J. L., S. J. Oltmans, H. Levy II and J. T. Merrill, 1995: Transport climatology tropospheric ozone to Bermuda. *J. Geophys. Res*., **100**, 7179-7194.

Muhs, D.R., C.A. Bush, K.C. Stewart, T.R. Rowland and R.C. Crittenden, 1990. Geochemical evidence of Saharan dust parent material for soils developed on Quaternary limestones of Caribbean and Western Atlantic Islands. *Quaternary Research Letters*, **33**, 157-177.

Namias, J. and P. F. Clapp, 1949: Confluence theory of the high-tropospheric jet stream. *J. Meteorol*. **6**, 330-360.

Newell, R. E., J. W. Kidson, D. G. Vincent and G. J. Boer, 1972: The general circulation of the tropical atmosphere and interactions with extratropical latitudes, Vol. **1**, MIT Press. 258 pp.

Newell, R. E., J, W. Kidson, D. G. Vincent and G. J. Boer, 1974: The general circulation of the tropical atmosphere, Vol. **2**, MIT Press. 371 pp.

Newton, C. W., 1986: Erik Palmén; Synthesizer of the atmospheric general circulation. *Bull*. *Amer. Meteor. Soc*., **67**, 282-293.

Nichols, N., 1984: The Southern Oscillation and Indonesian sea surface temperature. *Mon. Wea. Rev*., **112**, 424-432.

NOAA, 1999: NOAA technical memorandum *ERL ARL*-**230**, 35pp.

Padya, B. M., 1984: The climate of Mauritius, Meteorological Office, Vacoas, Mauritius Meteorological Office Report, 217pp.

Palmén, E., 1951: The role of atmospheric disturbances in the general circulation. *Q. J. R. Meteor*. Soc. **77**, 337-354.

Palmén, E., and C. W Newton, 1969: Atmospheric circulation systems. Academic press.

Petisco, E., and J. M. Martín, 1995: Characterization of the atmospheric general circulation in the Iberian Peninsula and Balearic Islands. *Tech. Note* **5**, Service of Numerical Weather Prediction, Instituto Nacional de Meteorología, Madrid.

Philander, S. G. H., 1983: El Niño Southern Oscillation phenomena. *Nature,* **302**, 295-301.

Pitty, A. F., 1968: Particle size of the Saharan dust which fell into Britain in July 1968. *Nature*, **220**, 364-365.

Poissant, L., 1999: Potential sources of atmospheric total gaseous mercury in the St. Lawrence River Valley. *Atmos, Environ., 33, 2537-2547*

Potgieter, C. J., 2006: Accuracy and skill of the conformal-cubic atmospheric model in short-range weather forecasting over southern Africa. Unpublished MSc. Thesis, University of Pretoria.

Prospero, J. M., R. A. GLaccum and R. T. Nees, 1981: Atmospheric transport of soil dust from Africa to South America. *Nature*, **289**, 570- 572.

Rasmusson, E. M. and T. H. Carpenter, 1982: Variations in tropical sea surface temperature and sea surface wind fields associated with the Southern Oscillation/El Niño. *Mon. Wea. Rev*., **110**, 354-384.

Reason C.J.C. and M. R. Jury, 1990: On the generation and propagation of the southern African coastal low. *Q. J. R. Meteor. Soc*., **116**, 1133-1151.

Ribalaygua, J. and R Borén, 1995: Classification of daily spatial patterns of precipitation of peninsular Spain and Balearic Islands. Tech. Note **3**, Service of Numerical Weather Prediction, Instituto Nacional de Meteorología, Madrid.

Riehl, H., 1954: Tropical meteorology. Mc Graw-Hill, New York. 93-97, 374-375pp.

Romesburg, H. C., 1984: Cluster analysis for researchers. Lifetime Learning, Belmont, Calif., 334pp.

Rosenlof, K. H., D. E. Stevens, J. R. Anderson and P. E. Ciesielski, 1986: The Walker circulation with observed zonal winds, a mean Hadley cell, and cumulus friction. *Bull, Amer. Meteor. Soc*., **43**, 449-467.

Sasamori, T., 1982: Stability of the Walker circulation. *Bull, Amer. Meteor. Soc*., 39, 518-527.

Schulze, B. R., 1965: Climate South of Africa, general survey, *part* **8**.Weather Bureau, Pretoria, South Africa.

Schneider, T, 2006: The general circulation of the atmosphere. *Annu. Rev. Earth Planet. Sci*. **34**: 655-688.

Schumann, E. H., 1992: Interannual wind variability on the south and east coasts of South Africa. *J. Geophys. Res*., **97**, 20397-20403.

Schumann, E. H. and J. A. Martin, 1991: Climatology aspects of the coastal wind field at Cape Town, Port Elizabeth and Durban.

Shannon, L. V., A. J. Boyd, G. B. Brundrit and J. Taunton-Clark, 1986: On the existence of an El Niño-type phenomena in the Benguela system. *J. Mar. Res*., **44**, 495- 520.

Sodemann, H., 2000: Relationships between the origin of air masses and Carbon Monoxide measurements at the Cape Point Trace Gas Monitoring Station, Unpublished Honours Thesis, Department of Environmental and Geographical Science, University of Cape Town, South Africa, 75 pp.

Spellman, G., 2000: The application of an objective weather-type system for the Iberian Peninsula. *Weather*, **55**, 375-385.

Stohl, A., 1998: Computation, accuracy and applications of trajectories; a review and bibliography. Atmos. Environ., **32**, 947-966.

Stohl, A. and P. Siebert, 1998: Accuracy of trajectories as determined from the conservation of meteorological tracers. *Q. J. R. Meteor. Soc*. **124**, 1465- 1484.

Stunder, B. J.B., 1996: An assessment of the quality of forecast trajectories. *J. Appl. Meteor*. **35**, 1319-1331.

Swap R. J., M. Garstang, S. Greco, R. Talbot and P. Kållberg, 1992: Saharan Dust in the Amazon Basin. *Tellus* **44(B)**:133-149.

Swap, R. J., M. Garstang, S. A. Macko, P. D. Tyson, W. Maenhaut, P. Artaxo, P. Kallberg and R. Talbot, 1995: The long range transport of southern African aerosols to the tropical south Atlantic, *J. Geophys. Res*., ***101***, 23,777–23,791, .

Taljaard, J. J., 1953: The mean circulation in the lower troposphere over southern Africa. *S. Afr. Geogr. J*. **35**, 33-45.

Taljaard, J. J., 1955: Stable stratification in the atmosphere over southern Africa. *Notos*, **4**, 217-230.

Taljaard, J. J., 1967: Development, distribution and movement of cyclones and anticyclones in the southern hemisphere during the IGY. *J. Appl. Meteor*. **6**, 973-987.

Taljaard, J. J., 1972: Synoptic meteorology of the Southern Hemisphere. *Meotorol. Monogr.*, **13**. No 35, American Meteorological Society, Boston.

Taljaard, J. J., 1995a: Atmospheric circulation systems, synoptic climatology and weather phenomena of South Africa. Part **2**. Atmospheric circulation systems in the South African region. *Technical Paper* **28**, SA Weather Bureau, Department of transport, Pretoria.

Taljaard, J. J., 1995b: Atmospheric circulation systems, synoptic climatology and weather phenomena of South Africa. Part **3**. The synoptic climatology of South African region. *Technical Paper* **29**, SA Weather Bureau, Department of transport, Pretoria.

Taljaard, J. J., 1995c: Atmospheric circulation systems, synoptic climatology and weather phenomena of South Africa. Part **4**. Surface pressure and wind phenomena in South Africa. *Technical Paper* **30**, SA Weather Bureau, Department of transport, Pretoria.

Taylor, A. D., 1997: Conformal map transformation for meteorological modelers. *Computers and Geosciences*, **23**, 63-75.

Triegaardt, D.O. and W. A. Landman, 1992: Charts of the mean circulation over the Monsoon regions of the world. South African Weather Bureau, *Technical Paper No*. **25**. 32pp.

Tyson P.D., 1986: Climatic Change and Variability in southern Africa. Oxford University Press, Cape Town, 220pp.

Tyson, P. D., M. Garstang and R. Swap, 1996a: Large-scale recirculation of air over southern Africa. *J. Appl. Meteor.*, **35**, 2218-2236.

Tyson, P. D., M. Garstang, R. Swap, P. Kållberg and M. Edwards, 1996b: An air transport climatology for subtropical southern Africa. *Int. J. Climatol*., **16**, 265-291.

Tyson, P. D. and R. A. Preston-Whyte, 2000: Atmospheric circulation and weather over southern Africa, Oxford University Press, Cape Town, 176pp.

van Heerden, J. H., 1987: Southern Africa's weather patterns ' an introductory guide' , Acacia books, via Africa limited, second edition, 29-71pp.

van Heerden, J., D. E. Terblanche and G. C. Schulze, 1988: The southern oscillation and South African summer rainfall, *J. Climatol*., **8**, 577-597.

van Loon, H., 1965: A climatology of the atmospheric circulation in the southern hemisphere during the IGY, Part **I**, 479-491.

van Rooy, M.P. 1936: Influence of berg winds on the temperatures along the west coast of South Africa. *S. Afr. J. Sci*, **22**, 94-95.

Walker, G. T., 1923: Correlation in seasonal variations of weather VIII. Mem. Indian Meoteor. Dept., **24**, 75-131.

Walker, G. T. and E. W. Bliss, 1932: "World Weather IV," Memoirs of the Royal Meterological Society, Vol. 4, No. **36**, London, 53-84pp.

Walker, N. D., 1990: Links between South African summer rainfall and temperature variability of the Agulhas and Benguela current systems, *J. Geophys. Res*., **95**, 3297-3319.

Watson, C. E., H. Fishman and H. J. Richie, 1990: The significance of biomass burning as a source of carbon monoxide and ozone in the southern hemisphere tropics; a satellite analysis. *J. Geophys. Res*., **95**, 16433-16450.

WMO TD, 2002; GAW Report No. 1077

Yarnal, B., 1993: Synoptic Climatology in Environmental Analysis. Bellhaven Press, 195pp.

Zannetti, P. and K. Puckett (Editors), 2004: Air quality modeling; theories, methodologies, computational techniques, and available database and software, Vol **1**-Fundamentals, A & WMA and the Enviro. Comp Institute. 430pp.

http://gap-vm-pub1.gap.fzk.de/319.php

http://gap-vm-pub1.gap.fzk.de/529.php

http://go.hrw.com/atlas/norm_htm/satlantc.html

http://sealevel.jpl.nasa.gov/overview/climate-climatic.html

http://weather.cod.edu/karl/chapter7.doc

http://wps.prenhall.com/ems_lutgens_atmoshere_9/0,7475,632096-,00.html

http://www.art.noaa.gov/ready/hysplit4.html

http://www.env.wustl.edu/archives/REU/2004/Students/Heinzerling/Heinzerlingrep01.html

http://gap-vm-pub1.gap.fzk.de/HYSPLIT_info.php

http://www.arl.noaa.gov/slides/ready/traj/traj4.html

http://auf.asn.au/meteorology/section4.html

http:/www.irbs.com/bowditch/pdf/chapter35.pdf

http://www.myweather.co.za/weatherinfo/SAWeather.html.

http://www.sci.ccny.edu/~stan/e31_glob.ppt

http://www.umweltbundesamt.de/luft-e/umweltbeobachtung/gaw/index.htm